Foregrounds Removal for Spectral Distortion Anisotropies

Mathieu Remazeilles

Instituto de Física de Cantabria

CSIC
Consejo Superior de Investigaciones Científicas

Remazeilles, Ravenni, Chluba, MNRAS 2022
Remazeilles & Chluba, MNRAS 2018

Dissipation of primordial acoustic modes

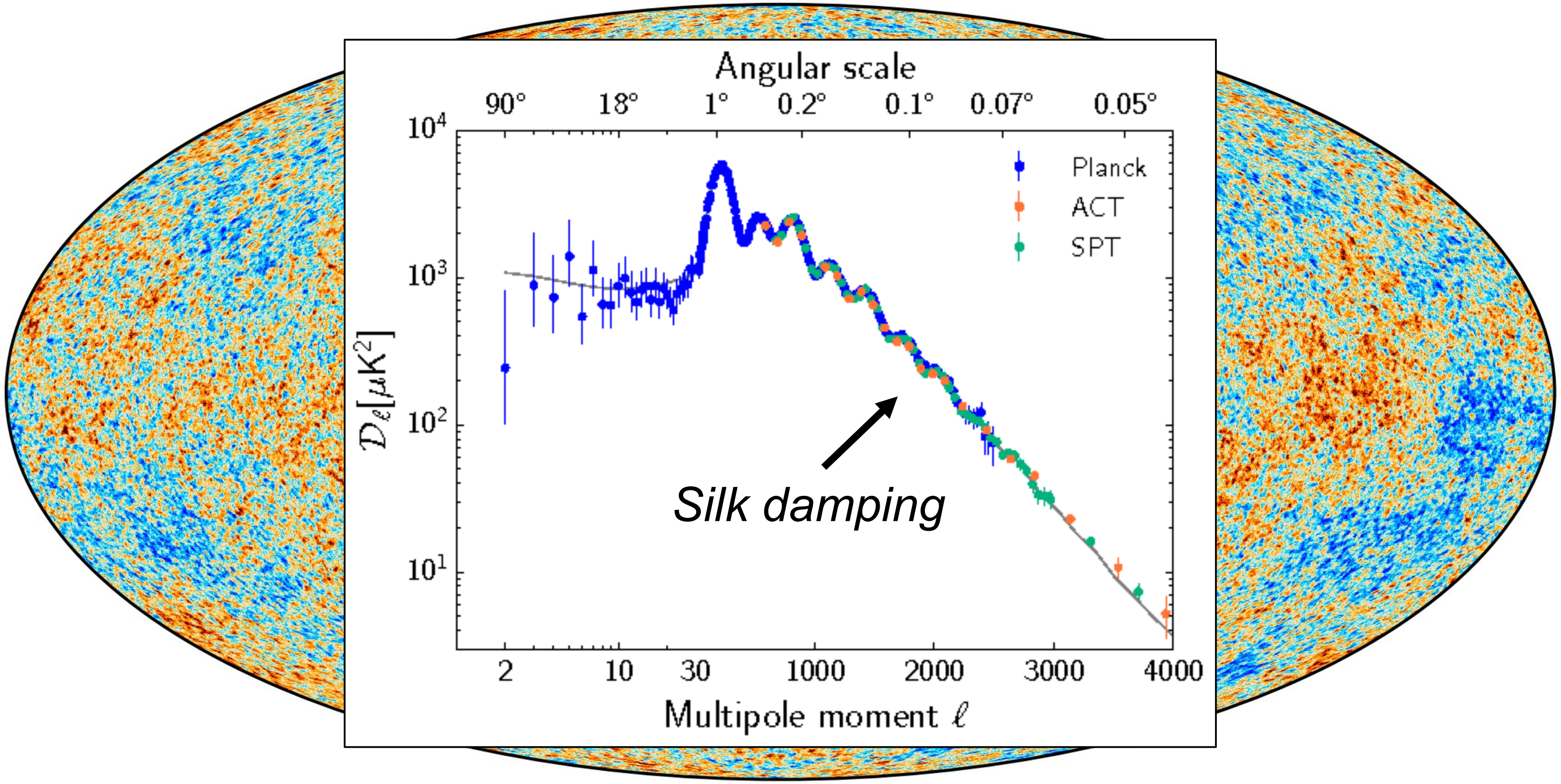

Photons random-walk out of **overdense/hot** regions towards **underdense/cold** regions, thus uniformizing the temperature and erasing anisotropies at small scales foremost

Dissipation of primordial acoustic modes

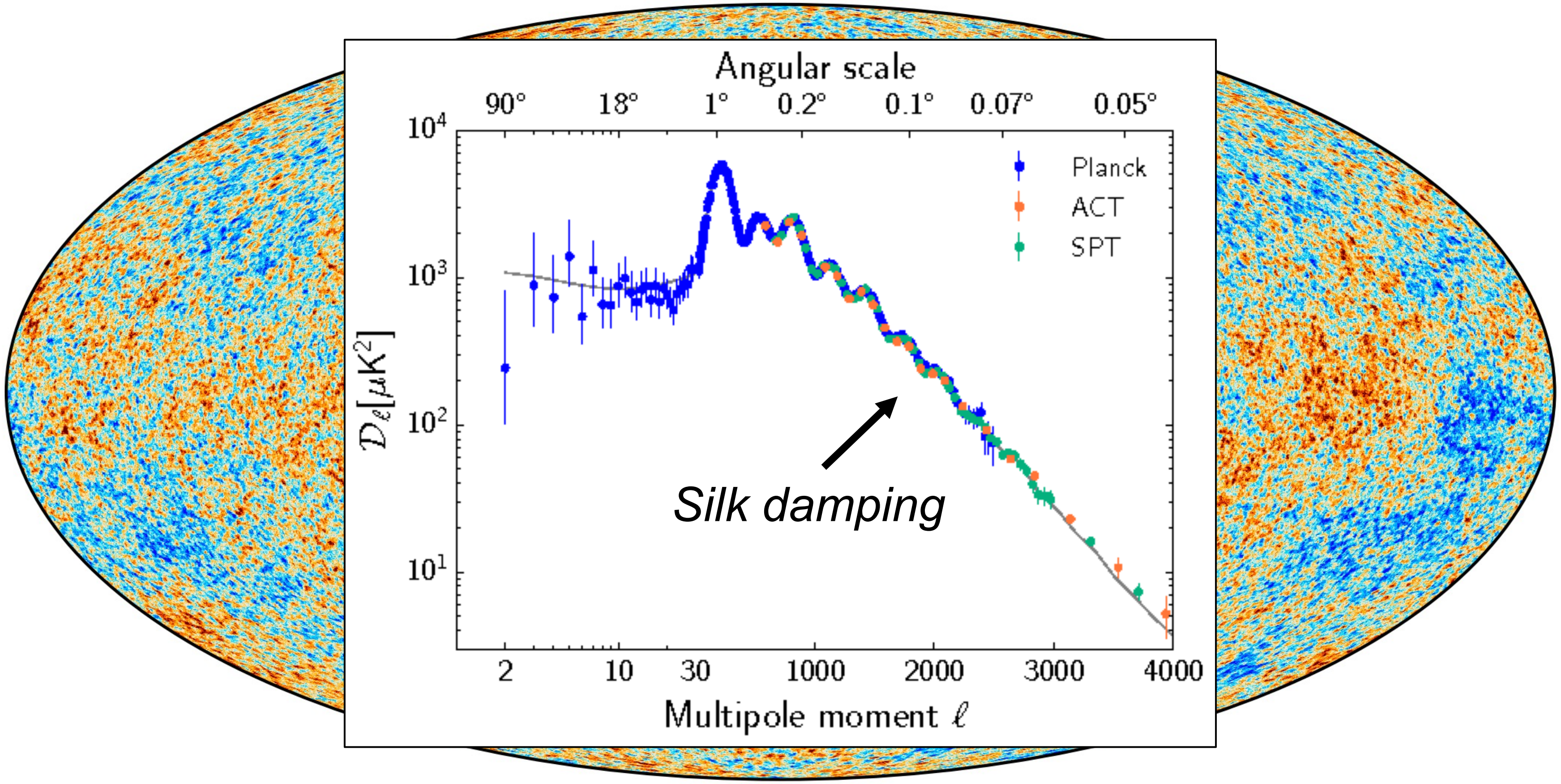

Photons random-walk out of **overdense/hot** regions towards **underdense/cold** regions, thus uniformizing the temperature and erasing anisotropies at small scales foremost

⟹ mixing blackbodies of different temperatures

Dissipation of primordial acoustic modes

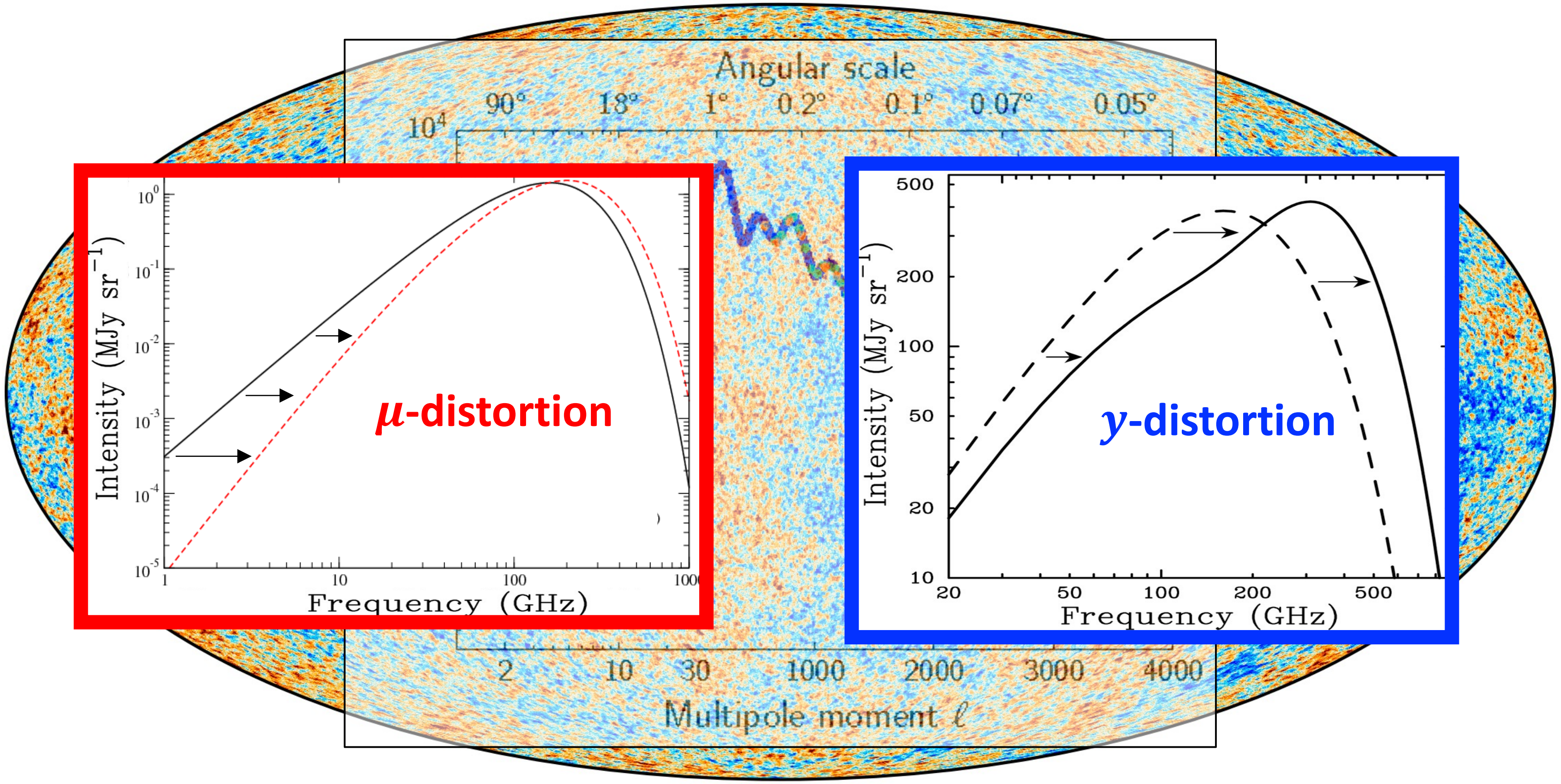

Photons random-walk out of **overdense/hot** regions towards **underdense/cold** regions, thus uniformizing the temperature and erasing anisotropies at small scales foremost

$\Longrightarrow$ ***mixing blackbodies of different temperatures***

CMB spectral distortions

Important at early times
$z > 10^4$

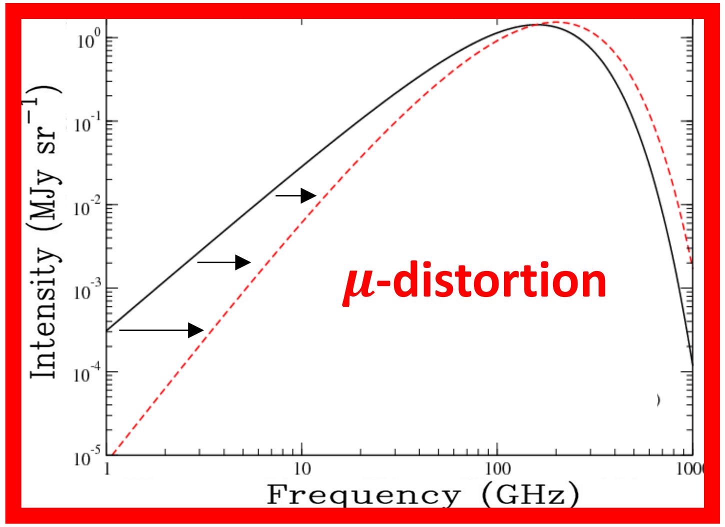

Sunyaev & Zeldovich, ApSS (1970)

Important at late times
$z < 10^4$

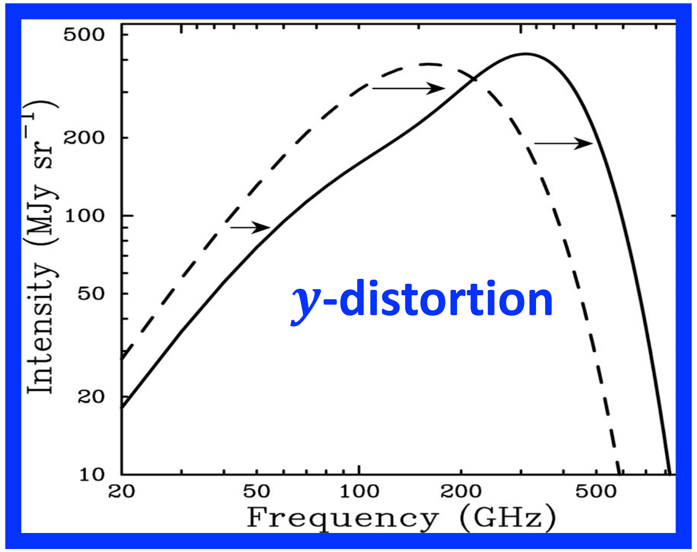

Zeldovich & Sunyaev, ApSS (1969)

CMB spectral distortions

Important at early times

$z > 10^4$

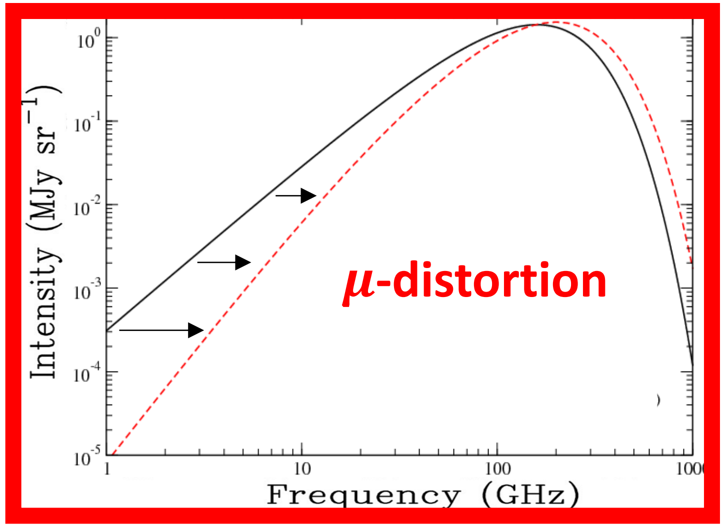

Sunyaev & Zeldovich, ApSS (1970)

Important at late times

$z < 10^4$

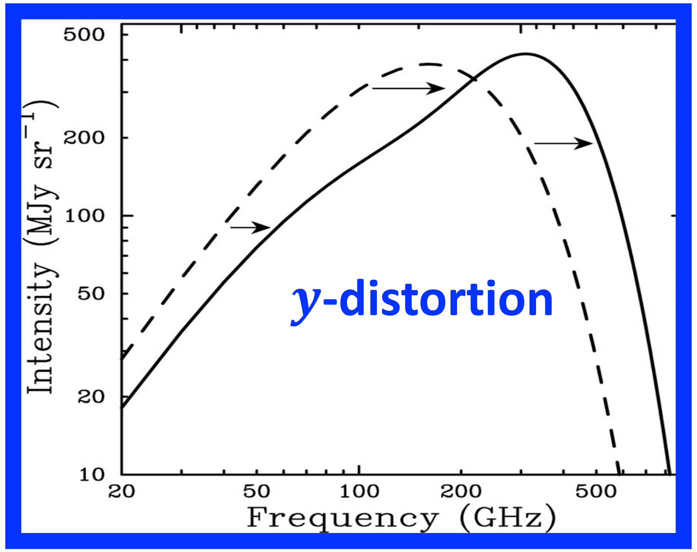

Zeldovich & Sunyaev, ApSS (1969)

$x \equiv h\nu/kT$

$$I_\nu^{\rm CMB} \simeq I_\nu^{\rm Planck}\left(1 + \mu \underbrace{\frac{xe^x}{e^x - 1}\left[\frac{\pi^2}{18\zeta(3)} - \frac{1}{x}\right]}_{\text{spectral signature of } \mu\text{-distortion}}\right)$$

Blackbody

$$I_\nu^{\rm CMB} \simeq I_\nu^{\rm Planck}\left(1 + y \underbrace{\frac{xe^x}{e^x - 1}\left[x\coth\frac{x}{2} - 4\right]}_{\text{spectral signature of } y\text{-distortion}}\right)$$

Blackbody

Spectral shapes of the distortions

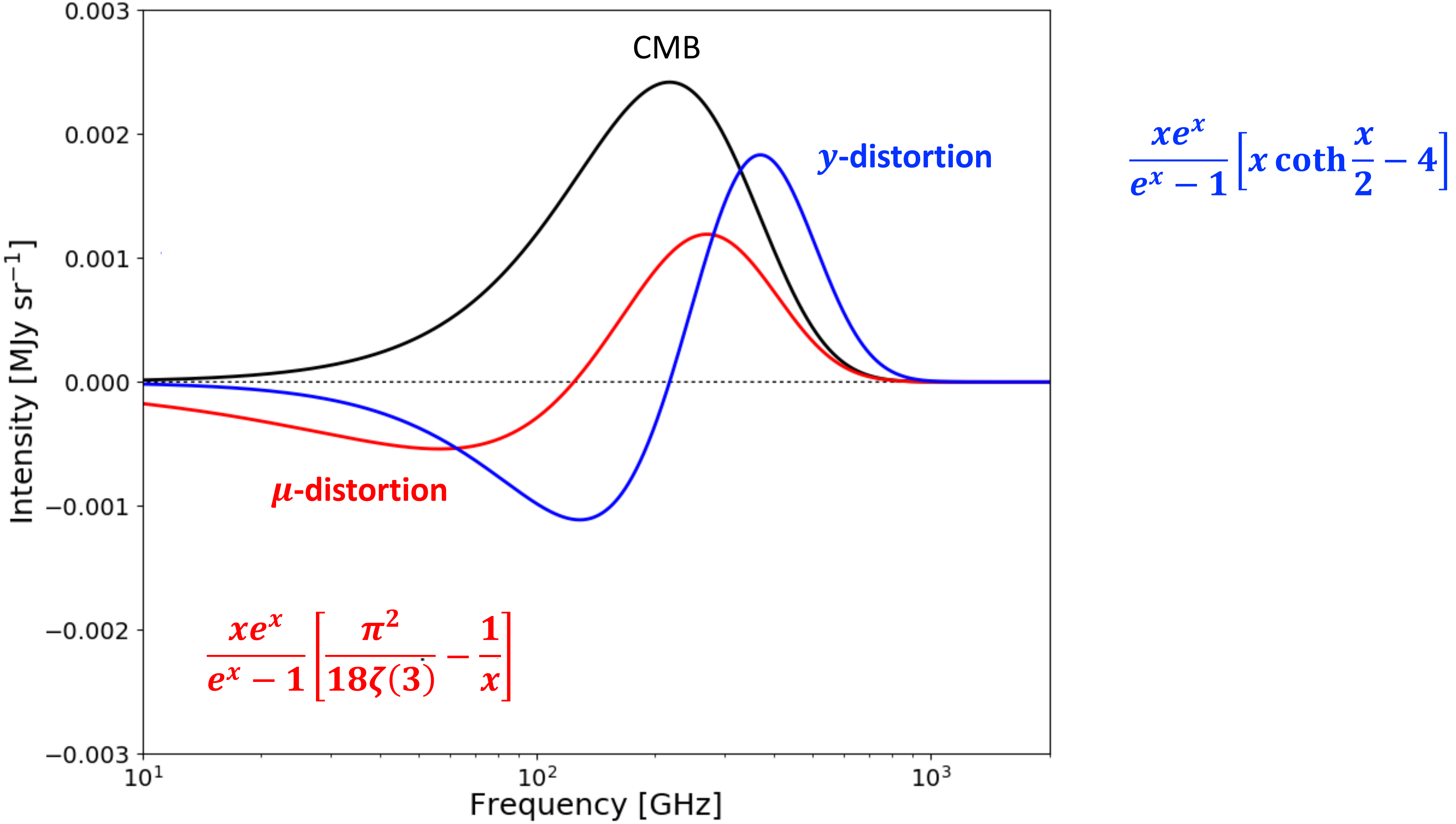

Spectral distortions probe the primordial power spectrum at very small scales

The primordial power spectrum is mostly unknown at scales $k > 3\ Mpc^{-1}$

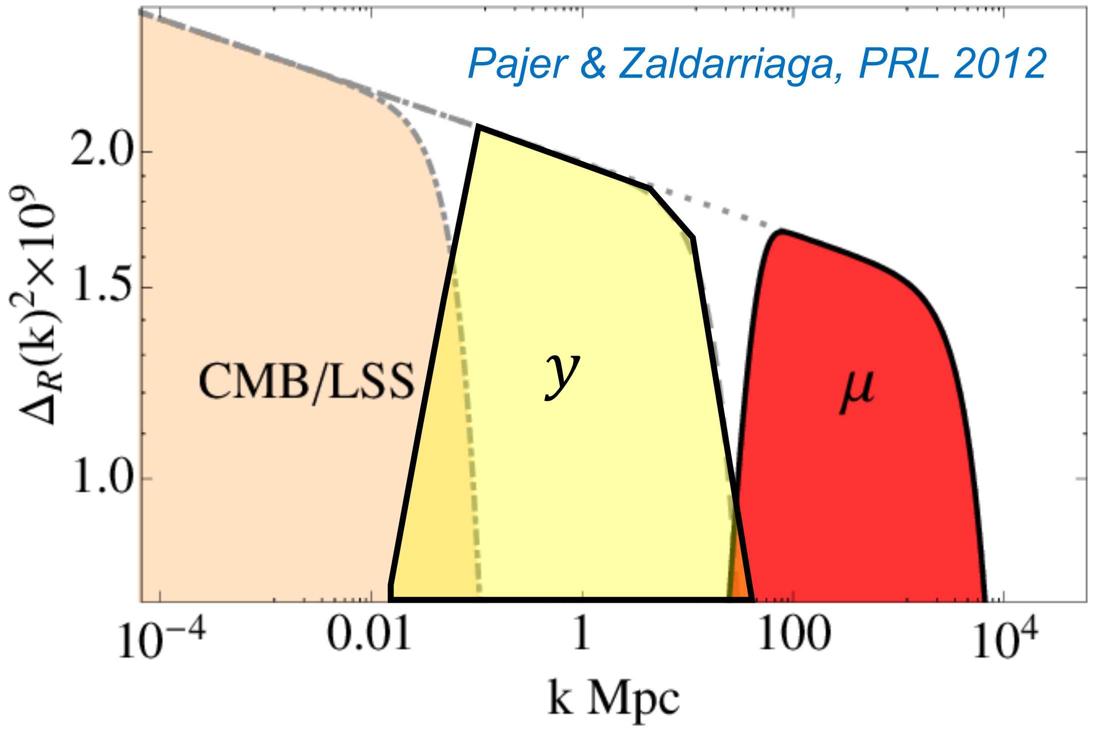

- CMB: $k > 0.2$ Mpc^{-1} erased by Silk damping
- LSS: $k > 0.2$ Mpc^{-1} very non-linear
- Spectral distortions can extend our lever arm up to $k \simeq 10^4\ \mathrm{Mpc}^{-1}$ in the linear regime!

Aside from average distortions…

Anisotropies of spectral distortions from non-Gaussian primordial perturbations

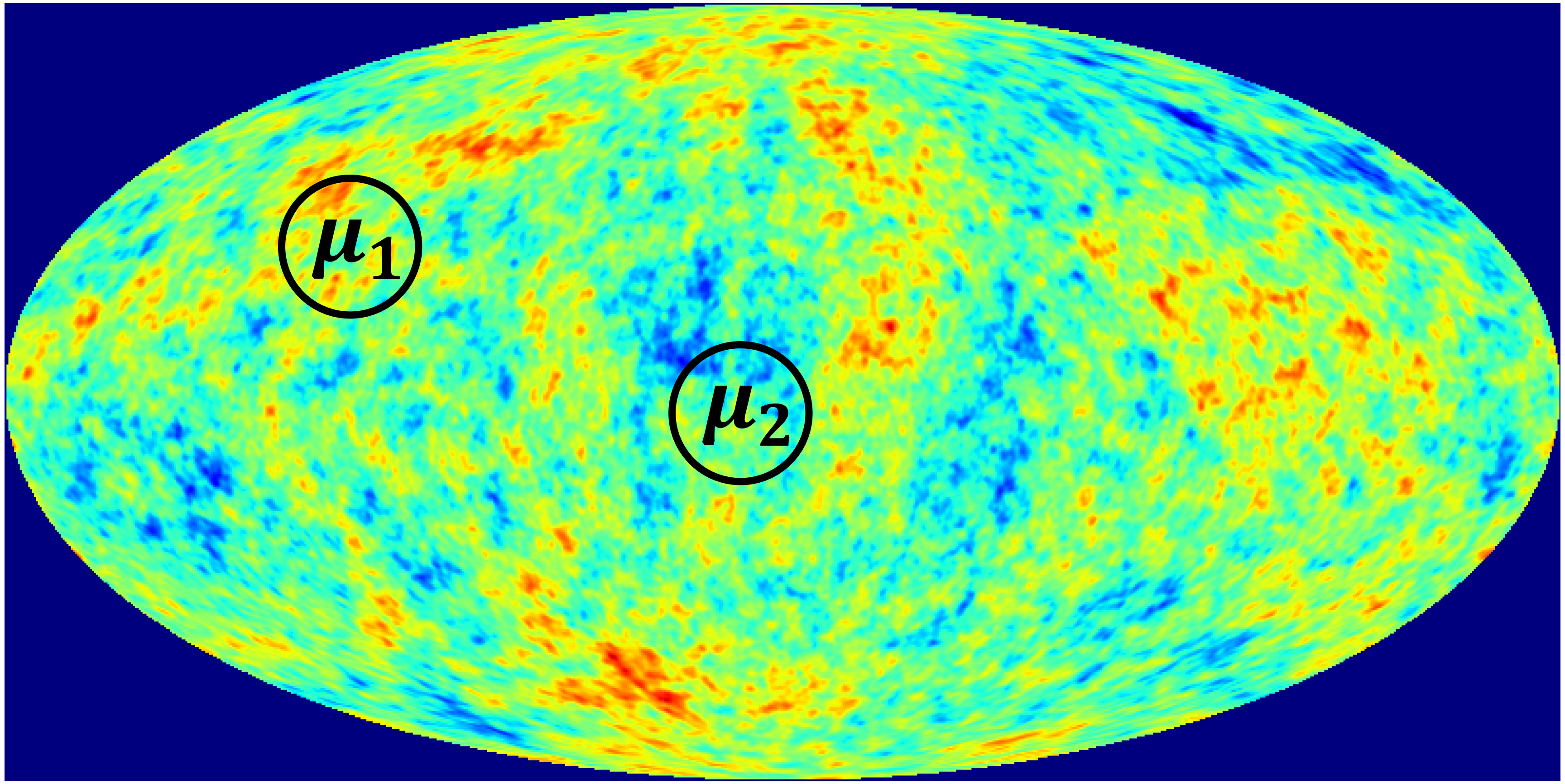

Anisotropic distortions from non-Gaussianity

Local type non-Gaussianity
"ultra squeezed"

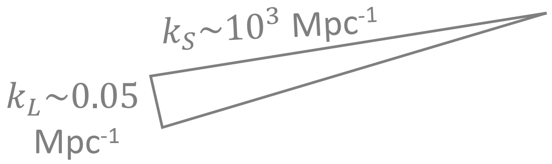

Pajer & Zaldarriaga, PRL 2012
Ganc & Komatsu, PRD 2012
Dimastrogiovanni et al JCAP 2016

- Multi-field inflation and non-Bunch-Davies vacuum models predict sizeable, scale-dependent, non-Gaussianity of the primordial perturbation field

- Non-gaussian couplings between short- and long-wavelength modes modulate the damping of primordial perturbations across different directions in the sky

$\Longrightarrow$ Anisotropic μ-distortions $\sim C_\ell^{\mu\mu}$

- Non-gaussian couplings $\Longrightarrow$ correlation between CMB temperature and μ-distortion anisotropies!

$$\Longrightarrow C_\ell^{\mu T} \simeq f_{\rm NL}(k \simeq 10^3\ \mathrm{Mpc}^{-1})\,\langle\mu\rangle\,\rho(\ell) C_\ell^{TT,\mathrm{SW}}$$

Anisotropic distortions from non-Gaussianity

Local type non-Gaussianity
"ultra squeezed"

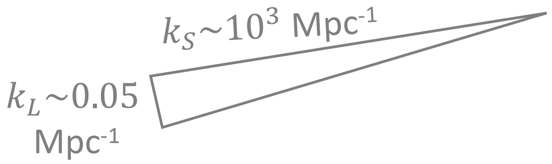

Pajer & Zaldarriaga, PRL 2012
Ganc & Komatsu, PRD 2012
Dimastrogiovanni et al JCAP 2016

- Multi-field inflation and non-Bunch-Davies vacuum models predict sizeable, scale-dependent, non-Gaussianity of the primordial perturbation field

- Non-gaussian couplings between short- and long-wavelength modes modulate the damping of primordial perturbations across different directions in the sky

$\Longrightarrow$ Anisotropic μ- and y-distortions $\sim C_\ell^{\mu\mu}$, C_ℓ^{yy}

- Non-gaussian couplings $\Longrightarrow$ correlation between CMB temperature and μ-distortion anisotropies!

$$\Longrightarrow C_\ell^{\mu T} \simeq f_{\rm NL}(k \simeq 10^3\ \mathrm{Mpc}^{-1})\, \langle\mu\rangle\, \rho(\ell) C_\ell^{TT,SW}$$
$$\Longrightarrow C_\ell^{yT} \simeq f_{\rm NL}(k \simeq 10\ \mathrm{Mpc}^{-1})\, \langle y\rangle\, \tilde{\rho}(\ell) C_\ell^{TT,SW}$$

Anisotropic distortions from non-Gaussianity

Local type non-Gaussianity
"ultra squeezed"

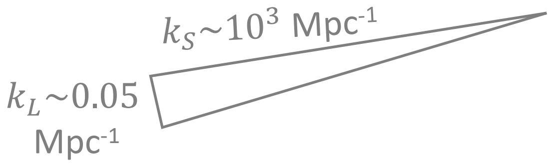

Pajer & Zaldarriaga, PRL 2012
Ganc & Komatsu, PRD 2012
Dimastrogiovanni et al JCAP 2016

- Multi-field inflation and non-Bunch-Davies vacuum models predict sizeable, scale-dependent, non-Gaussianity of the primordial perturbation field

- Non-gaussian couplings between short- and long-wavelength modes modulate the damping of primordial perturbations across different directions in the sky

$\Longrightarrow$ Anisotropic μ- and y-distortions $\sim C_\ell^{\mu\mu}$, C_ℓ^{yy}

- Non-gaussian couplings $\Longrightarrow$ correlation between CMB temperature and μ-distortion anisotropies!

$$\Longrightarrow C_\ell^{\mu T} \simeq f_{\rm NL}(k \simeq 10^3\ {\rm Mpc}^{-1})\, \langle\mu\rangle\, \rho(\ell) C_\ell^{TT,SW}$$
$$\Longrightarrow C_\ell^{yT} \simeq f_{\rm NL}(k \simeq 10\ {\rm Mpc}^{-1})\, \langle y\rangle\, \tilde{\rho}(\ell) C_\ell^{TT,SW}$$

Enhanced distortion signals by cross-correlation with CMB temperature anisotropies!

Anisotropic distortions from non-Gaussianity

Local type non-Gaussianity
"ultra squeezed"

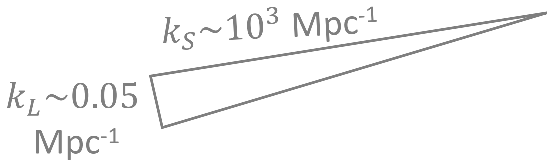

Pajer & Zaldarriaga, PRL 2012
Ganc & Komatsu, PRD 2012
Dimastrogiovanni et al JCAP 2016

- Multi-field inflation and non-Bunch-Davies vacuum models predict sizeable, scale-dependent, non-Gaussianity of the primordial perturbation field

- Non-gaussian couplings between short- and long-wavelength modes modulate the damping of primordial perturbations across different directions in the sky

$\Longrightarrow$ Anisotropic μ- and y-distortions $\sim C_\ell^{\mu\mu}$, C_ℓ^{yy}

- Non-gaussian couplings $\Longrightarrow$ correlation between CMB temperature and μ-distortion anisotropies!

$$\Longrightarrow C_\ell^{\mu T} \simeq f_{\rm NL}(\underline{k \simeq 10^3\ {\rm Mpc}^{-1}})\,\langle\mu\rangle\,\rho(\ell)C_\ell^{TT,SW}$$
$$\Longrightarrow C_\ell^{yT} \simeq f_{\rm NL}(\underline{k \simeq 10\ {\rm Mpc}^{-1}})\,\langle y\rangle\,\tilde{\rho}(\ell)C_\ell^{TT,SW}$$

New pivot scales to probe the scale-dependence of primordial non-Gaussianity!

Theory

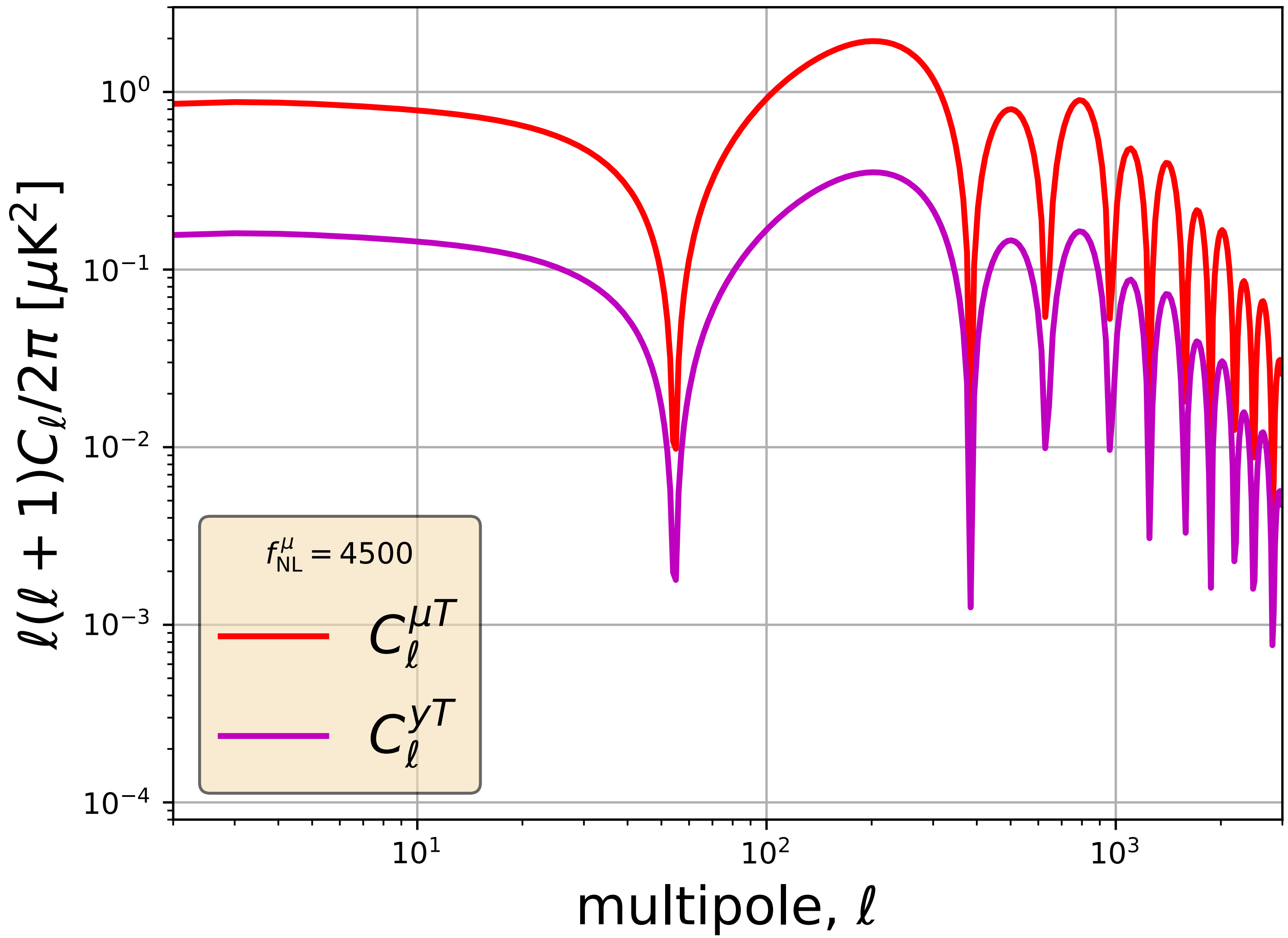

Ravenni et al JCAP 2017

CMB polarization adds more leverage!

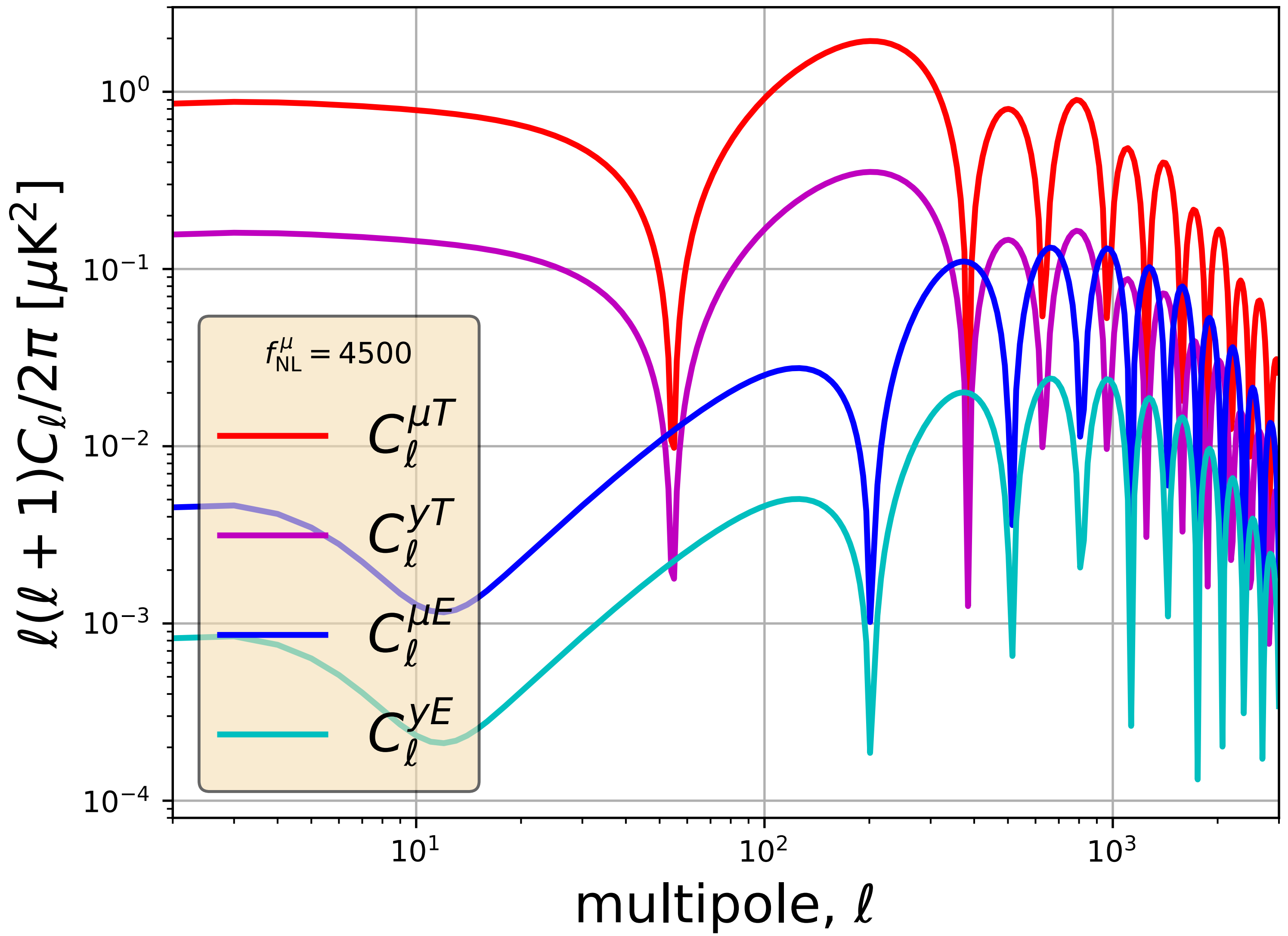

Ravenni et al JCAP 2017

Extra bits of information from μE, yE correlations!

Huge dynamic range of scales between CMB and μ-distortion probes

Mild scale dependence allows for large $f_{\rm NL}$ values at large wavenumber k

$$f_{\rm NL}(k) = f_{\rm NL}(k_0)\left(\frac{k}{k_0}\right)^{n_{\rm NL} \lesssim 0.6}$$

$f_{\rm NL}(k\sim 10^{-2}\ {\rm Mpc}^{-1}) \simeq 5$

CMB anisotropies

$f_{\rm NL}(k\sim 10^{3}\ {\rm Mpc}^{-1}) \simeq 5000$

μ-distortion anisotropies

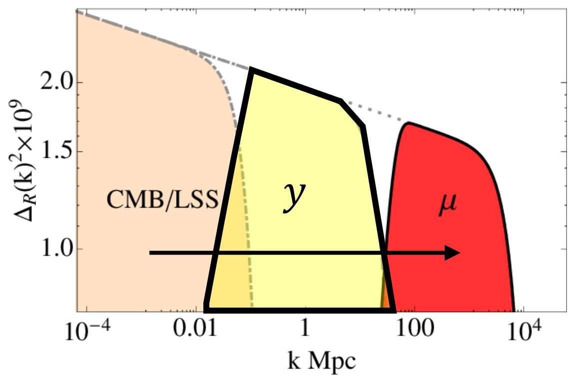

Orders of magnitude

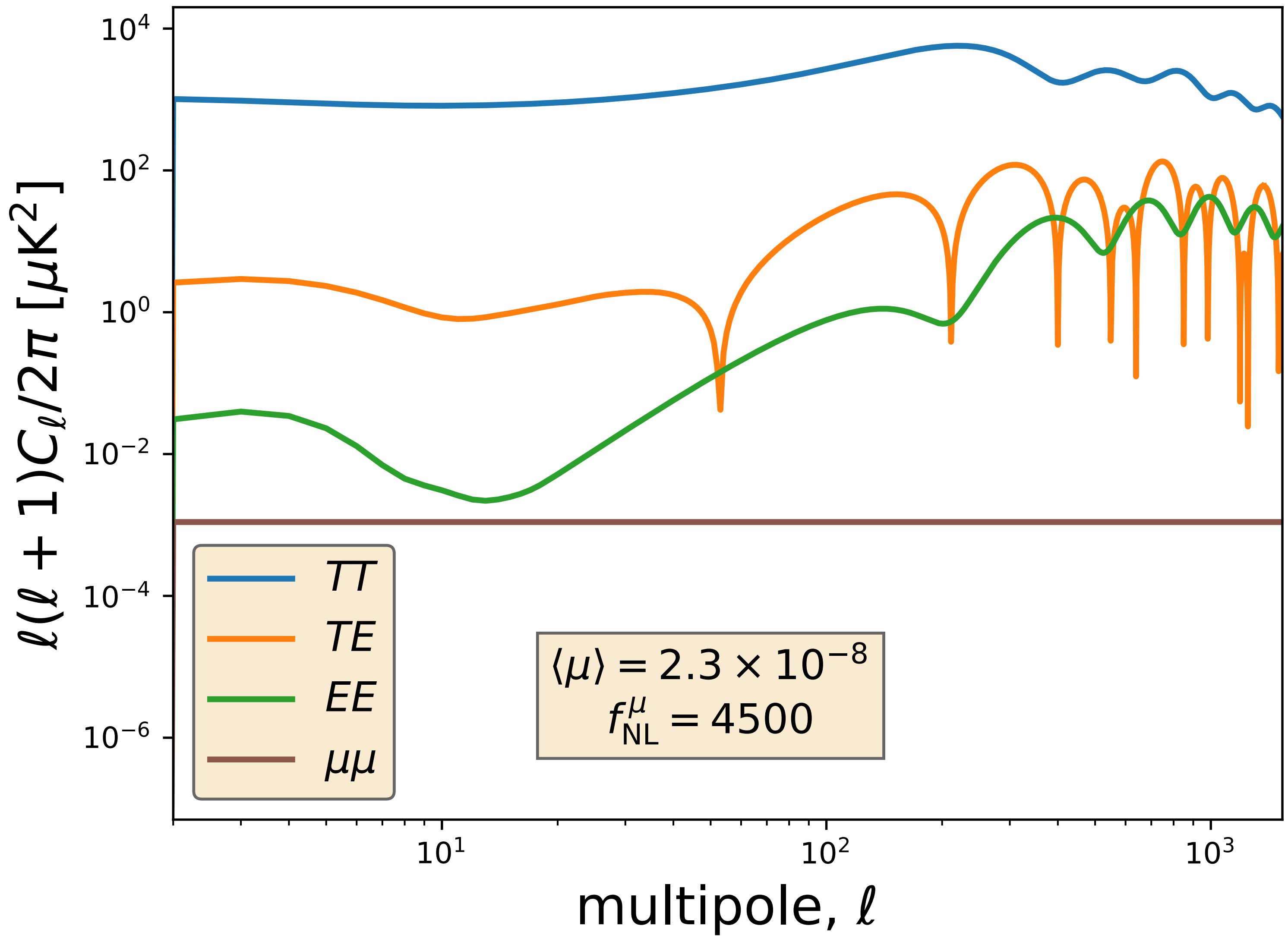

Orders of magnitude

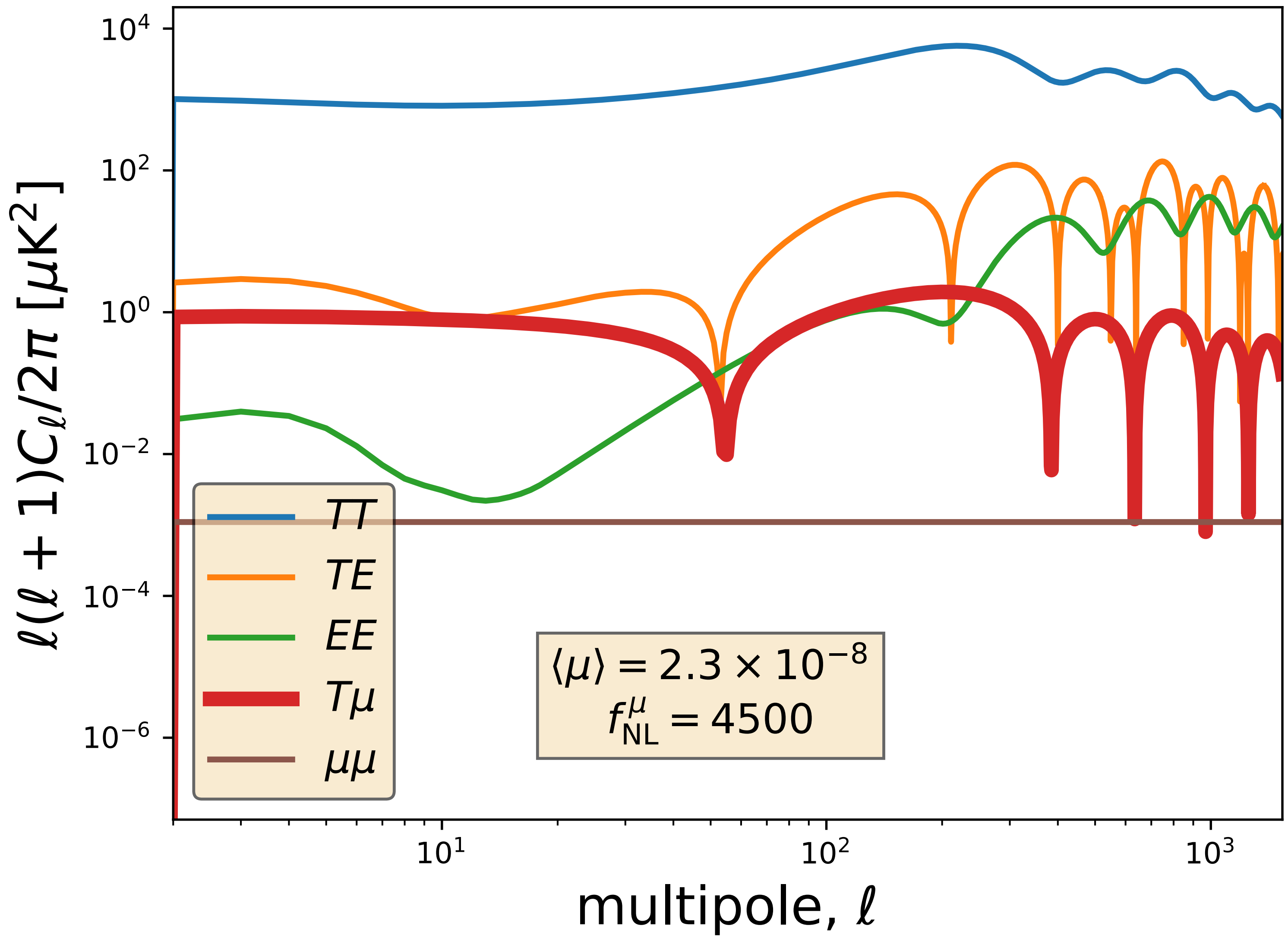

For $f_{\rm NL}^{\mu} \simeq 4500$
μT comparable
to TE and EE

Orders of magnitude

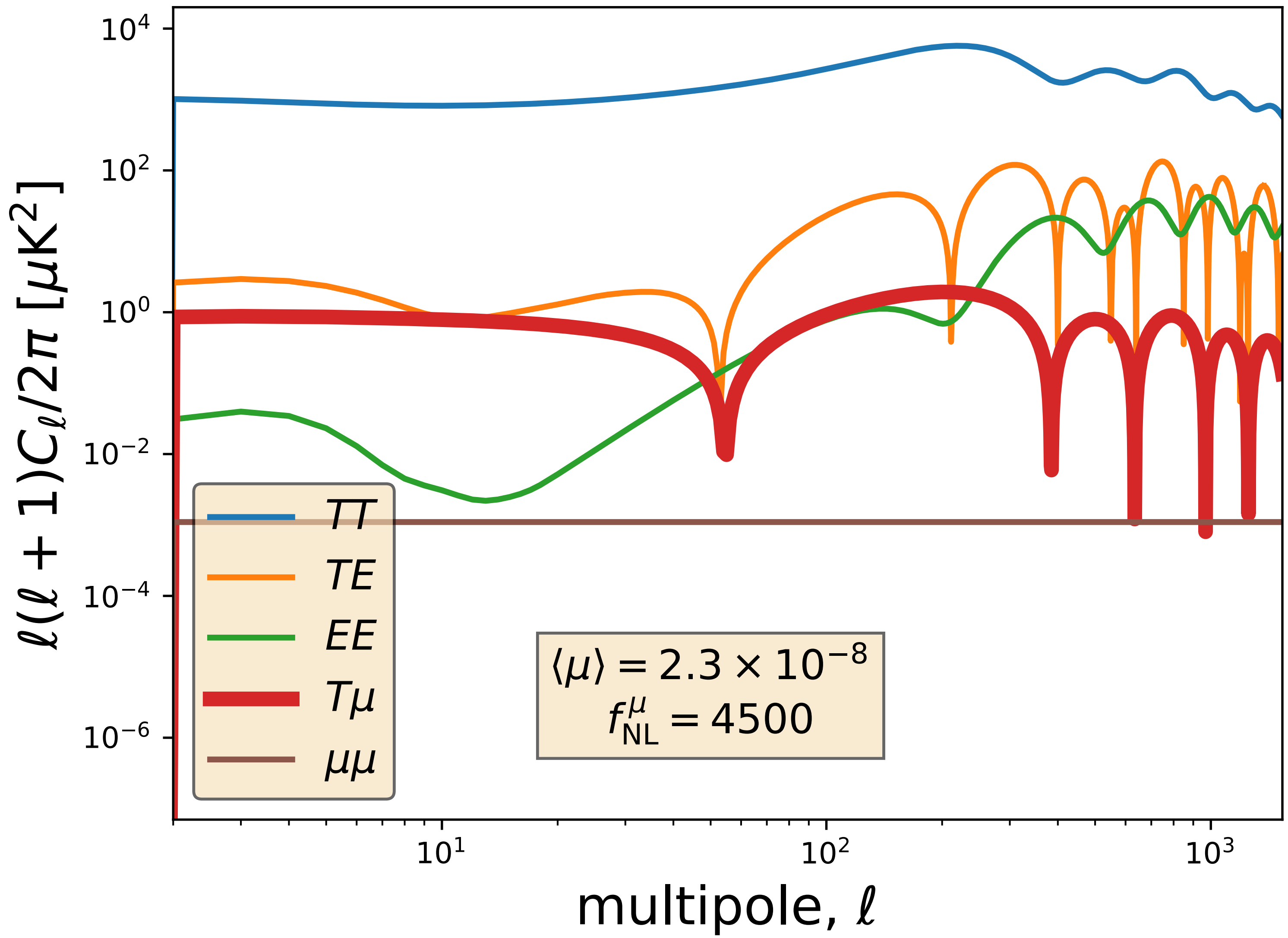

For $f_{\rm NL}^{\mu} \simeq 4500$
μT comparable
to TE and EE

A science goal for future CMB imagers!

Orders of magnitude

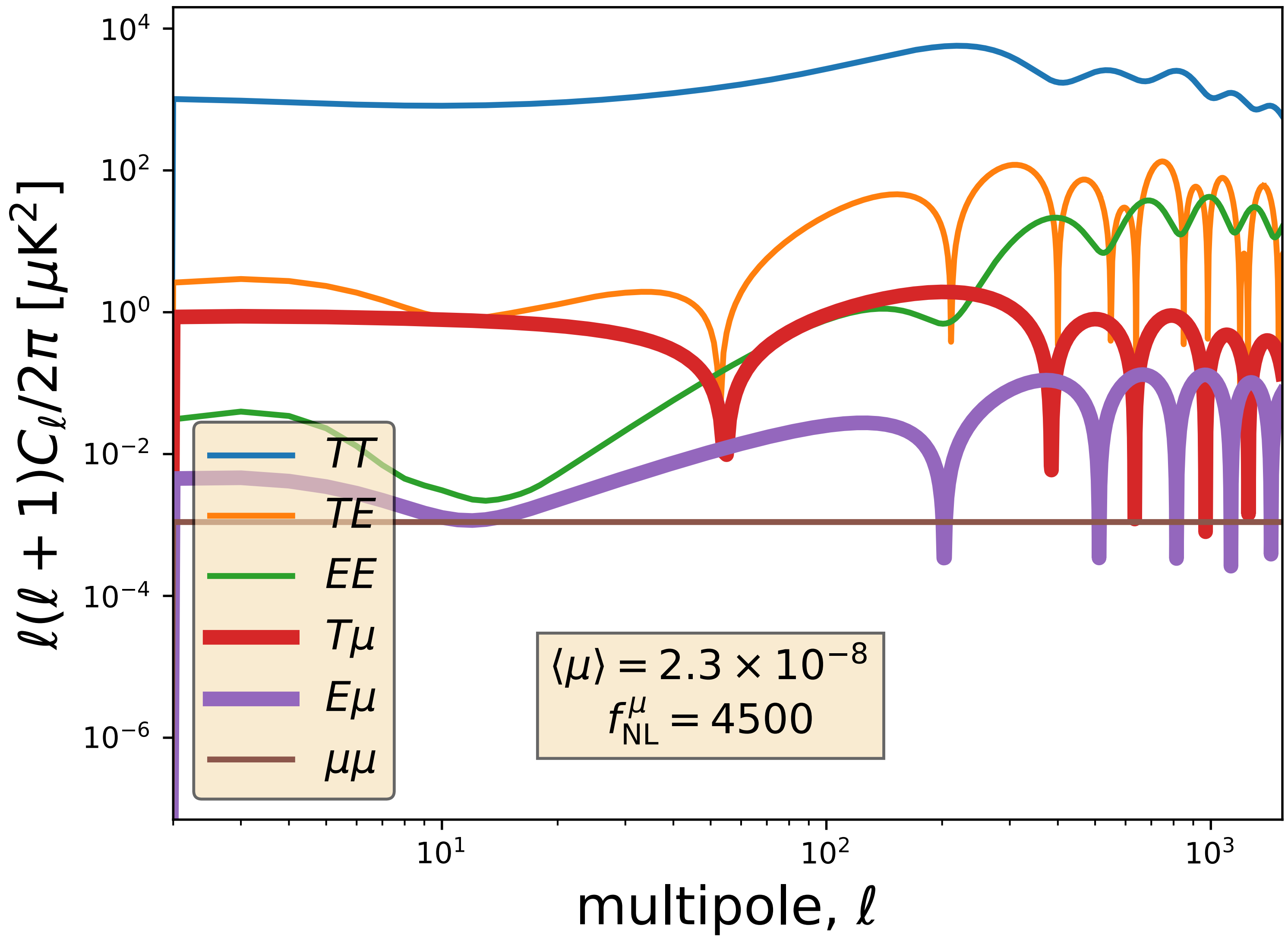

For $f_{\rm NL}^{\mu} \simeq 4500$ μT comparable to TE and EE

A science goal for future CMB imagers!

Degree of correlation: $\mu{\times}E$ vs $\mu{\times}T$

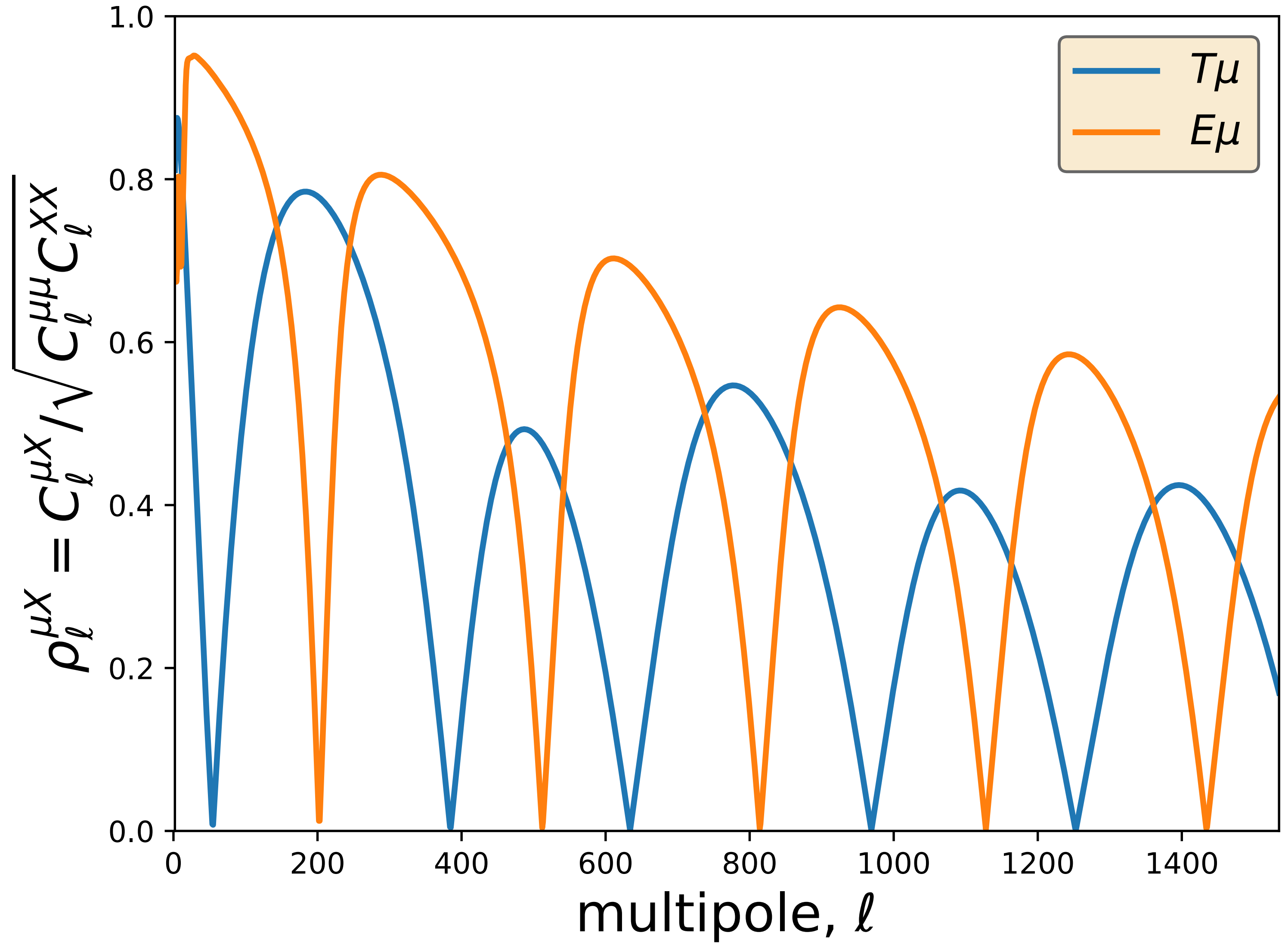

Remazeilles et al MNRAS 2022

$\boldsymbol{\mu E}$ correlation larger than $\boldsymbol{\mu T}$ correlation!

Questions

- Can we detect μT and μE correlated anisotropies with a future CMB satellite like *LiteBIRD*?
- What constraints on $f_{\mathrm{NL}}^{\mu}(k \simeq 740\,\mathrm{Mpc}^{-1})$ can be achieved with *LiteBIRD* in the presence of foregrounds?
- How much do we gain on f_{NL} sensitivity by including cross-correlations with CMB E-mode polarization?

Distinct spectral signatures of the distortions

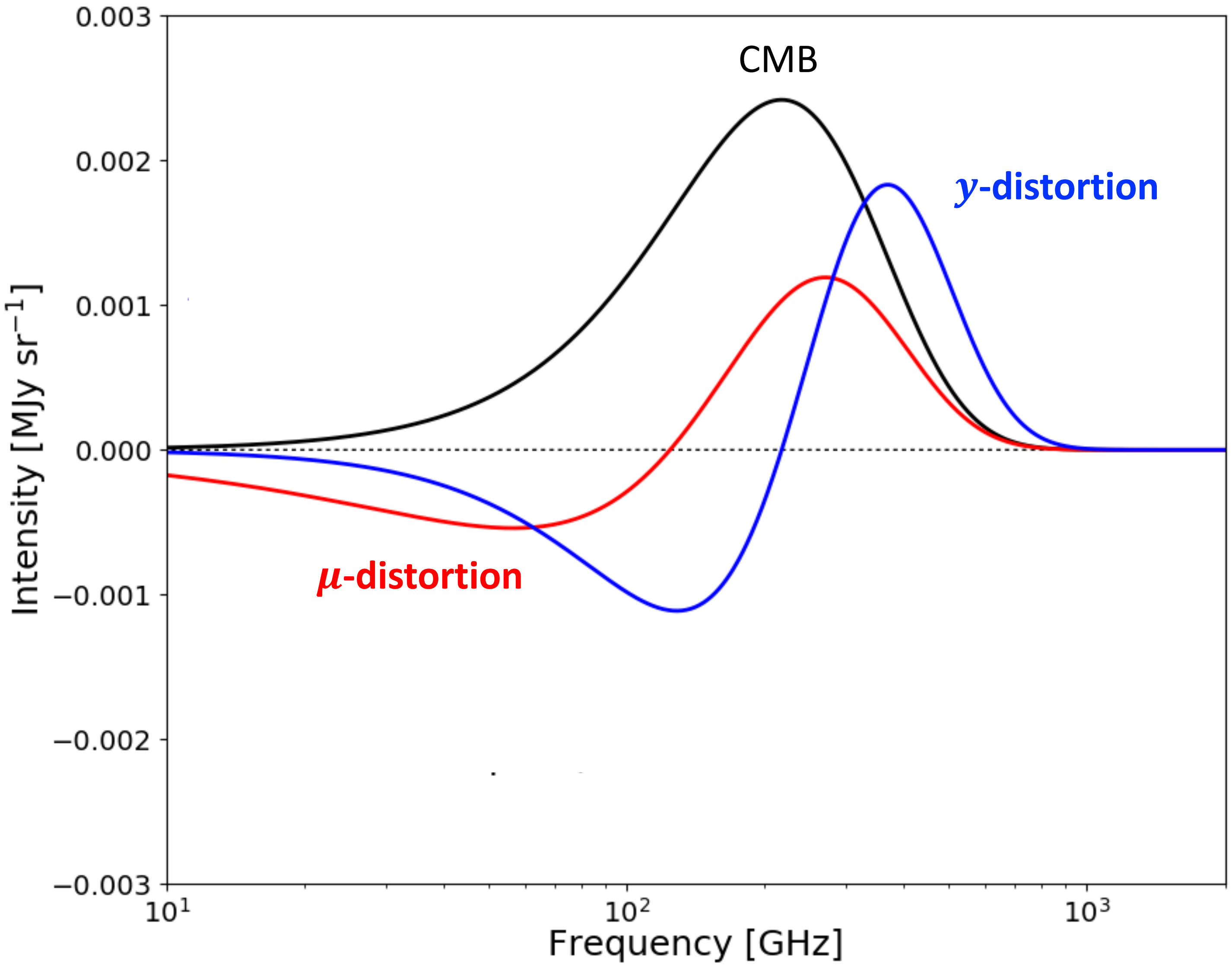

Multi-frequency observations should allow us to disentangle them

Spectral signatures in temperature units

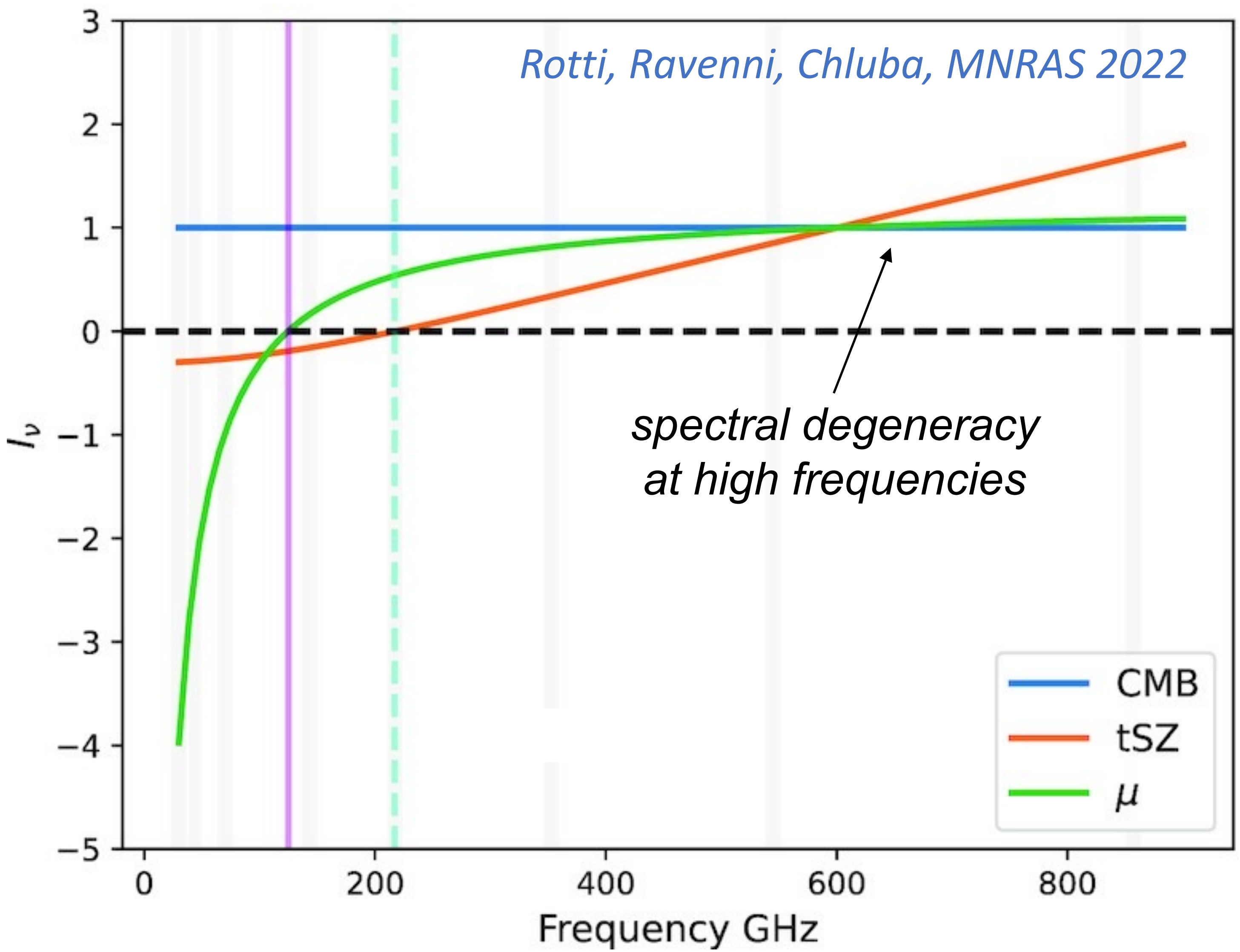

Spectral signatures in temperature units

Low frequencies are essential to disentangle CMB and μ-distortion anisotropies!

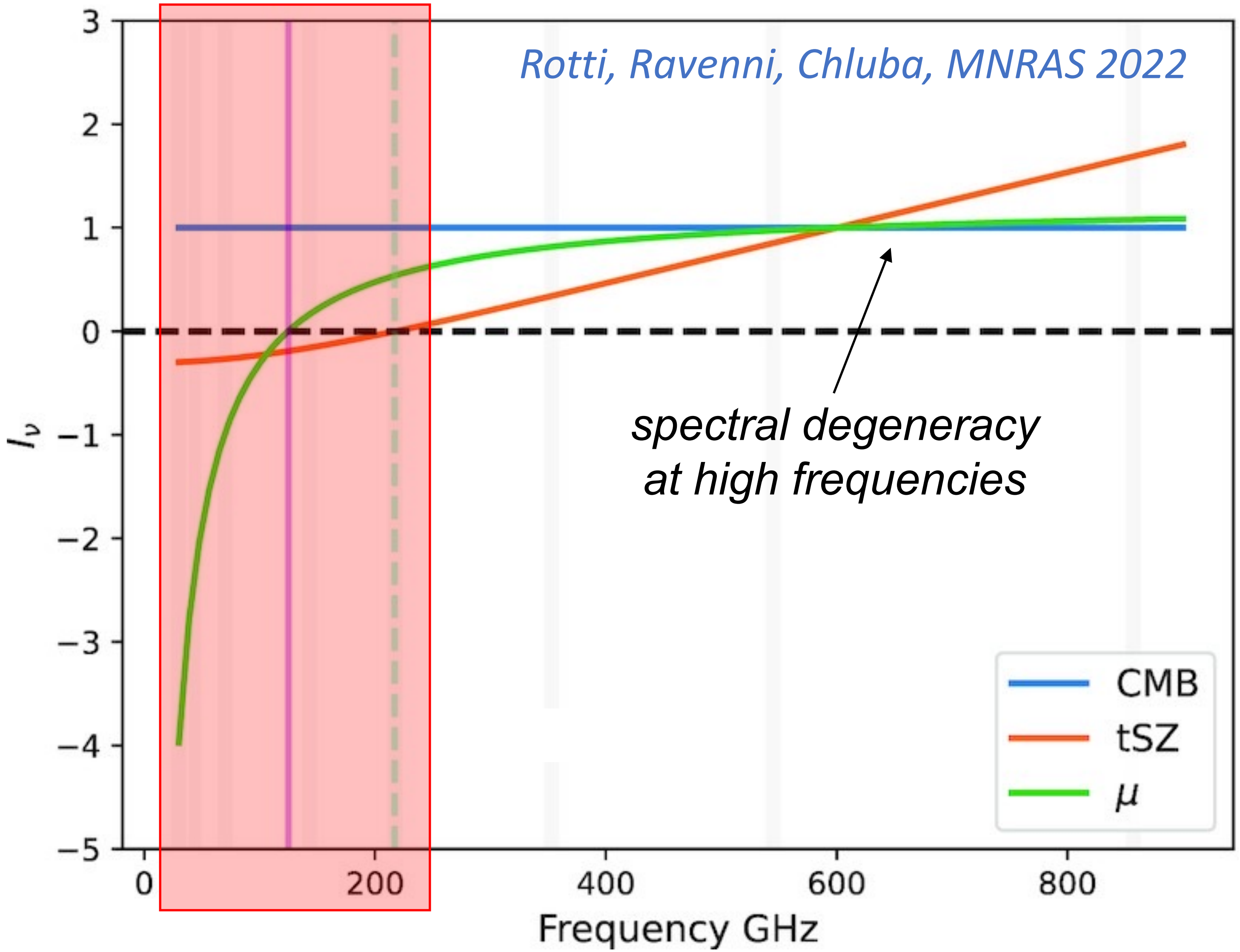

Spectral signatures in temperature units

Low frequencies are essential to disentangle CMB and μ-distortion anisotropies!

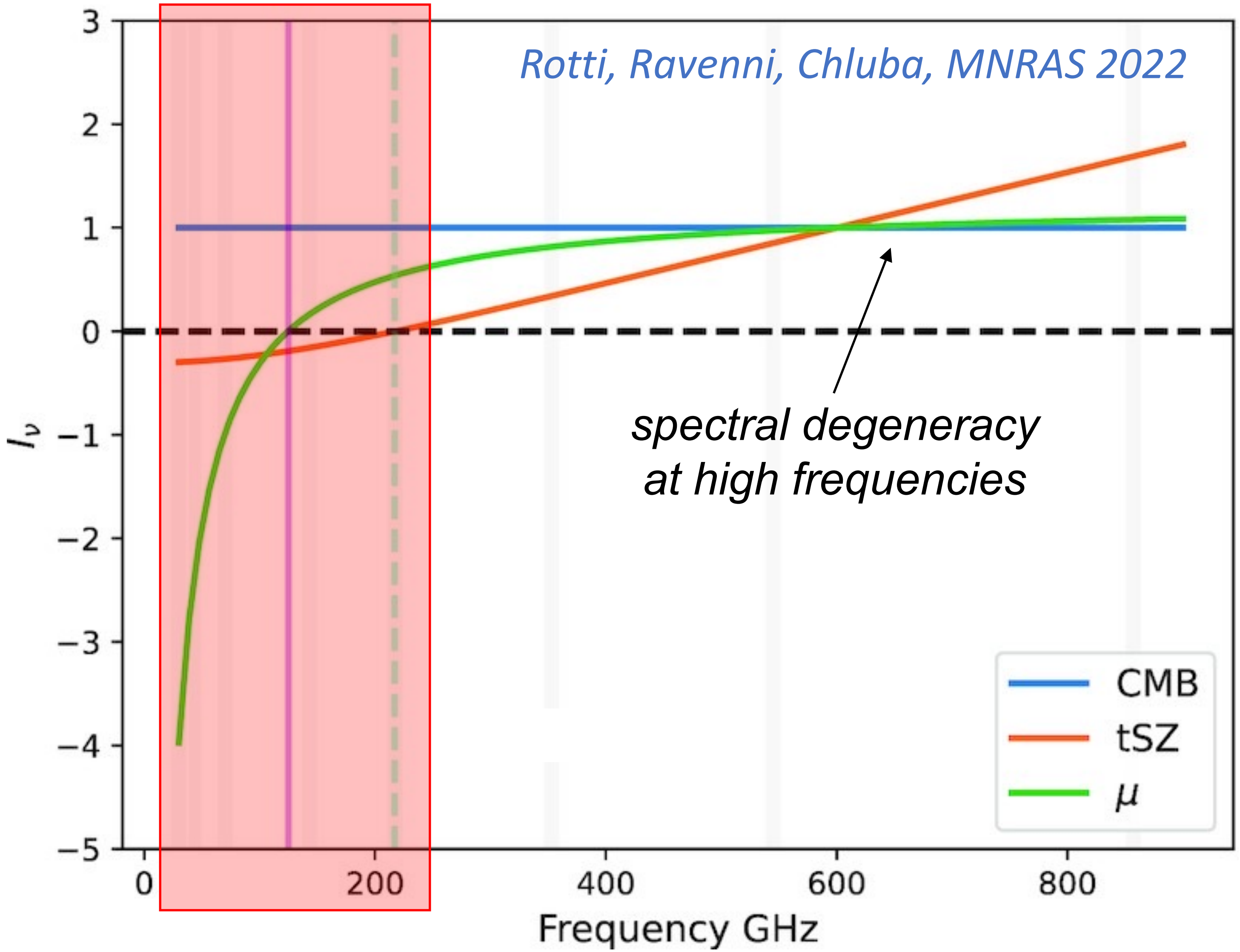

⟶ see talk by David Zegeye about using SKA

Foregrounds obscure SD anisotropies

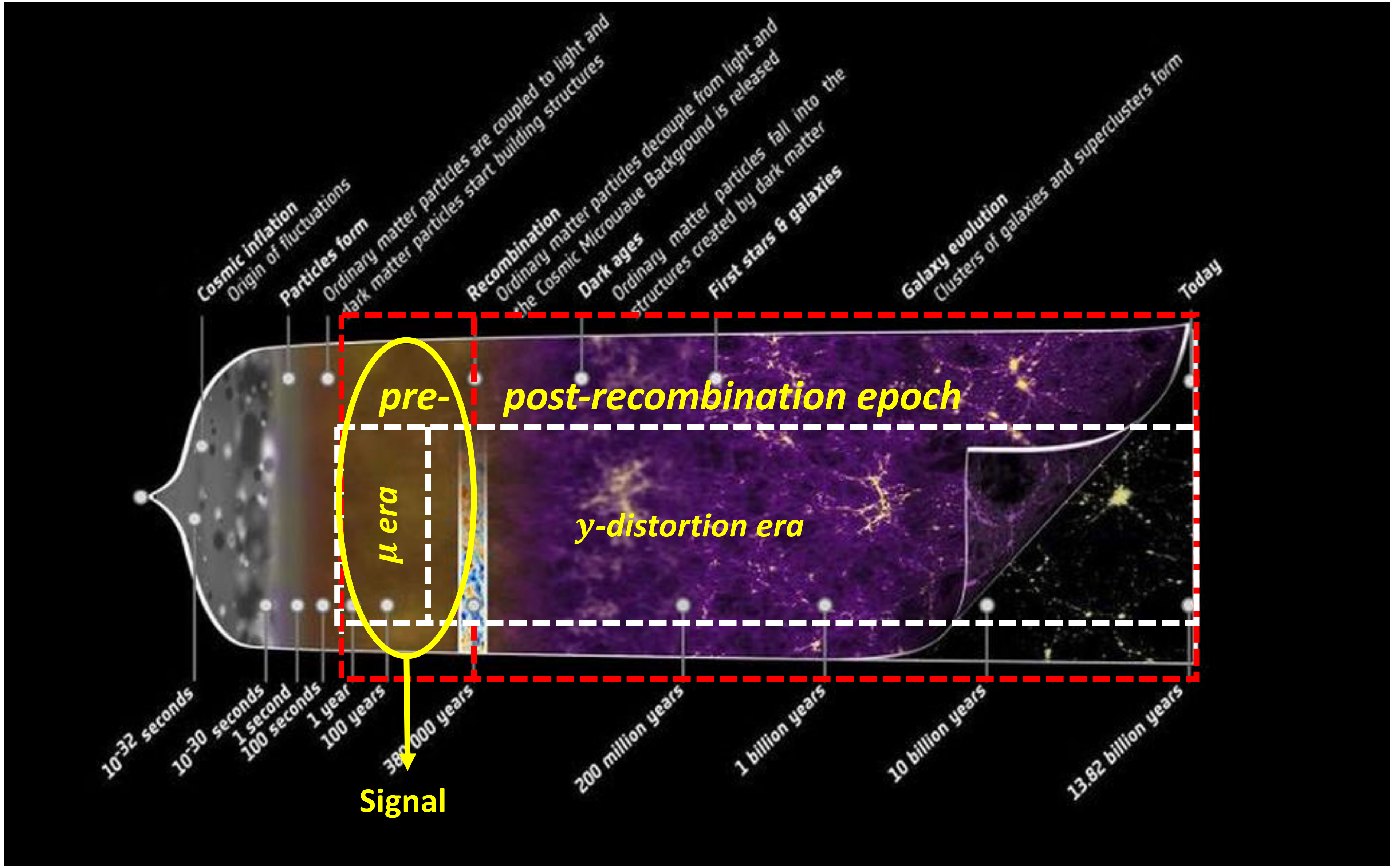

M. Remazeilles

Foregrounds obscure SD anisotropies

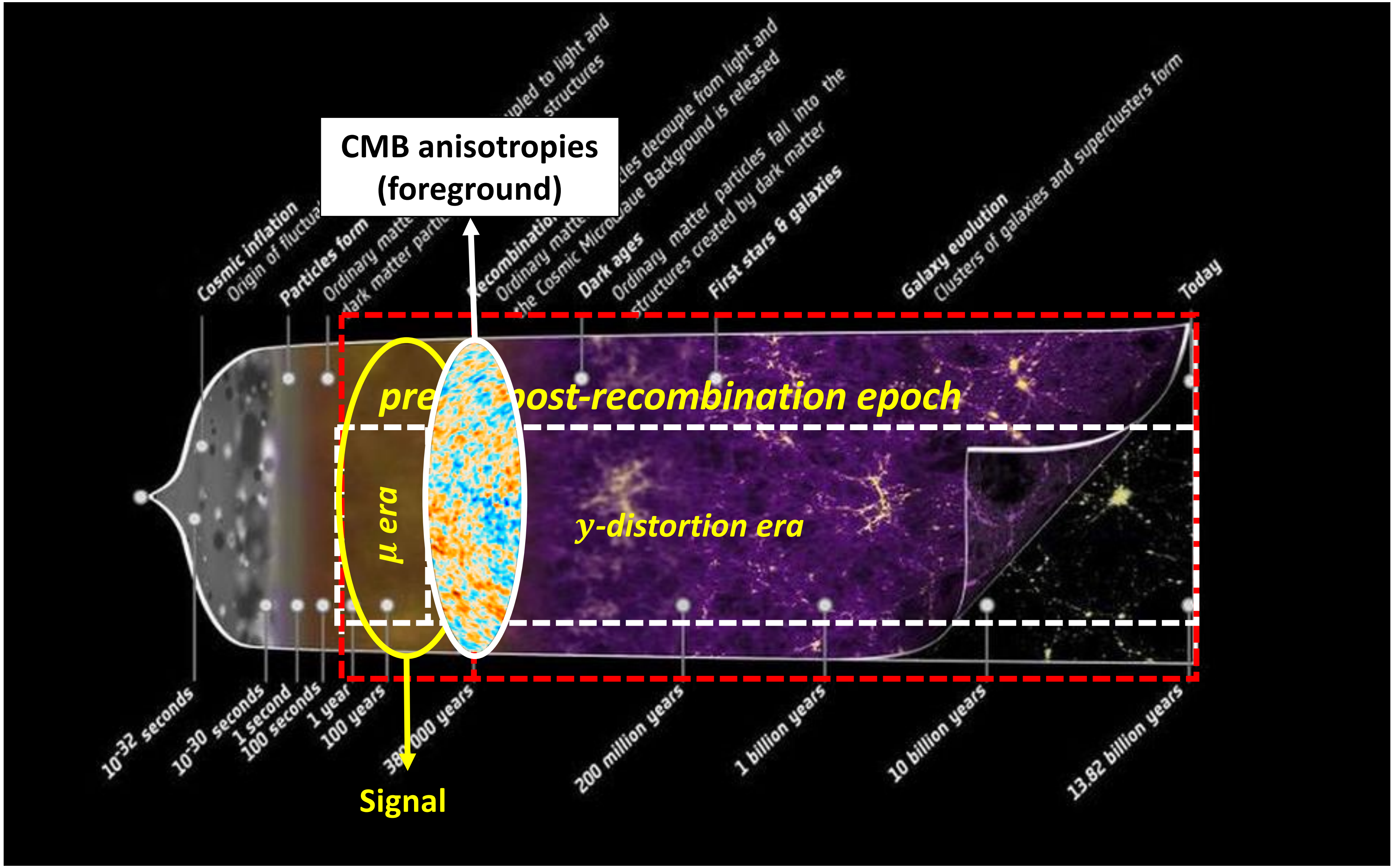

M. Remazeilles

Foregrounds obscure SD anisotropies

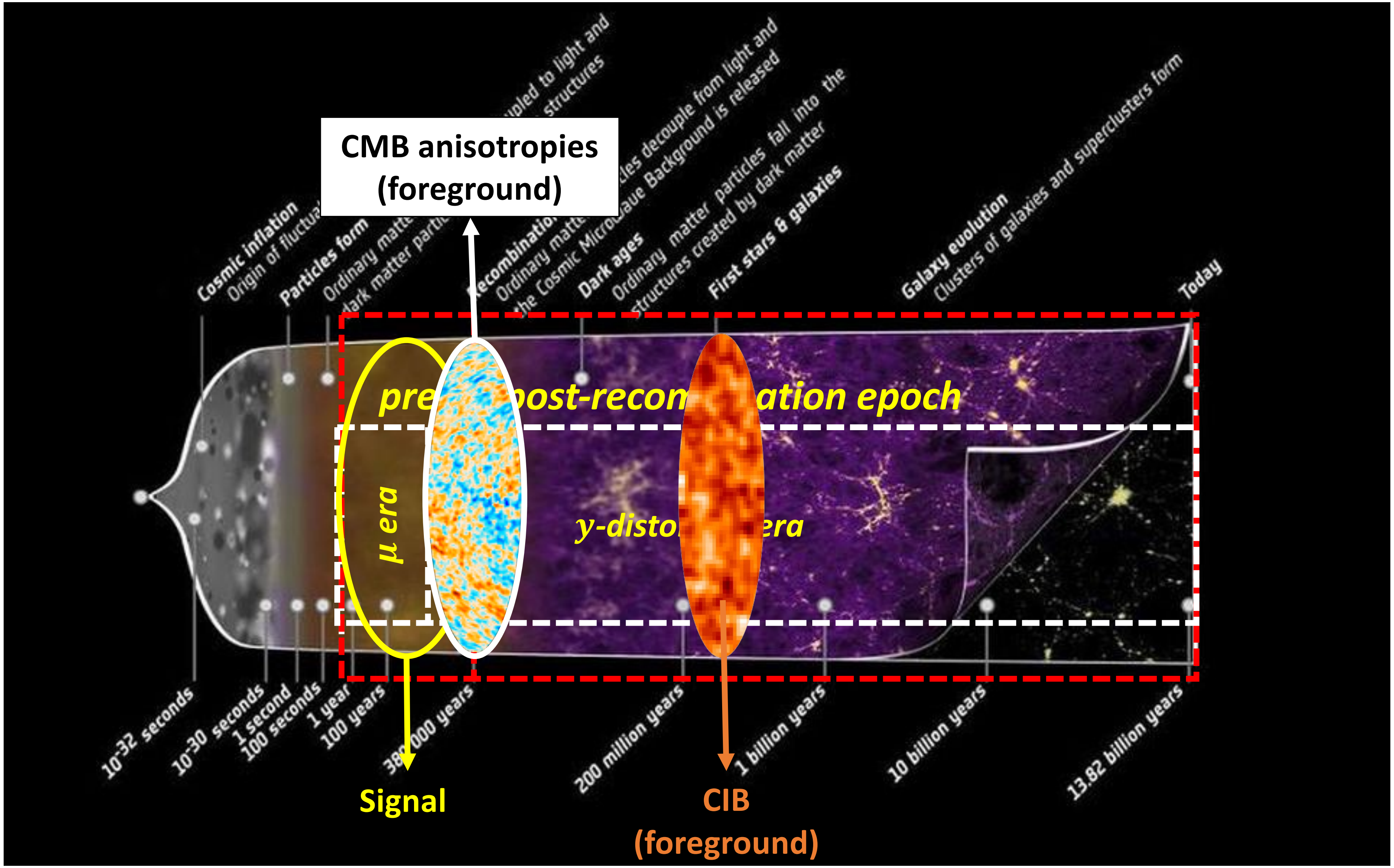

M. Remazeilles

Foregrounds obscure SD anisotropies

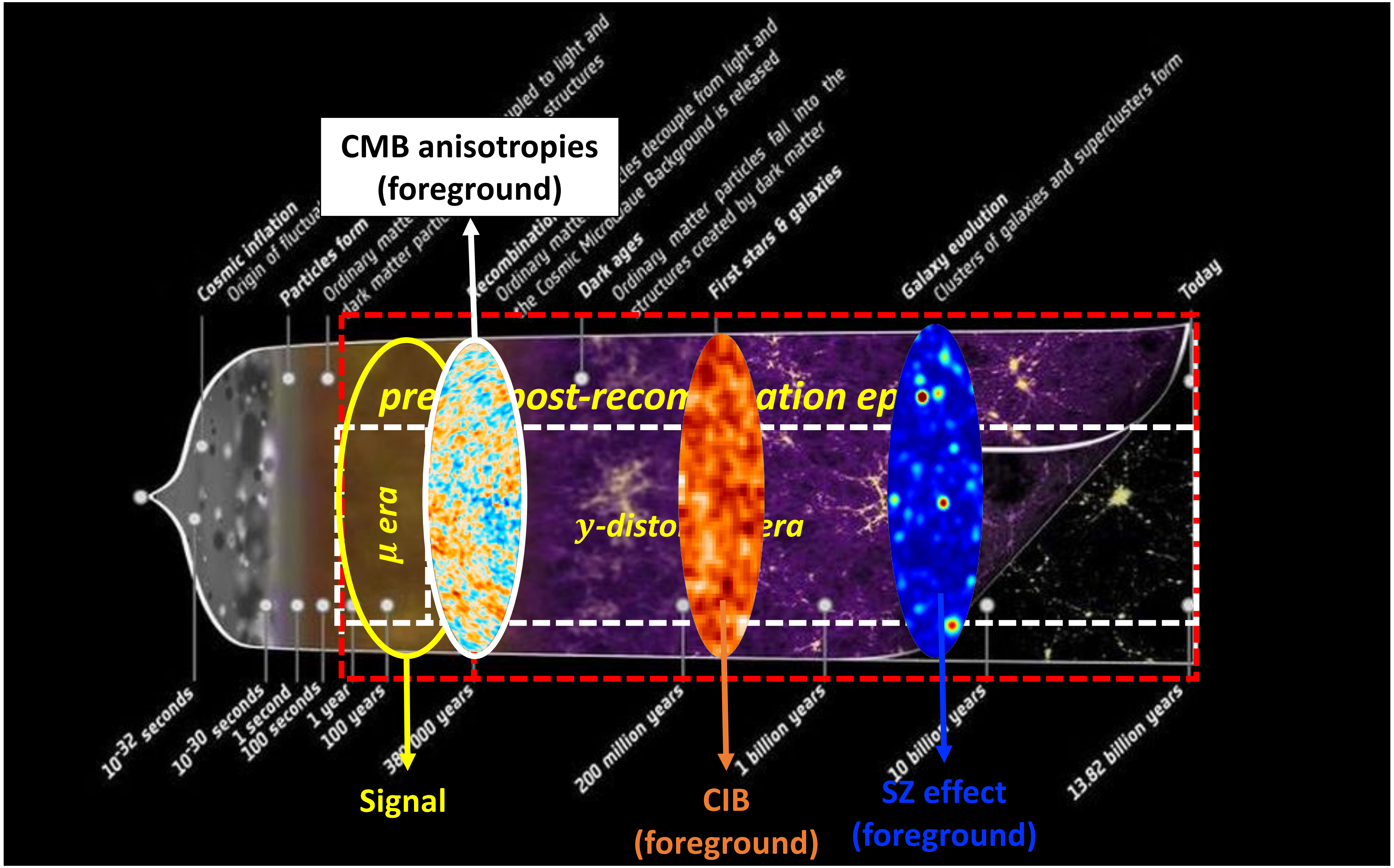

M. Remazeilles

Foregrounds obscure SD anisotropies

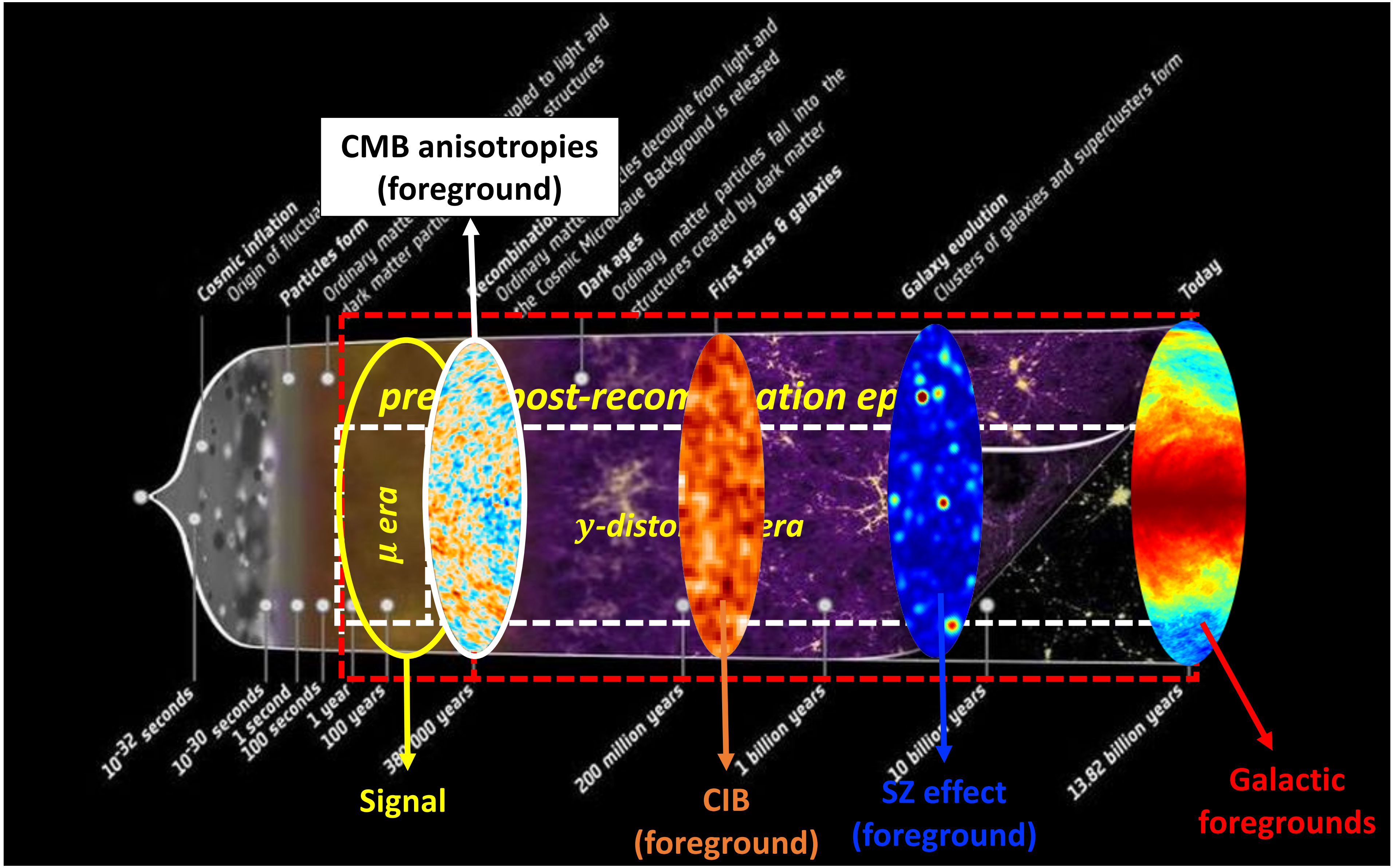

M. Remazeilles

Foregrounds obscure SD anisotropies

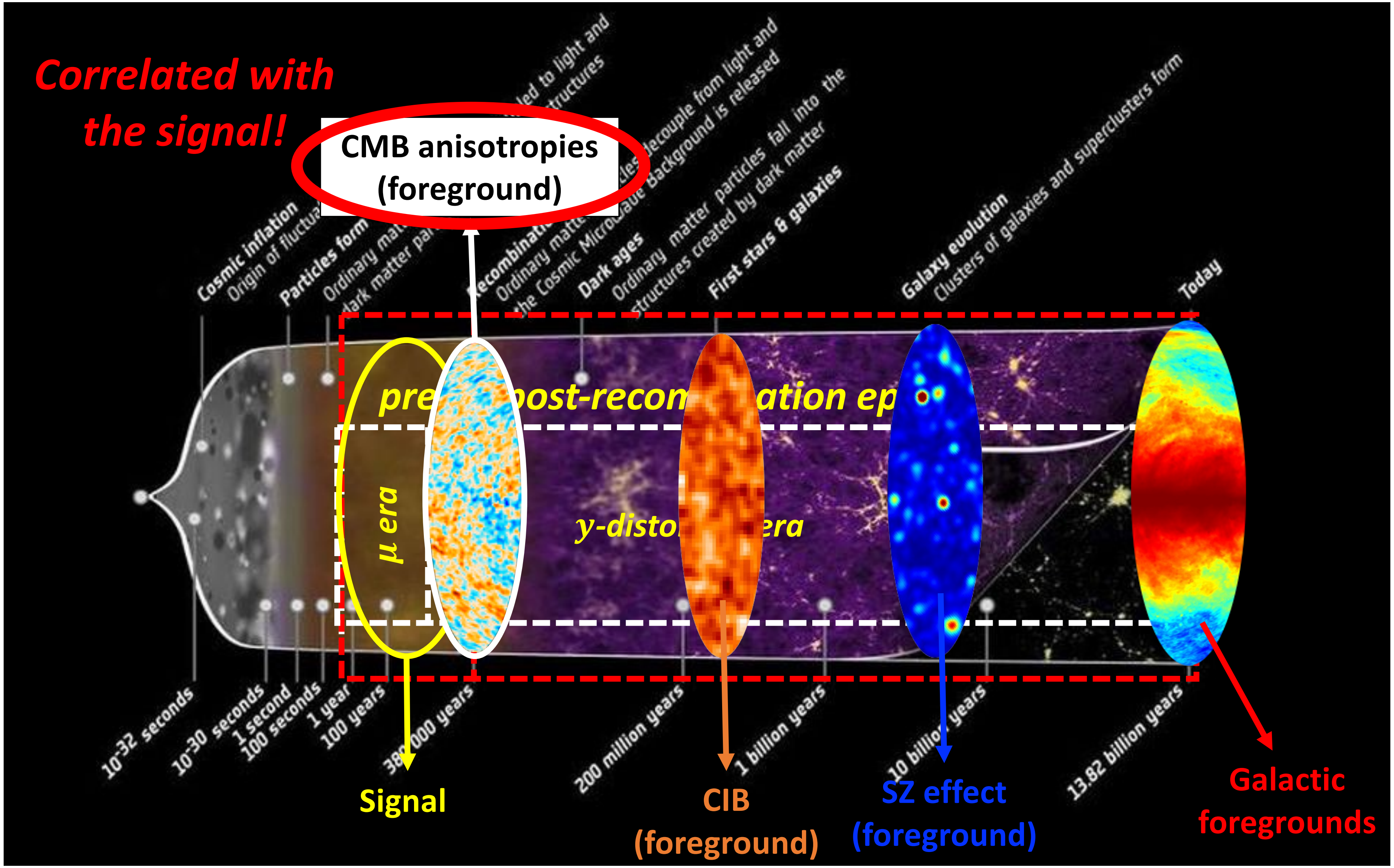

M. Remazeilles

Foregrounds vs Spectral Distortions (SD)

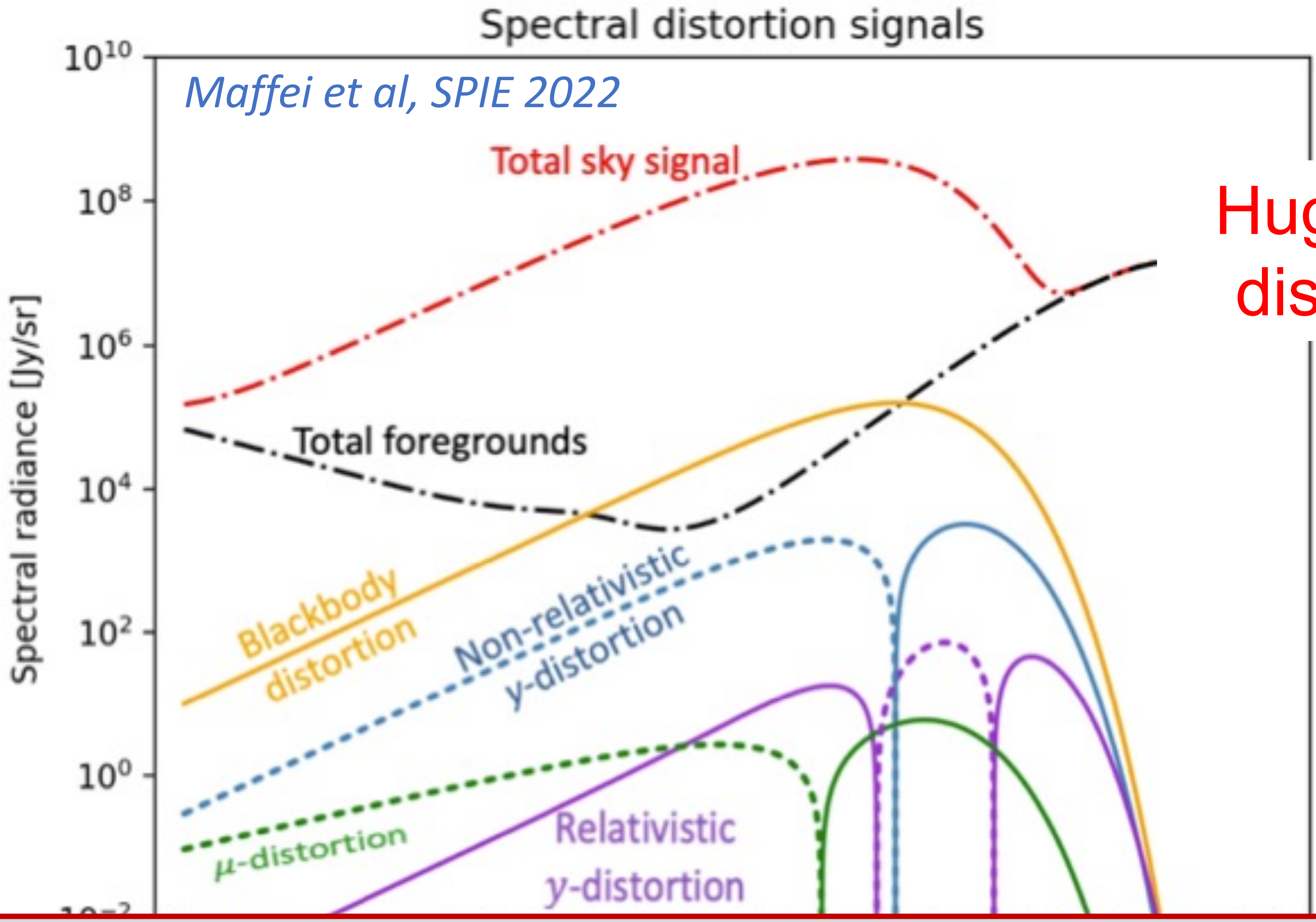

Huge amplitude discrepancies!

Tiny modelling errors on the foregrounds $\Longrightarrow$ Large error / bias on the SD signal!

The "smoothness" of foregrounds is a myth

Baseline SEDs (spectral signatures)

power-law?

ν^{β}

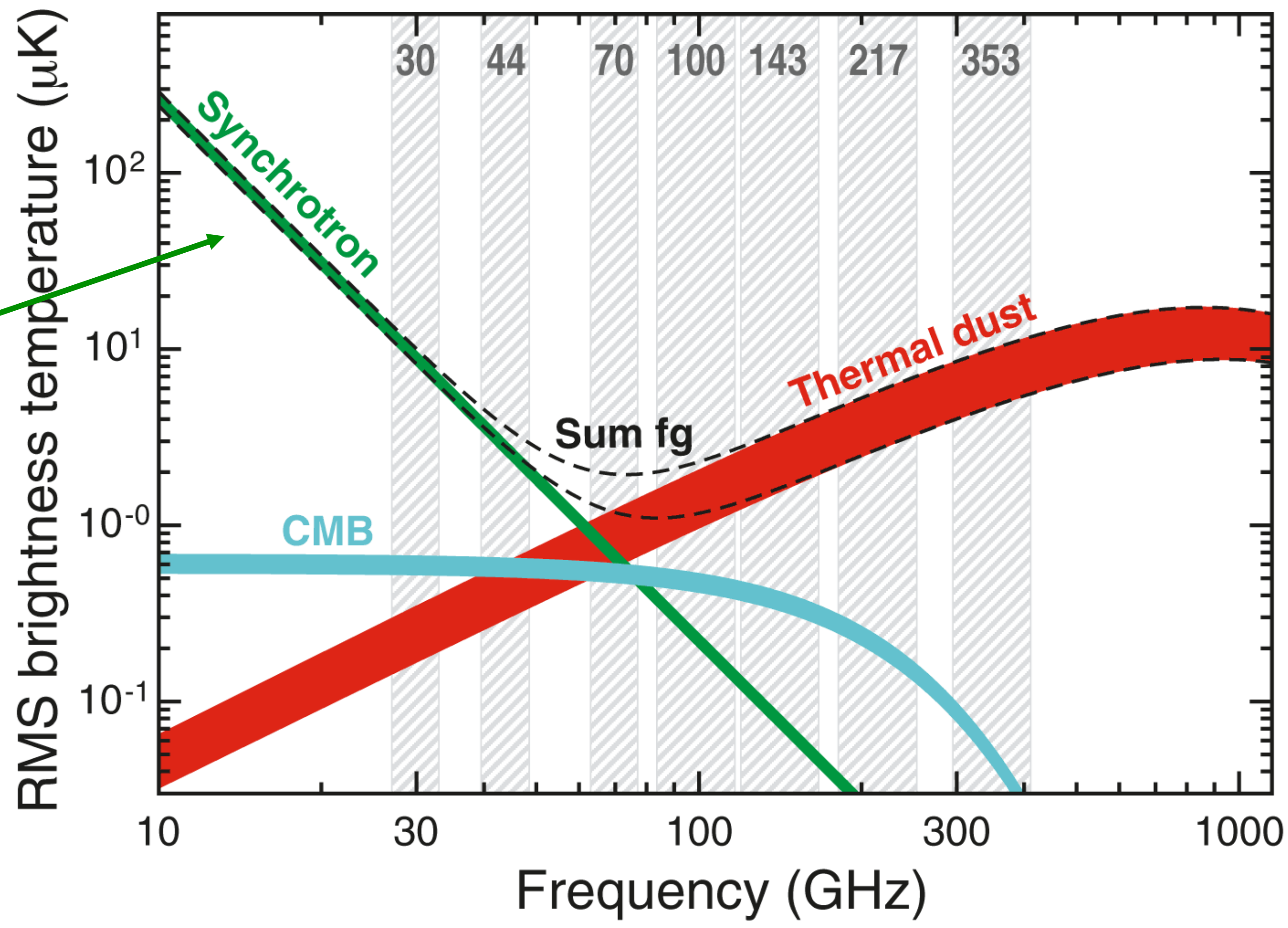

modified blackbody?

$\nu^{\beta} B_{\nu}(T)$

The "smoothness" of foregrounds is a myth

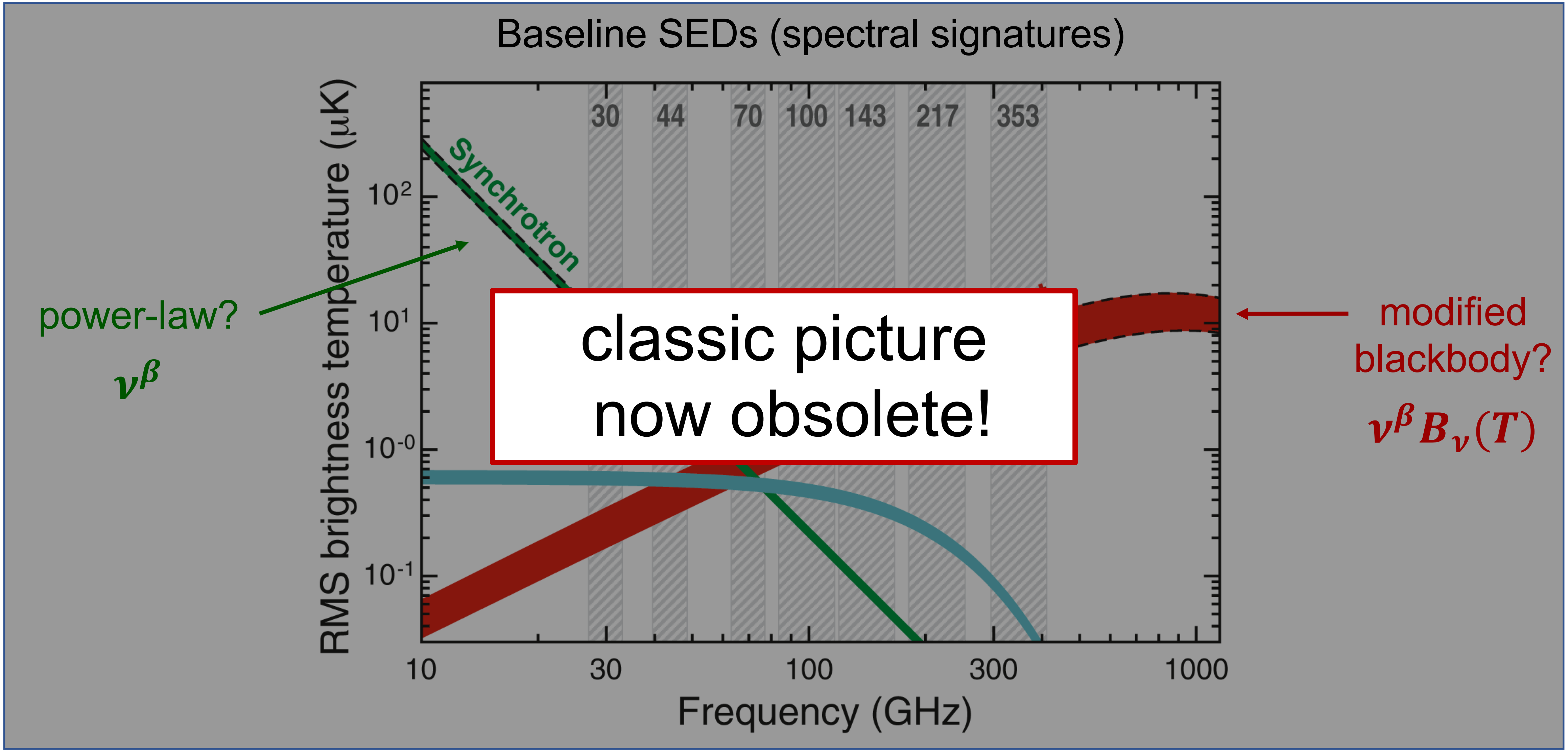

Spectral distortions of the foregrounds!

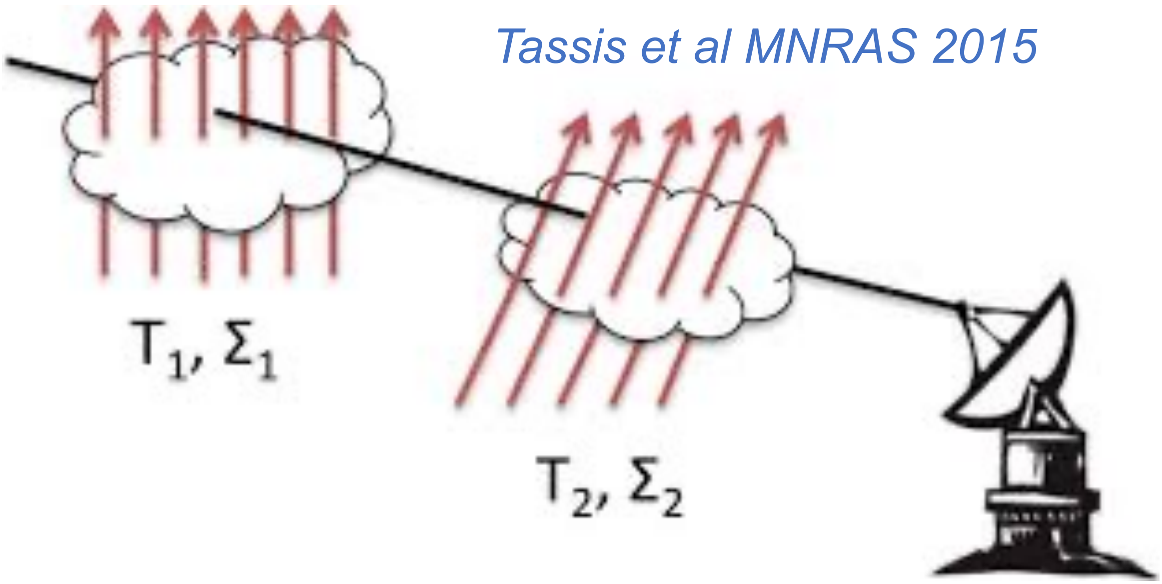

Tassis et al MNRAS 2015

Spectral variations averaged along the line of sight

$$\left\langle \nu^{\beta_1} B_\nu(T_1) + \nu^{\beta_2} B_\nu(T_2) + \cdots \right\rangle \neq \nu^{\langle\beta\rangle} B_\nu(\langle T \rangle)$$

Spectral distortions to the modified blackbody

Chluba, Hill, Abitbol, MNRAS 2017

Spectral distortions of the foregrounds!

Remazeilles, Rotti, Chluba, MNRAS 2021

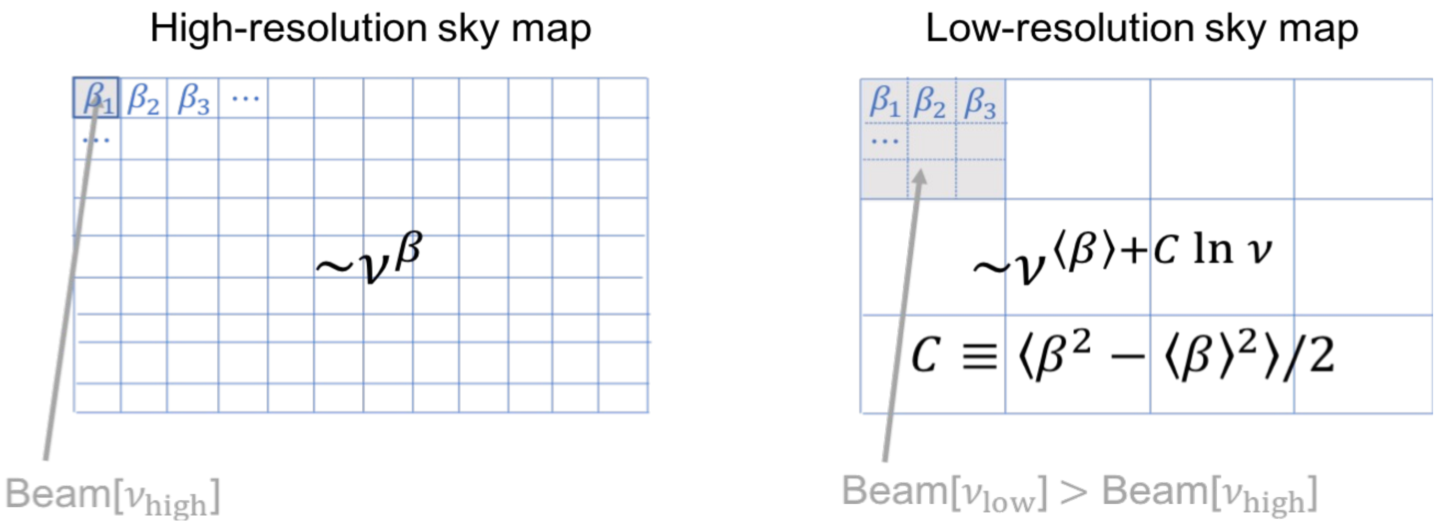

Spectral variations averaged within the beam

$$\left\langle \nu^{\beta_1} + \nu^{\beta_2} + \cdots \right\rangle = \nu^{\langle\beta\rangle + \frac{1}{2}\sigma_\beta^2 \ln \nu + \ldots}$$

Spectral distortions to the power-law (curvature terms)

Chluba, Hill, Abitbol, MNRAS 2017

Spectral distortions of the foregrounds

Foreground SED distortions

Averaging along the line of sight

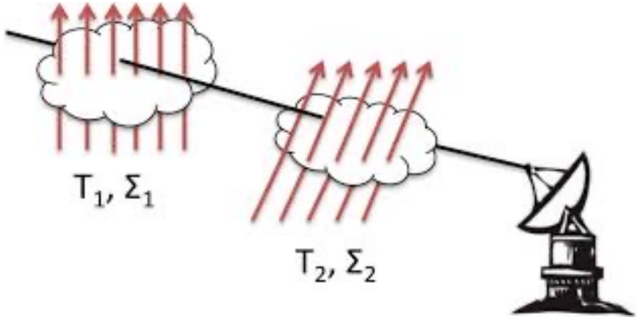

$$\left\langle \nu^{\beta_1} B_\nu(T_1) + \nu^{\beta_2} B_\nu(T_2) + \cdots \right\rangle \neq \nu^{\langle\beta\rangle} B_\nu(\langle T\rangle)$$

Averaging within the beam

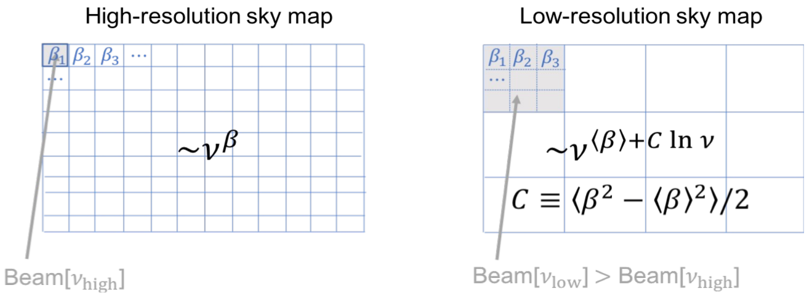

- Spectral distortions of the baseline foreground SEDs
- Complicates foreground modelling for parametric fitting
- Could mimic CMB spectral distortion signals

Chluba, Hill, Abitbol, MNRAS (2017)
Remazeilles, Rotti, Chluba, MNRAS (2021)

Spectral distortions of the foregrounds

Foreground SED distortions

Averaging along the line of sight

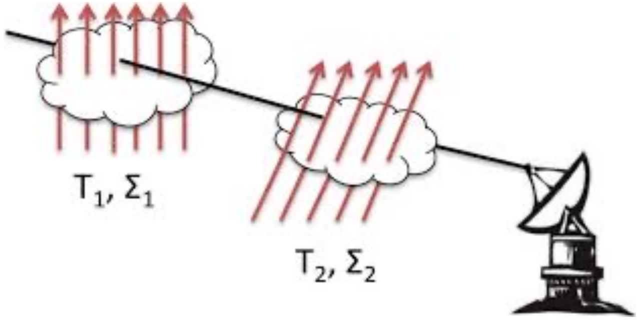

$$\left\langle \nu^{\beta_1} B_\nu(T_1) + \nu^{\beta_2} B_\nu(T_2) + \cdots \right\rangle \neq \nu^{\langle\beta\rangle} B_\nu(\langle T \rangle)$$

Averaging within the beam

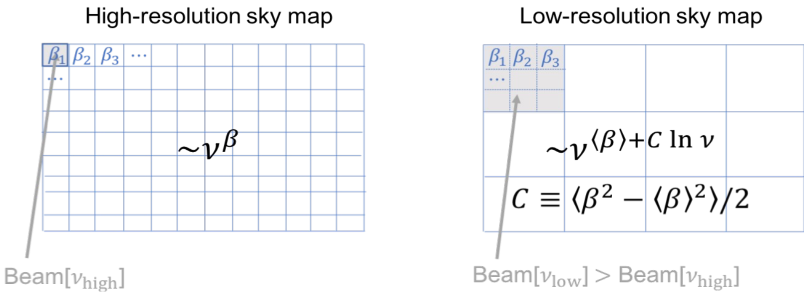

- Spectral distortions of the baseline foreground SEDs
- Complicates foreground modelling for parametric fitting
- Could mimic CMB spectral distortion signals

Tiny distortions to foregrounds $\gg$ μ-distortion !

Chluba, Hill, Abitbol, MNRAS (2017)
Remazeilles, Rotti, Chluba, MNRAS (2021)

Analysis

Theory

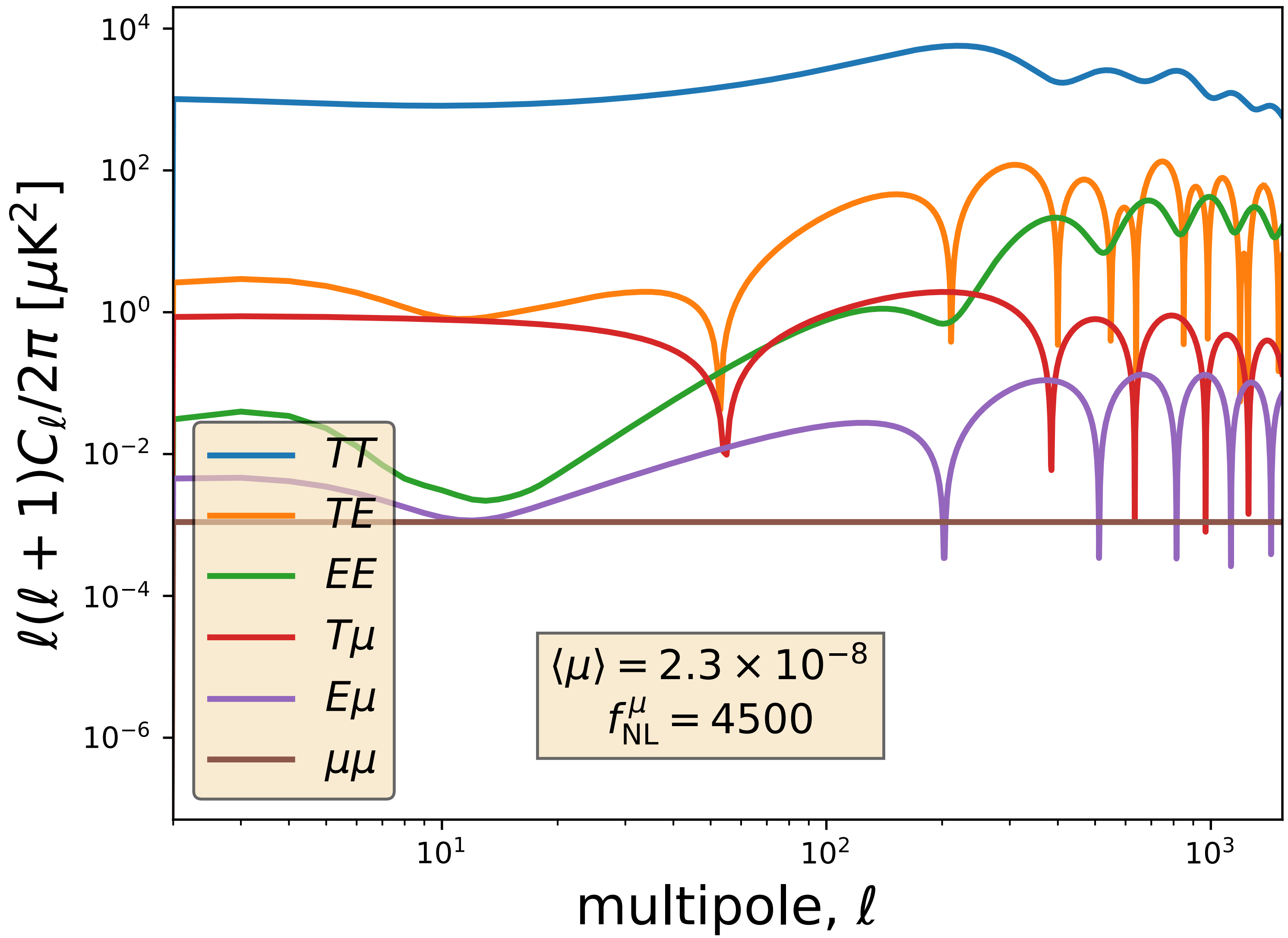

Ravenni et al JCAP 2017

Correlated map simulations using Cholesky

μ-distortion anisotropies ($f_{\rm NL}^{\mu} = 4500$)

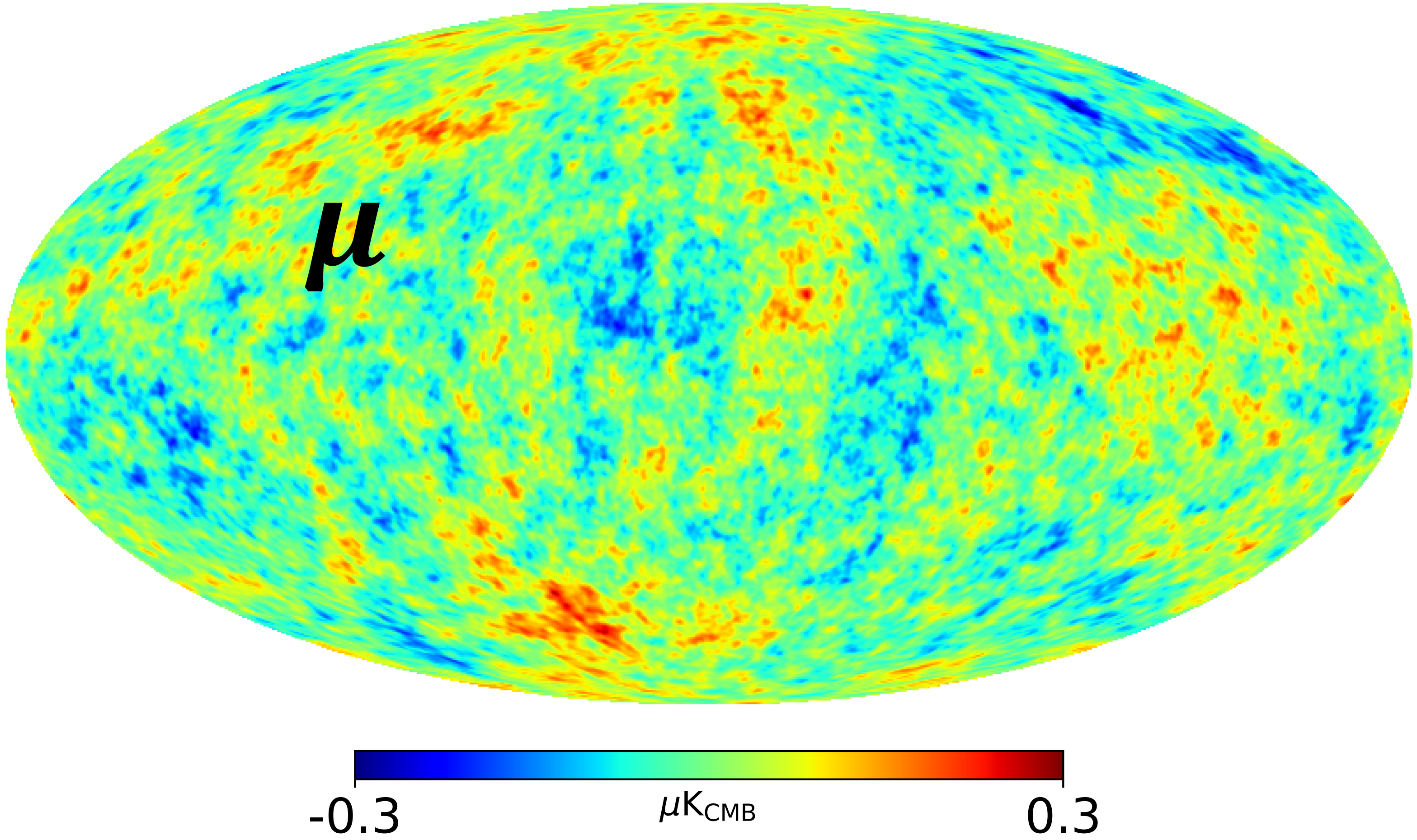

60′ resolution

Remazeilles, Ravenni, Chluba MNRAS 2022

Correlated map simulations using Cholesky

CMB temperature anisotropies

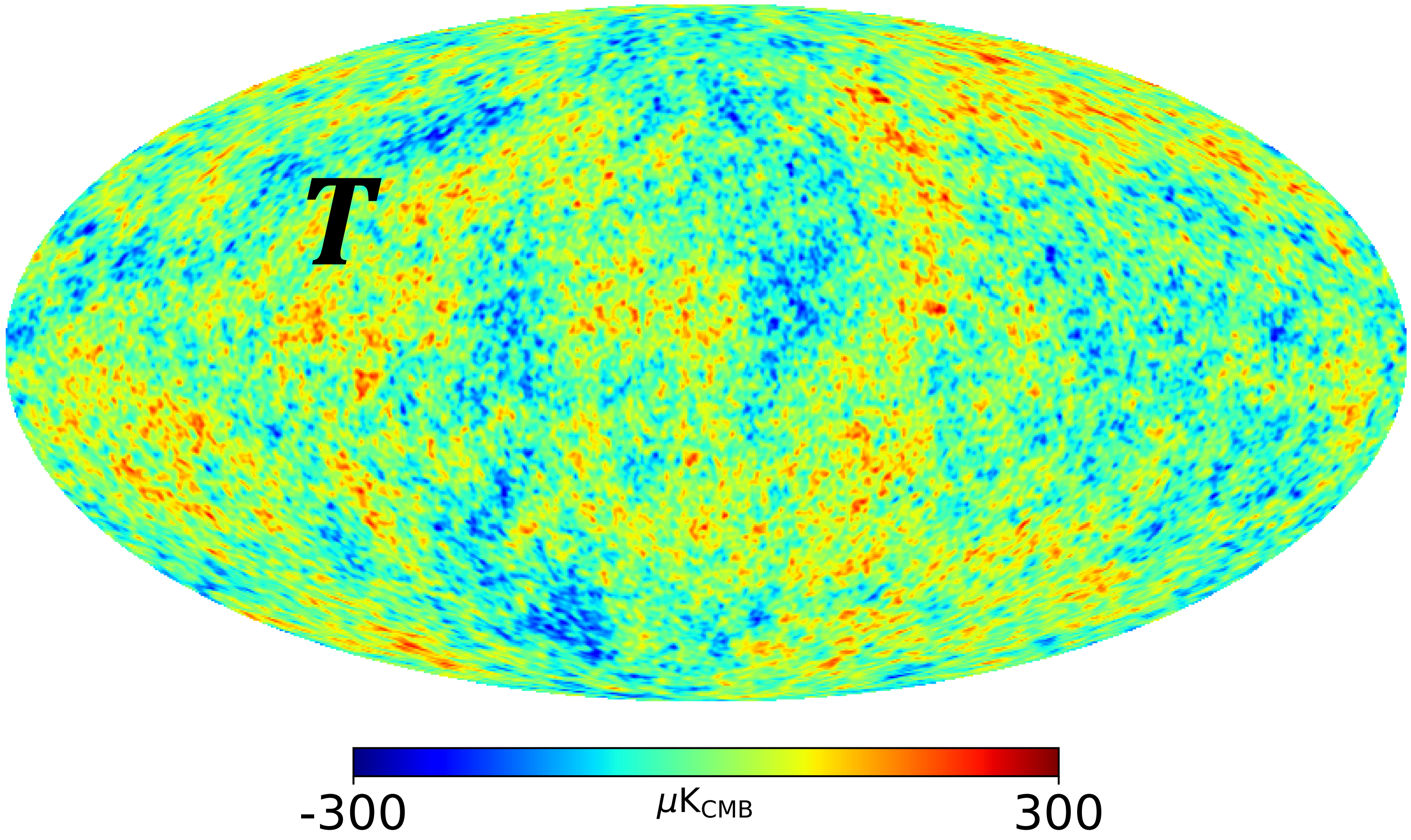

60′ resolution

Remazeilles, Ravenni, Chluba MNRAS 2022

Correlated map simulations using Cholesky

CMB E-mode polarization anisotropies

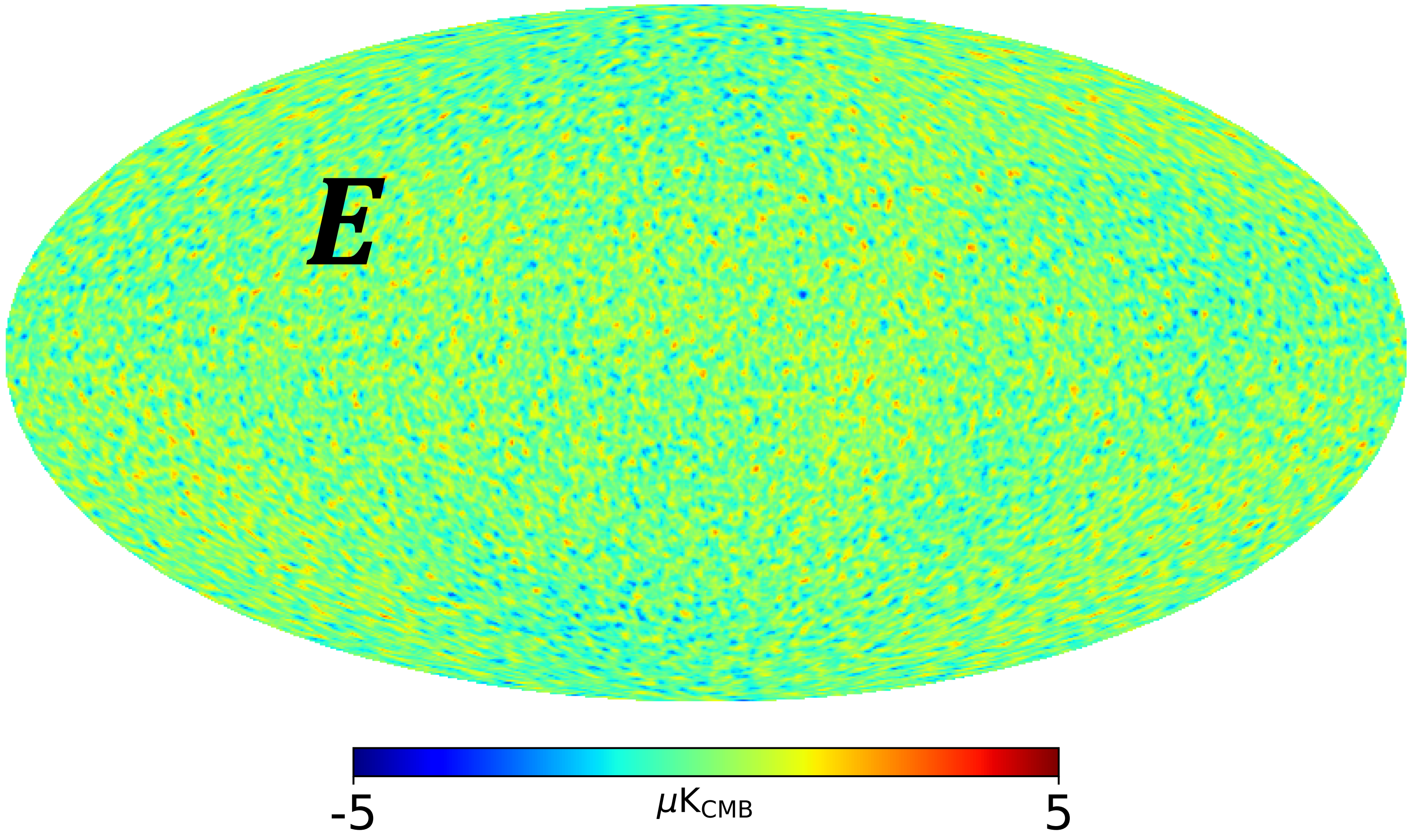

$60'$ resolution

Remazeilles, Ravenni, Chluba MNRAS 2022

Correlated map simulations using Cholesky

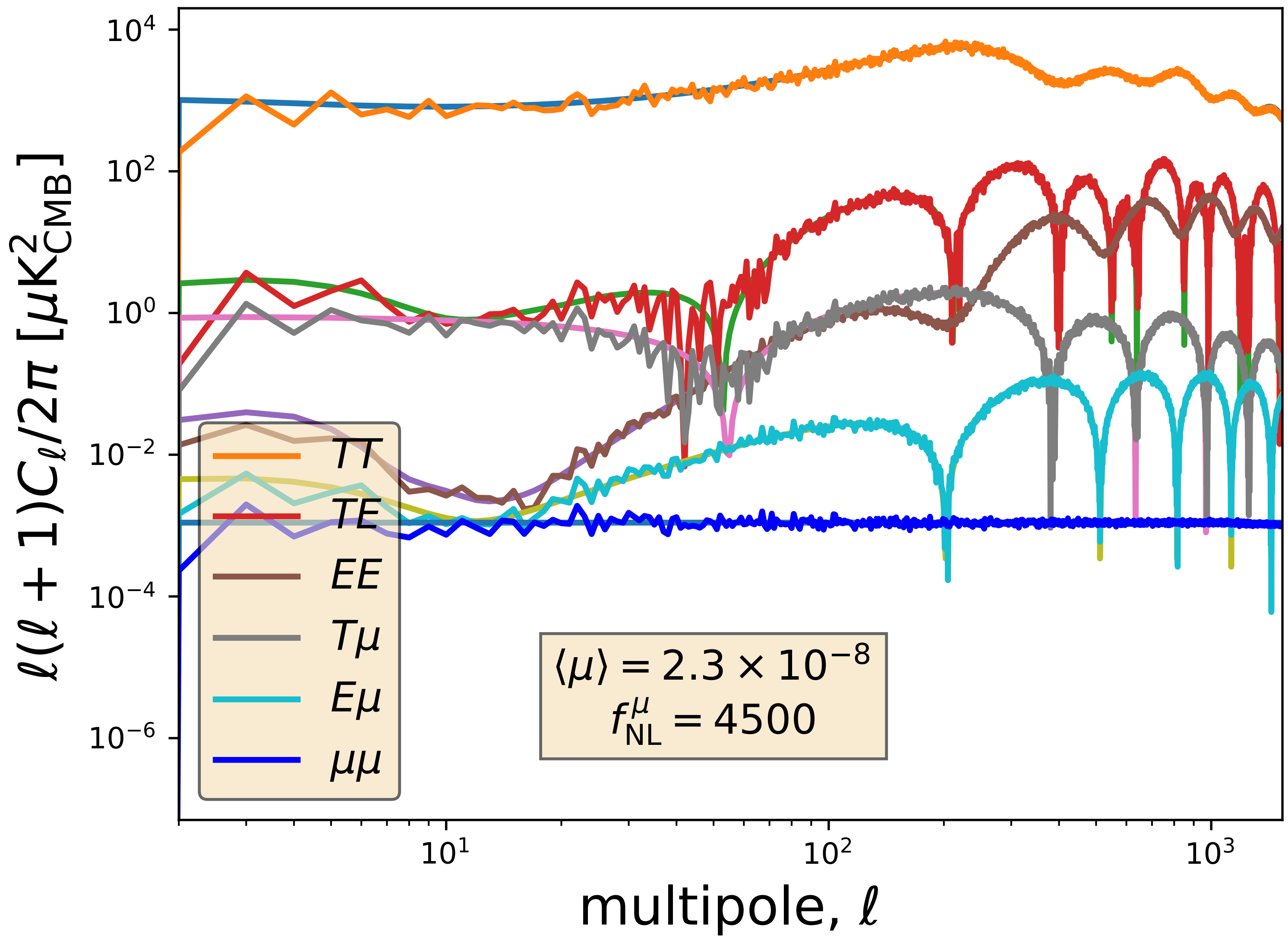

Remazeilles, Ravenni, Chluba MNRAS 2022

Foregrounds simulation (temperature)

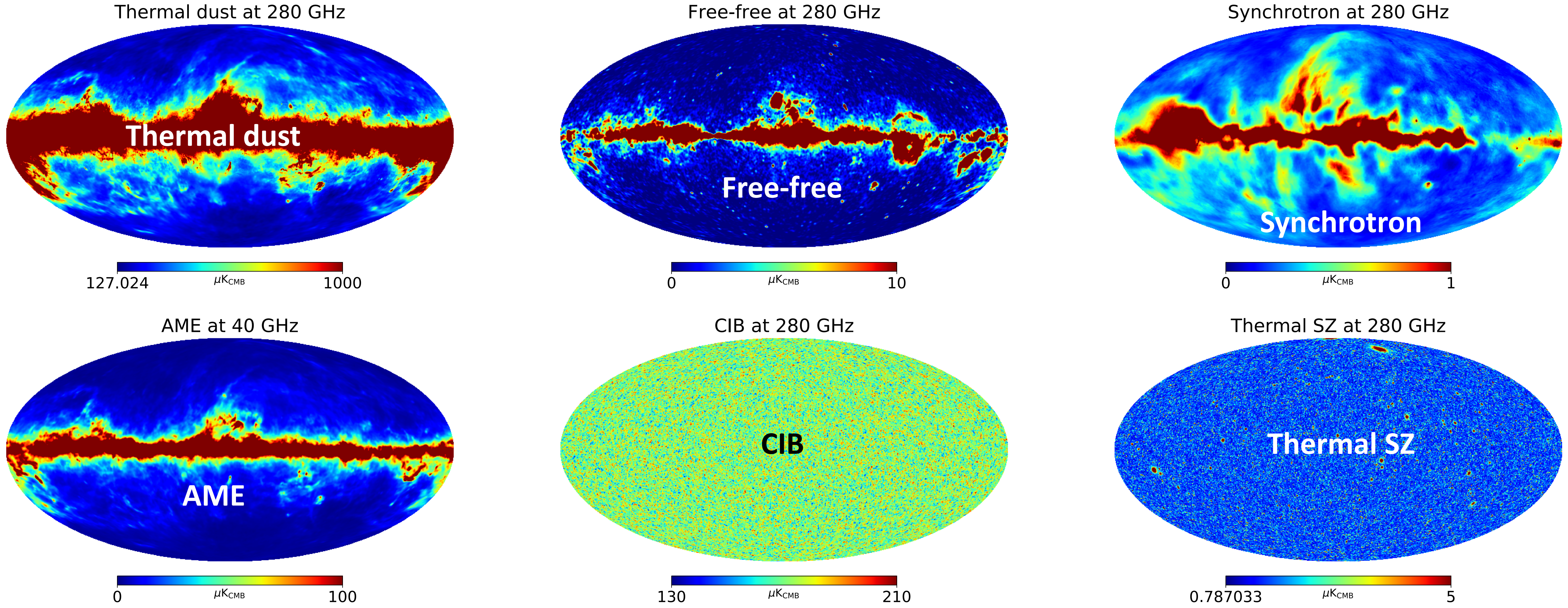

Remazeilles, Ravenni, Chluba, MNRAS 2022

Foregrounds simulation (polarization)

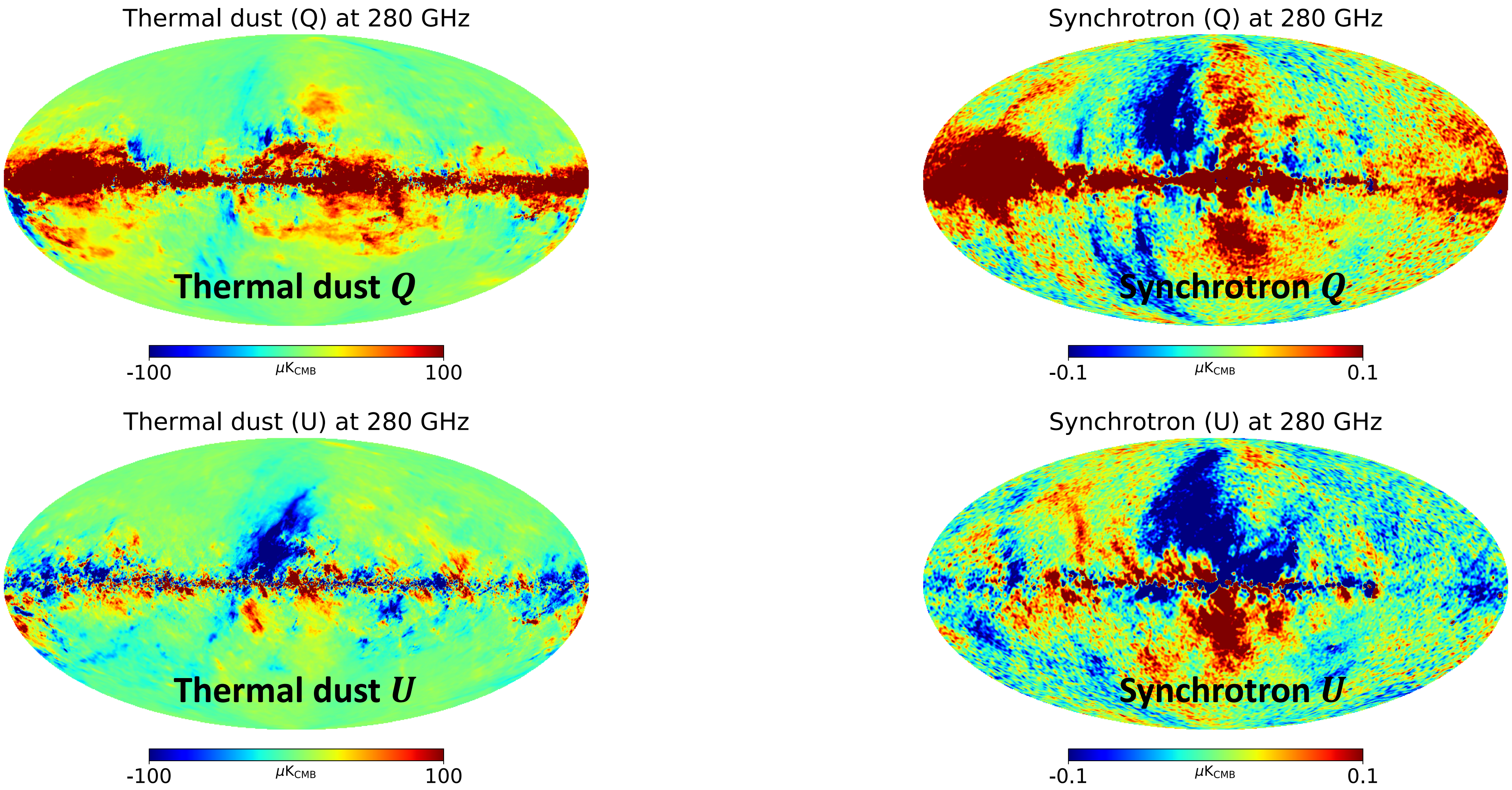

Remazeilles, Ravenni, Chluba, MNRAS 2022

Component separation: standard ILC ?

$$\boldsymbol{d}(\boldsymbol{\nu},\vec{\boldsymbol{n}}) = \boldsymbol{a}(\boldsymbol{\nu})\boldsymbol{\mu}(\vec{\boldsymbol{n}}) + \boldsymbol{b}(\boldsymbol{\nu})\boldsymbol{T}(\vec{\boldsymbol{n}}) + \text{foregrounds}(\nu,\vec{n}) + \text{noise}(\nu,\vec{n})$$

data

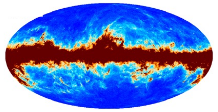

μ-distortion anisotropies

CMB temperature anisotropies

The standard ILC method forms an estimate of the μ-map as

$$\hat{\boldsymbol{\mu}}\,(\vec{\boldsymbol{n}}) = \sum_{\boldsymbol{\nu}} \boldsymbol{w}(\boldsymbol{\nu})\,\boldsymbol{d}(\boldsymbol{\nu},\vec{\boldsymbol{n}}) \quad \text{such that} \quad \begin{cases} \langle \hat{\boldsymbol{\mu}}\,(\vec{\boldsymbol{n}})^2 \rangle \text{ of minimum variance} \\ \sum_{\boldsymbol{\nu}} \boldsymbol{w}(\boldsymbol{\nu})\,\boldsymbol{a}(\boldsymbol{\nu}) = \mathbf{1} \end{cases}$$

Remazeilles & Chluba, MNRAS 2018

Component separation: standard ILC ?

$$\boldsymbol{d}(\boldsymbol{\nu},\vec{\boldsymbol{n}}) = \boldsymbol{a}(\boldsymbol{\nu})\boldsymbol{\mu}(\vec{\boldsymbol{n}}) + \boldsymbol{b}(\boldsymbol{\nu})\boldsymbol{T}(\vec{\boldsymbol{n}}) + \text{foregrounds}(\nu,\vec{n}) + \text{noise}(\nu,\vec{n})$$

data

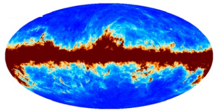

μ-distortion anisotropies

CMB temperature anisotropies

The standard ILC method forms an estimate of the μ-map as

$$\widehat{\boldsymbol{\mu}}\,(\vec{\boldsymbol{n}}) = \sum_{\boldsymbol{\nu}} \boldsymbol{w}(\boldsymbol{\nu})\,\boldsymbol{d}(\boldsymbol{\nu},\vec{\boldsymbol{n}}) \quad \text{such that} \quad \begin{cases} \langle \widehat{\boldsymbol{\mu}}\,(\vec{\boldsymbol{n}})^2 \rangle \text{ of minimum variance} \\ \sum_{\boldsymbol{\nu}} \boldsymbol{w}(\boldsymbol{\nu})\,\boldsymbol{a}(\boldsymbol{\nu}) = \mathbf{1} \end{cases}$$

$$\widehat{\boldsymbol{\mu}}\,(\vec{\boldsymbol{n}}) = \left(\sum_{\boldsymbol{\nu}} \boldsymbol{w}(\boldsymbol{\nu})\,\boldsymbol{a}(\boldsymbol{\nu})\right)\boldsymbol{\mu}(\vec{\boldsymbol{n}}) + \left(\sum_{\boldsymbol{\nu}} \boldsymbol{w}(\boldsymbol{\nu})\,\boldsymbol{b}(\boldsymbol{\nu})\right)\boldsymbol{T}(\vec{\boldsymbol{n}}) + \cdots$$

Remazeilles & Chluba, MNRAS 2018

Component separation: standard ILC ?

$$\boldsymbol{d}(\boldsymbol{\nu},\vec{\boldsymbol{n}}) = \boldsymbol{a}(\boldsymbol{\nu})\boldsymbol{\mu}(\vec{\boldsymbol{n}}) + \boldsymbol{b}(\boldsymbol{\nu})\boldsymbol{T}(\vec{\boldsymbol{n}}) + \text{foregrounds}(\nu,\vec{n}) + \text{noise}(\nu,\vec{n})$$

data

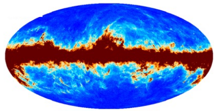

μ-distortion anisotropies

CMB temperature anisotropies

The standard ILC method forms an estimate of the μ-map as

$$\hat{\boldsymbol{\mu}}\,(\vec{\boldsymbol{n}}) = \sum_{\boldsymbol{\nu}} \boldsymbol{w}(\boldsymbol{\nu})\,\boldsymbol{d}(\boldsymbol{\nu},\vec{\boldsymbol{n}}) \quad \text{such that} \quad \begin{cases} \langle \hat{\boldsymbol{\mu}}\,(\vec{\boldsymbol{n}})^2 \rangle \text{ of minimum variance} \\ \sum_{\boldsymbol{\nu}} \boldsymbol{w}(\boldsymbol{\nu})\,\boldsymbol{a}(\boldsymbol{\nu}) = \boldsymbol{1} \end{cases}$$

$$\hat{\boldsymbol{\mu}}\,(\vec{\boldsymbol{n}}) = \left(\overbrace{\sum_{\boldsymbol{\nu}} \boldsymbol{w}(\boldsymbol{\nu})\,\boldsymbol{a}(\boldsymbol{\nu})}^{=\,\boldsymbol{1}}\right)\boldsymbol{\mu}(\vec{\boldsymbol{n}}) + \left(\sum_{\boldsymbol{\nu}} \boldsymbol{w}(\boldsymbol{\nu})\,\boldsymbol{b}(\boldsymbol{\nu})\right)\boldsymbol{T}(\vec{\boldsymbol{n}}) + \cdots$$

Remazeilles & Chluba, MNRAS 2018

Component separation: standard ILC ?

$$\boldsymbol{d}(\boldsymbol{\nu},\vec{\boldsymbol{n}}) = \boldsymbol{a}(\boldsymbol{\nu})\boldsymbol{\mu}(\vec{\boldsymbol{n}}) + \boldsymbol{b}(\boldsymbol{\nu})\boldsymbol{T}(\vec{\boldsymbol{n}}) + \text{foregrounds}(\nu,\vec{n}) + \text{noise}(\nu,\vec{n})$$

data

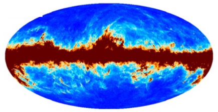

μ-distortion anisotropies

CMB temperature anisotropies

The standard ILC method forms an estimate of the μ-map as

$$\widehat{\boldsymbol{\mu}}\,(\vec{\boldsymbol{n}}) = \sum_{\boldsymbol{\nu}} \boldsymbol{w}(\boldsymbol{\nu})\,\boldsymbol{d}(\boldsymbol{\nu},\vec{\boldsymbol{n}}) \quad \text{such that} \quad \begin{cases} \langle \widehat{\boldsymbol{\mu}}\,(\vec{\boldsymbol{n}})^2 \rangle \text{ of minimum variance} \\ \sum_{\boldsymbol{\nu}} \boldsymbol{w}(\boldsymbol{\nu})\,\boldsymbol{a}(\boldsymbol{\nu}) = \mathbf{1} \end{cases}$$

$$\widehat{\boldsymbol{\mu}}\,(\vec{\boldsymbol{n}}) = \boldsymbol{\mu}(\vec{\boldsymbol{n}}) + \left(\sum_{\boldsymbol{\nu}} \boldsymbol{w}(\boldsymbol{\nu})\,\boldsymbol{b}(\boldsymbol{\nu})\right)\boldsymbol{T}(\vec{\boldsymbol{n}}) + \cdots$$

Remazeilles & Chluba, MNRAS 2018

Component separation: standard ILC ?

$$\boldsymbol{d}(\boldsymbol{\nu},\vec{\boldsymbol{n}}) = \boldsymbol{a}(\boldsymbol{\nu})\boldsymbol{\mu}(\vec{\boldsymbol{n}}) + \boldsymbol{b}(\boldsymbol{\nu})\boldsymbol{T}(\vec{\boldsymbol{n}}) + \text{foregrounds}(\nu,\vec{n}) + \text{noise}(\nu,\vec{n})$$

data

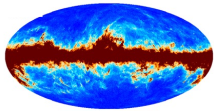

μ-distortion anisotropies

CMB temperature anisotropies

The standard ILC method forms an estimate of the μ-map as

$$\hat{\boldsymbol{\mu}}\,(\vec{\boldsymbol{n}}) = \sum_{\boldsymbol{\nu}} \boldsymbol{w}(\boldsymbol{\nu})\,\boldsymbol{d}(\boldsymbol{\nu},\vec{\boldsymbol{n}}) \quad \text{such that} \quad \begin{cases} \langle \hat{\boldsymbol{\mu}}\,(\vec{\boldsymbol{n}})^2 \rangle \text{ of minimum variance} \\ \sum_{\boldsymbol{\nu}} \boldsymbol{w}(\boldsymbol{\nu})\,\boldsymbol{a}(\boldsymbol{\nu}) = \mathbf{1} \end{cases}$$

$$\hat{\boldsymbol{\mu}}\,(\vec{\boldsymbol{n}}) = \boldsymbol{\mu}(\vec{\boldsymbol{n}}) + \overbrace{\left(\sum_{\boldsymbol{\nu}} \boldsymbol{w}(\boldsymbol{\nu})\,\boldsymbol{b}(\boldsymbol{\nu})\right)}^{\textit{residual CMB anisotropies!}} \boldsymbol{T}(\vec{\boldsymbol{n}}) + \cdots$$

Remazeilles & Chluba, MNRAS 2018

Component separation: standard ILC ?

$$\boldsymbol{d}(\boldsymbol{\nu},\vec{\boldsymbol{n}}) = \boldsymbol{a}(\boldsymbol{\nu})\boldsymbol{\mu}(\vec{\boldsymbol{n}}) + \boldsymbol{b}(\boldsymbol{\nu})\boldsymbol{T}(\vec{\boldsymbol{n}}) + \text{foregrounds}(\nu,\vec{n}) + \text{noise}(\nu,\vec{n})$$

data

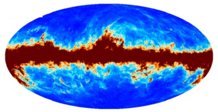

μ-distortion anisotropies

CMB temperature anisotropies

The standard ILC method forms an estimate of the μ-map as

$$\hat{\boldsymbol{\mu}}\,(\vec{\boldsymbol{n}}) = \sum_{\boldsymbol{\nu}} \boldsymbol{w}(\boldsymbol{\nu})\,\boldsymbol{d}(\boldsymbol{\nu},\vec{\boldsymbol{n}}) \quad \text{such that} \quad \begin{cases} \langle \hat{\boldsymbol{\mu}}\,(\vec{\boldsymbol{n}})^2 \rangle \text{ of minimum variance} \\ \sum_{\boldsymbol{\nu}} \boldsymbol{w}(\boldsymbol{\nu})\,\boldsymbol{a}(\boldsymbol{\nu}) = \boldsymbol{1} \end{cases}$$

$$\hat{\boldsymbol{\mu}}\,(\vec{\boldsymbol{n}}) = \boldsymbol{\mu}(\vec{\boldsymbol{n}}) + \overbrace{\left(\sum_{\boldsymbol{\nu}} \boldsymbol{w}(\boldsymbol{\nu})\,\boldsymbol{b}(\boldsymbol{\nu})\right)}^{\textit{residual CMB anisotropies!}} \boldsymbol{T}(\vec{\boldsymbol{n}}) + \cdots$$

$$\Longrightarrow C_\ell^{\hat{\mu}\times\hat{T}} = C_\ell^{\mu T} + \varepsilon C_\ell^{TT} + \cdots$$

Remazeilles & Chluba, MNRAS 2018

Component separation: standard ILC ?

$$\boldsymbol{d}(\boldsymbol{\nu},\vec{\boldsymbol{n}}) = \boldsymbol{a}(\boldsymbol{\nu})\boldsymbol{\mu}(\vec{\boldsymbol{n}}) + \boldsymbol{b}(\boldsymbol{\nu})\boldsymbol{T}(\vec{\boldsymbol{n}}) + \text{foregrounds}(\nu,\vec{n}) + \text{noise}(\nu,\vec{n})$$

data

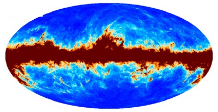

μ-distortion anisotropies

CMB temperature anisotropies

The standard ILC method forms an estimate of the μ-map as

$$\hat{\boldsymbol{\mu}}\,(\vec{\boldsymbol{n}}) = \sum_{\boldsymbol{\nu}} \boldsymbol{w}(\boldsymbol{\nu})\,\boldsymbol{d}(\boldsymbol{\nu},\vec{\boldsymbol{n}}) \quad \text{such that} \quad \begin{cases} \langle \hat{\boldsymbol{\mu}}\,(\vec{\boldsymbol{n}})^2 \rangle \text{ of minimum variance} \\ \sum_{\boldsymbol{\nu}} \boldsymbol{w}(\boldsymbol{\nu})\,\boldsymbol{a}(\boldsymbol{\nu}) = \mathbf{1} \end{cases}$$

$$\hat{\boldsymbol{\mu}}\,(\vec{\boldsymbol{n}}) = \boldsymbol{\mu}(\vec{\boldsymbol{n}}) + \overbrace{\left(\sum_{\boldsymbol{\nu}} \boldsymbol{w}(\boldsymbol{\nu})\,\boldsymbol{b}(\boldsymbol{\nu})\right)}^{\textit{residual CMB anisotropies!}}\boldsymbol{T}(\vec{\boldsymbol{n}}) + \cdots$$

$$\Longrightarrow C_\ell^{\hat{\mu}\times\hat{T}} = C_\ell^{\mu T} + \varepsilon C_\ell^{TT} + \cdots$$

residual TT correlations!

Remazeilles & Chluba, MNRAS 2018

Component separation: constrained ILC !

$$\boldsymbol{d}(\boldsymbol{\nu},\vec{\boldsymbol{n}}) = \boldsymbol{a}(\boldsymbol{\nu})\boldsymbol{\mu}(\vec{\boldsymbol{n}}) + \boldsymbol{b}(\boldsymbol{\nu})\boldsymbol{T}(\vec{\boldsymbol{n}}) + \text{foregrounds}(\nu,\vec{n}) + \text{noise}(\nu,\vec{n})$$

data

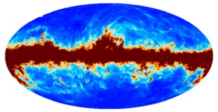

μ-distortion anisotropies

CMB temperature anisotropies

The ~~standard ILC~~ constrained ILC method forms an estimate of the μ-map as

$$\hat{\boldsymbol{\mu}}\,(\vec{\boldsymbol{n}}) = \sum_{\boldsymbol{\nu}} \boldsymbol{w}(\boldsymbol{\nu})\, \boldsymbol{d}(\boldsymbol{\nu},\vec{\boldsymbol{n}}) \quad \text{such that} \quad \begin{cases} \langle \hat{\boldsymbol{\mu}}\,(\vec{\boldsymbol{n}})^2 \rangle \text{ of minimum variance} \\ \sum_{\boldsymbol{\nu}} \boldsymbol{w}(\boldsymbol{\nu})\, \boldsymbol{a}(\boldsymbol{\nu}) = \mathbf{1} \\ \sum_{\boldsymbol{\nu}} \boldsymbol{w}(\boldsymbol{\nu})\, \boldsymbol{b}(\boldsymbol{\nu}) = \mathbf{0} \end{cases}$$

Remazeilles, Delabrouille, Cardoso, MNRAS 2011

Remazeilles & Chluba, MNRAS 2018

Component separation: constrained ILC !

$$\boldsymbol{d}(\boldsymbol{\nu},\vec{\boldsymbol{n}}) = \boldsymbol{a}(\boldsymbol{\nu})\boldsymbol{\mu}(\vec{\boldsymbol{n}}) + \boldsymbol{b}(\boldsymbol{\nu})\boldsymbol{T}(\vec{\boldsymbol{n}}) + \mathrm{foregrounds}(\nu,\vec{n}) + \mathrm{noise}(\nu,\vec{n})$$

data

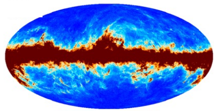

μ-distortion anisotropies

CMB temperature anisotropies

The ~~standard ILC~~ constrained ILC method forms an estimate of the μ-map as

$$\widehat{\boldsymbol{\mu}}\,(\vec{\boldsymbol{n}}) = \sum_{\boldsymbol{\nu}} \boldsymbol{w}(\boldsymbol{\nu})\,\boldsymbol{d}(\boldsymbol{\nu},\vec{\boldsymbol{n}}) \quad \text{such that} \quad \begin{cases} \langle \widehat{\boldsymbol{\mu}}\,(\vec{\boldsymbol{n}})^2 \rangle \text{ of minimum variance} \\ \displaystyle\sum_{\boldsymbol{\nu}} \boldsymbol{w}(\boldsymbol{\nu})\,\boldsymbol{a}(\boldsymbol{\nu}) = \mathbf{1} \\ \boxed{\displaystyle\sum_{\boldsymbol{\nu}} \boldsymbol{w}(\boldsymbol{\nu})\,\boldsymbol{b}(\boldsymbol{\nu}) = \mathbf{0}} \end{cases}$$

Extra constraint to guarantee the cancellation of residual CMB anisotropies

Remazeilles, Delabrouille, Cardoso, MNRAS 2011

Remazeilles & Chluba, MNRAS 2018

Component separation: constrained ILC !

$$\boldsymbol{d}(\boldsymbol{\nu},\vec{\boldsymbol{n}}) = \boldsymbol{a}(\boldsymbol{\nu})\boldsymbol{\mu}(\vec{\boldsymbol{n}}) + \boldsymbol{b}(\boldsymbol{\nu})\boldsymbol{T}(\vec{\boldsymbol{n}}) + \mathrm{foregrounds}(\nu,\vec{n}) + \mathrm{noise}(\nu,\vec{n})$$

data

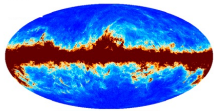

μ-distortion anisotropies

CMB temperature anisotropies

The ~~standard ILC~~ constrained ILC method forms an estimate of the μ-map as

$$\hat{\boldsymbol{\mu}}\,(\vec{\boldsymbol{n}}) = \sum_{\boldsymbol{\nu}} \boldsymbol{w}(\boldsymbol{\nu})\,\boldsymbol{d}(\boldsymbol{\nu},\vec{\boldsymbol{n}}) \quad \text{such that} \quad \begin{cases} \langle \hat{\boldsymbol{\mu}}\,(\vec{\boldsymbol{n}})^2 \rangle \text{ of minimum variance} \\ \sum_{\boldsymbol{\nu}} \boldsymbol{w}(\boldsymbol{\nu})\,\boldsymbol{a}(\boldsymbol{\nu}) = \mathbf{1} \\ \sum_{\boldsymbol{\nu}} \boldsymbol{w}(\boldsymbol{\nu})\,\boldsymbol{b}(\boldsymbol{\nu}) = \mathbf{0} \end{cases}$$

$$\hat{\boldsymbol{\mu}}\,(\vec{\boldsymbol{n}}) = \boldsymbol{\mu}(\vec{\boldsymbol{n}}) + \left(\overbrace{\sum_{\boldsymbol{\nu}} \boldsymbol{w}(\boldsymbol{\nu})\,\boldsymbol{b}(\boldsymbol{\nu})}^{=\,\mathbf{0}}\right)\boldsymbol{T}(\vec{\boldsymbol{n}}) + \cdots$$

$$\Longrightarrow C_\ell^{\hat{\mu}\times T} = C_\ell^{\mu\times T} + \cancel{\varepsilon C_\ell^{TT}} + \cdots$$

$\boxed{\textit{Zero residual TT correlation!}}$

Remazeilles, Delabrouille, Cardoso, MNRAS 2011

Remazeilles & Chluba, MNRAS 2018

Results

μ-map reconstruction with Constrained ILC

$$f_{\mathrm{NL}}^{\mu} = 10^4$$

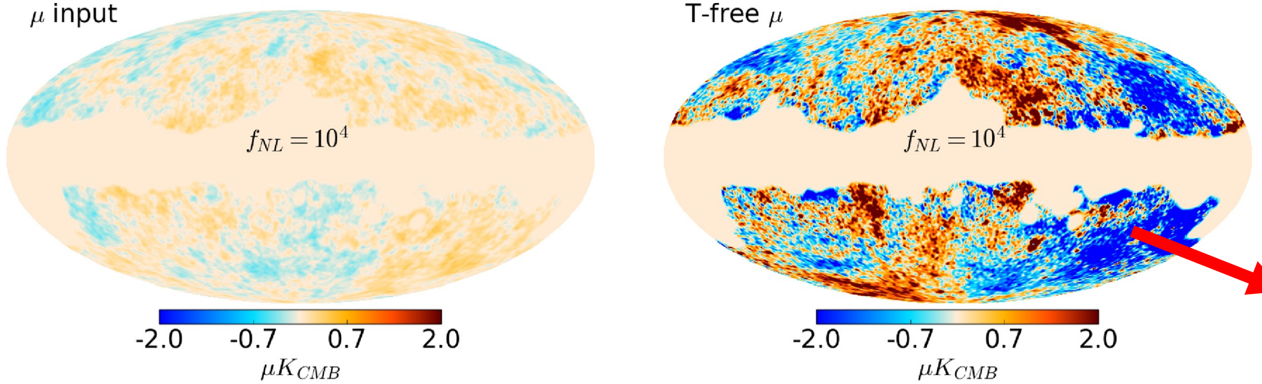

significant foreground contamination

Remazeilles & Chluba MNRAS 2018

μ-map reconstruction with Constrained ILC

$f_{\mathrm{NL}}^{\mu} = 10^4$

$f_{\mathrm{NL}}^{\mu} = 10^5$

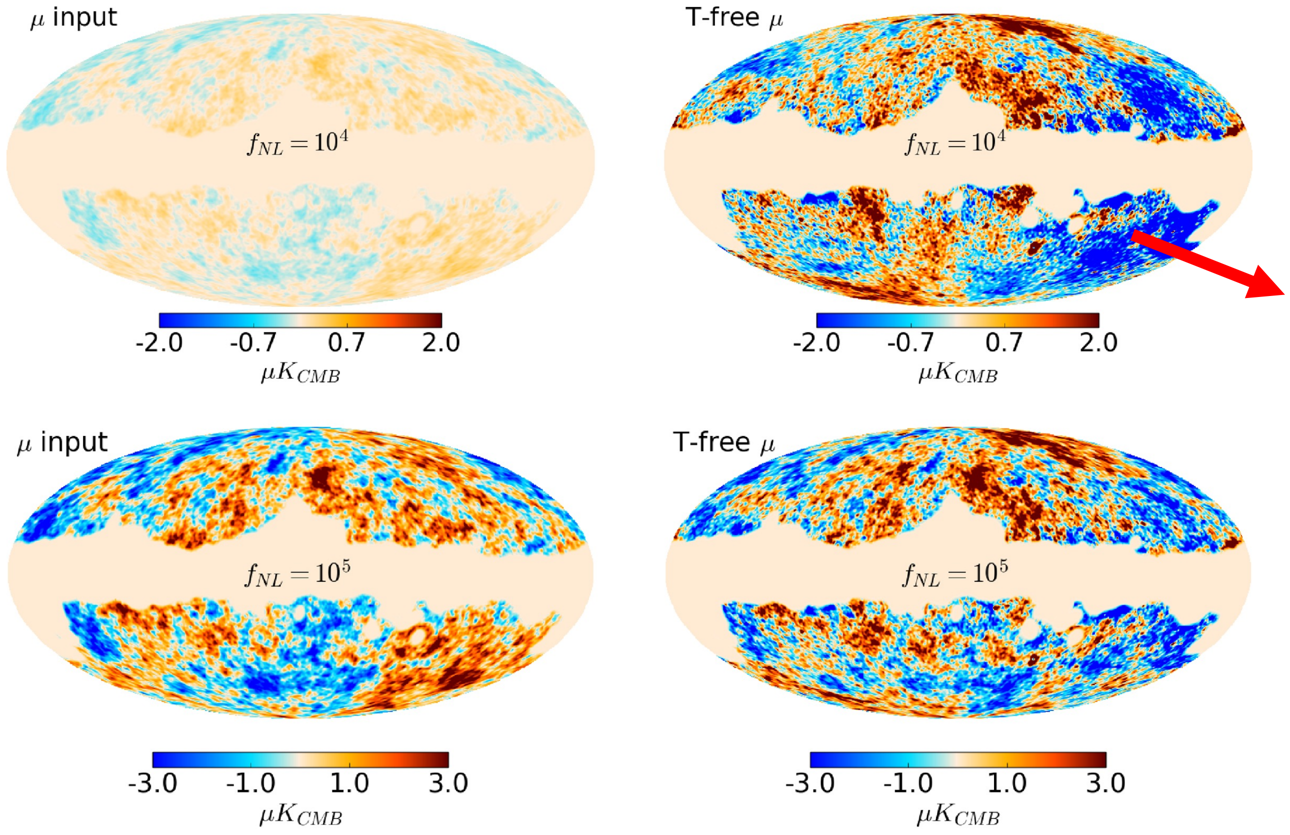

significant foreground contamination

Remazeilles & Chluba
MNRAS 2018

μ-map reconstruction with Constrained ILC

$f_{\rm NL}^{\mu} = 10^4$

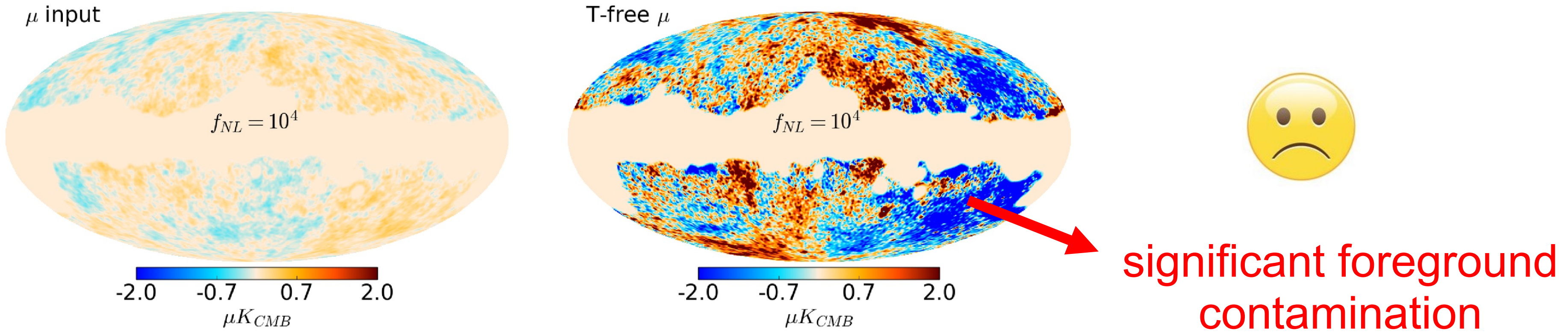

$f_{\rm NL}^{\mu} = 10^5$

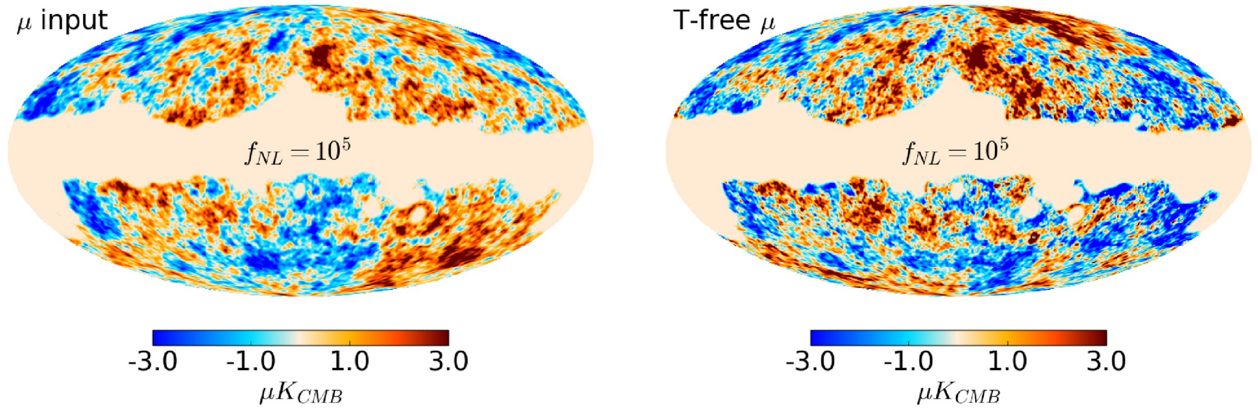

$f_{\rm NL}^{\mu} = 10^6$

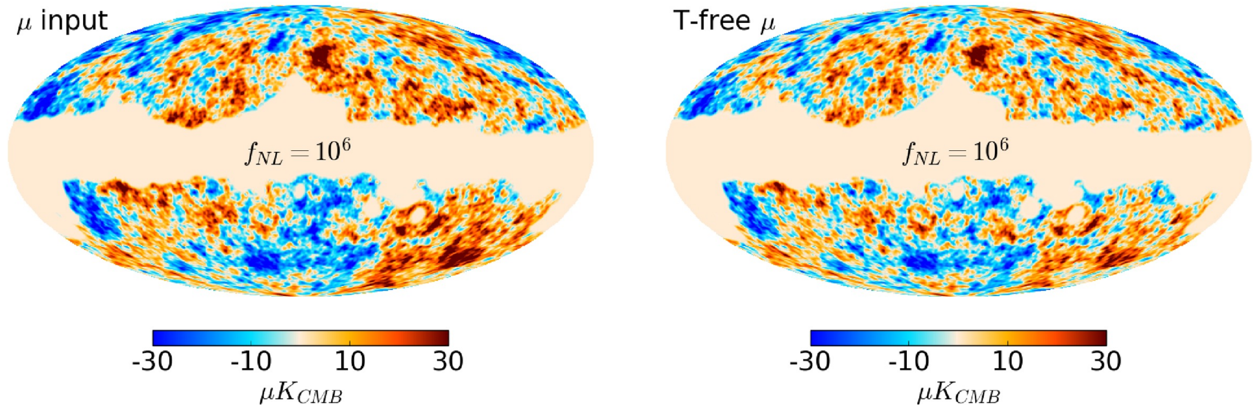

Remazeilles & Chluba MNRAS 2018

μ-map reconstruction with Constrained ILC

$f_{\rm NL}^{\mu} = 10^4$

$f_{\rm NL}^{\mu} = 10^5$

$f_{\rm NL}^{\mu} = 10^6$

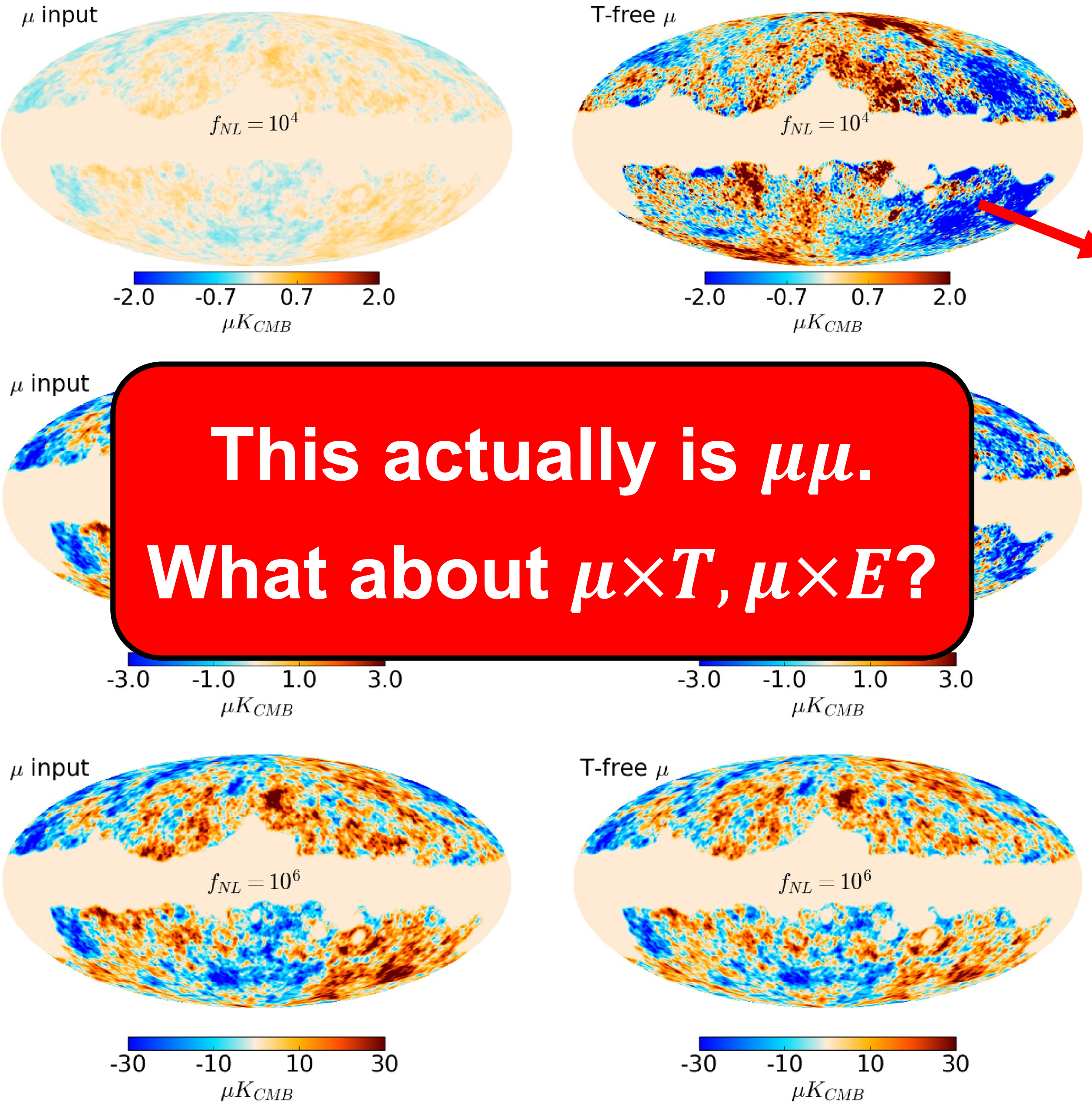

significant foreground contamination

This actually is $\mu\mu$.

What about $\mu\times T, \mu\times E$?

Remazeilles & Chluba MNRAS 2018

No binning

LiteBIRD, $f_{NL}^{\mu} = 4500$ without foregrounds

Remazeilles, Ravenni, Chluba MNRAS 2022

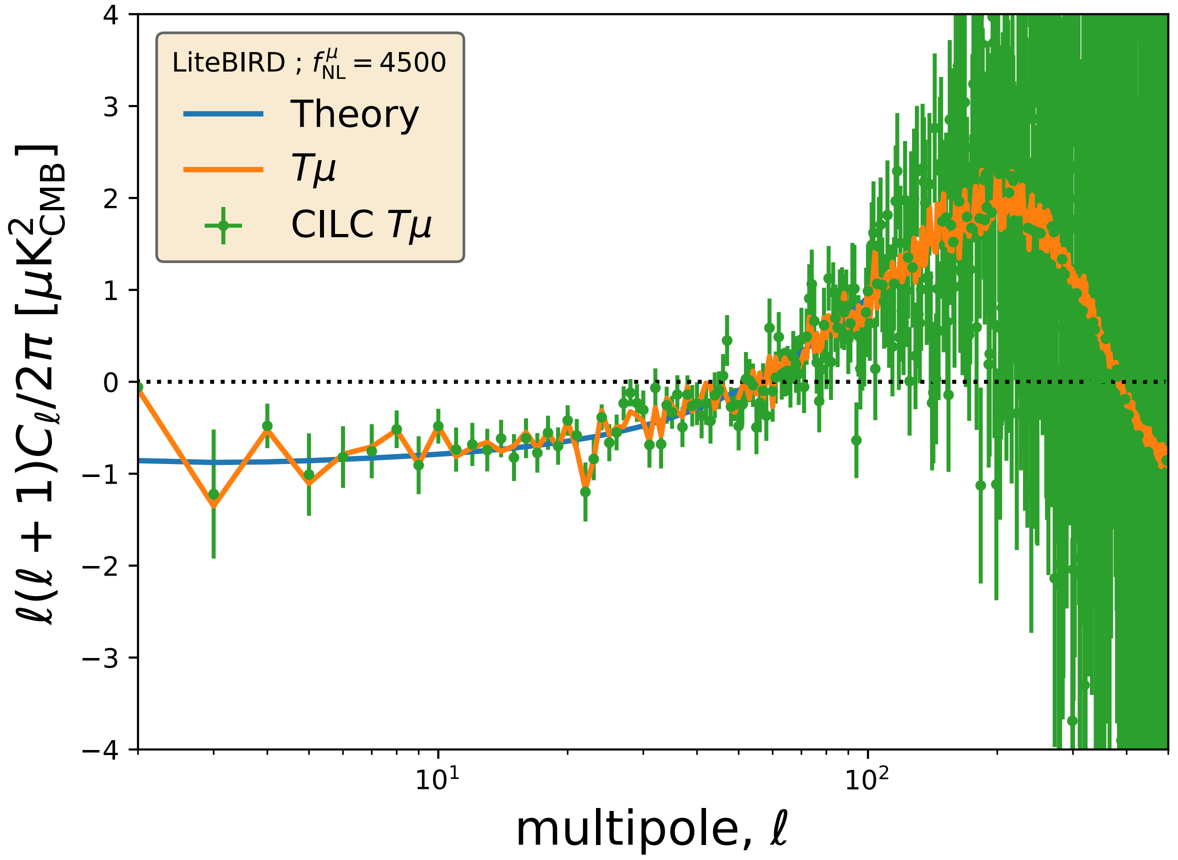

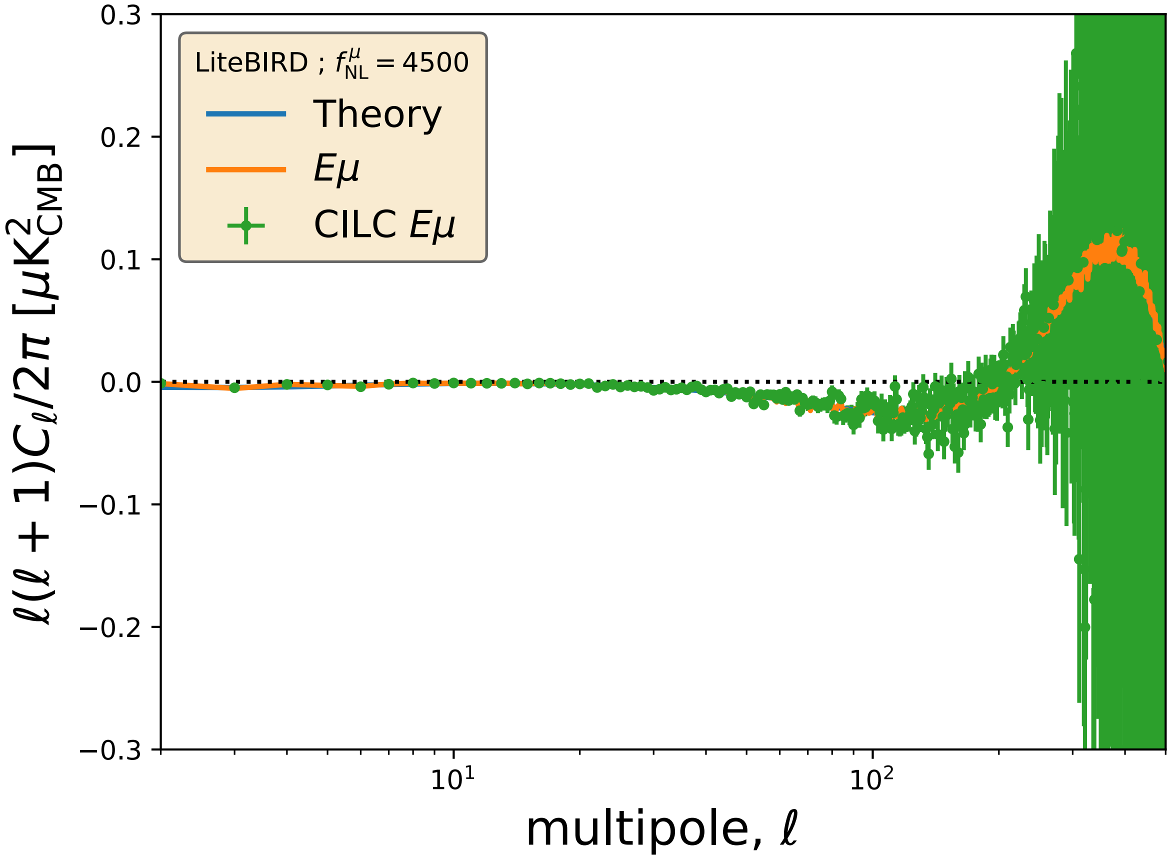

LiteBIRD, $f_{NL}^{\mu} = 4500$
without foregrounds

Remazeilles, Ravenni, Chluba MNRAS 2022

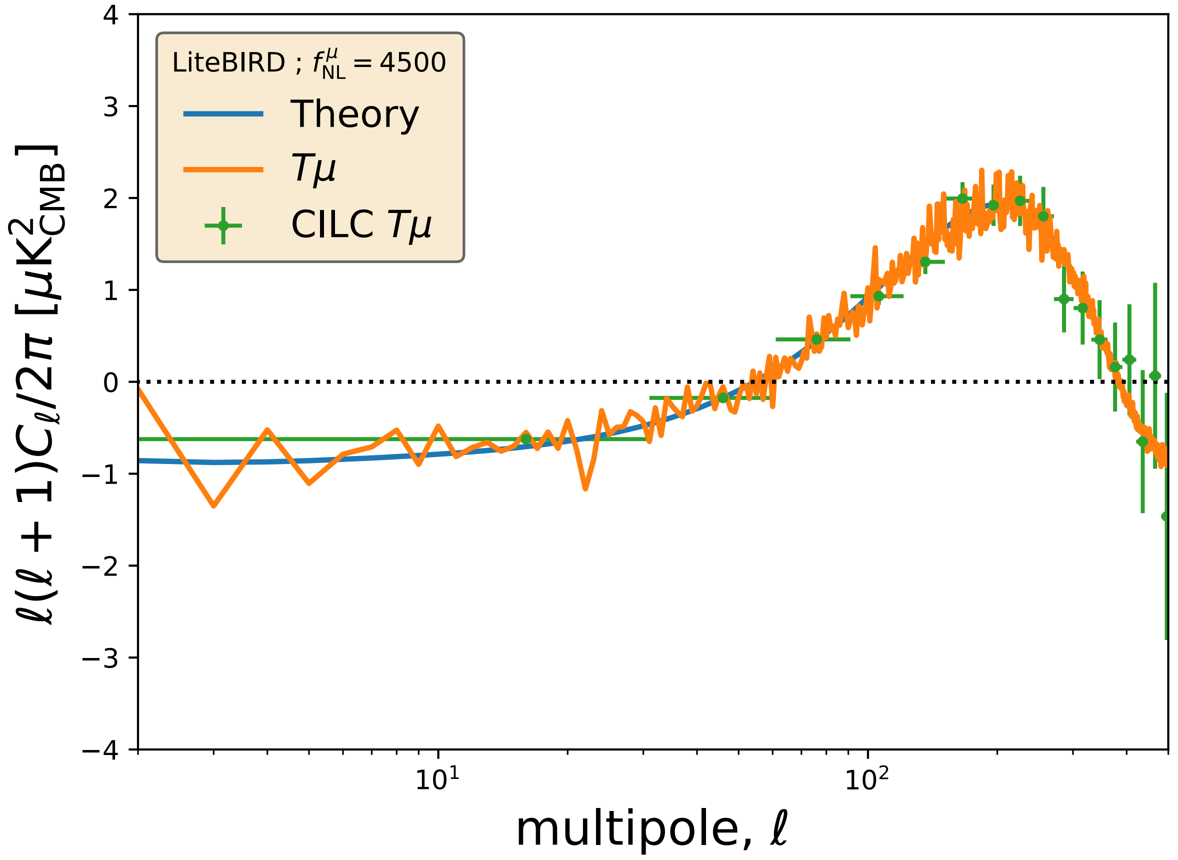

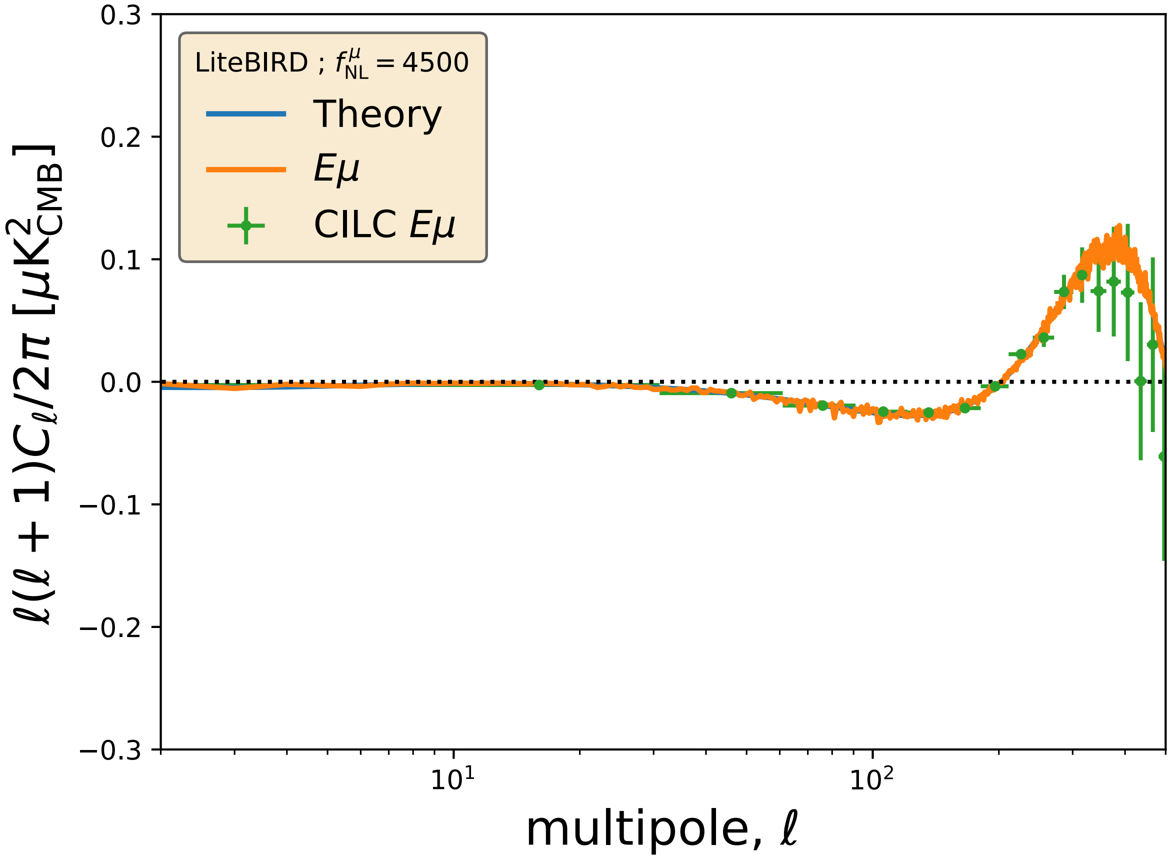

Standard ILC vs Constrained ILC

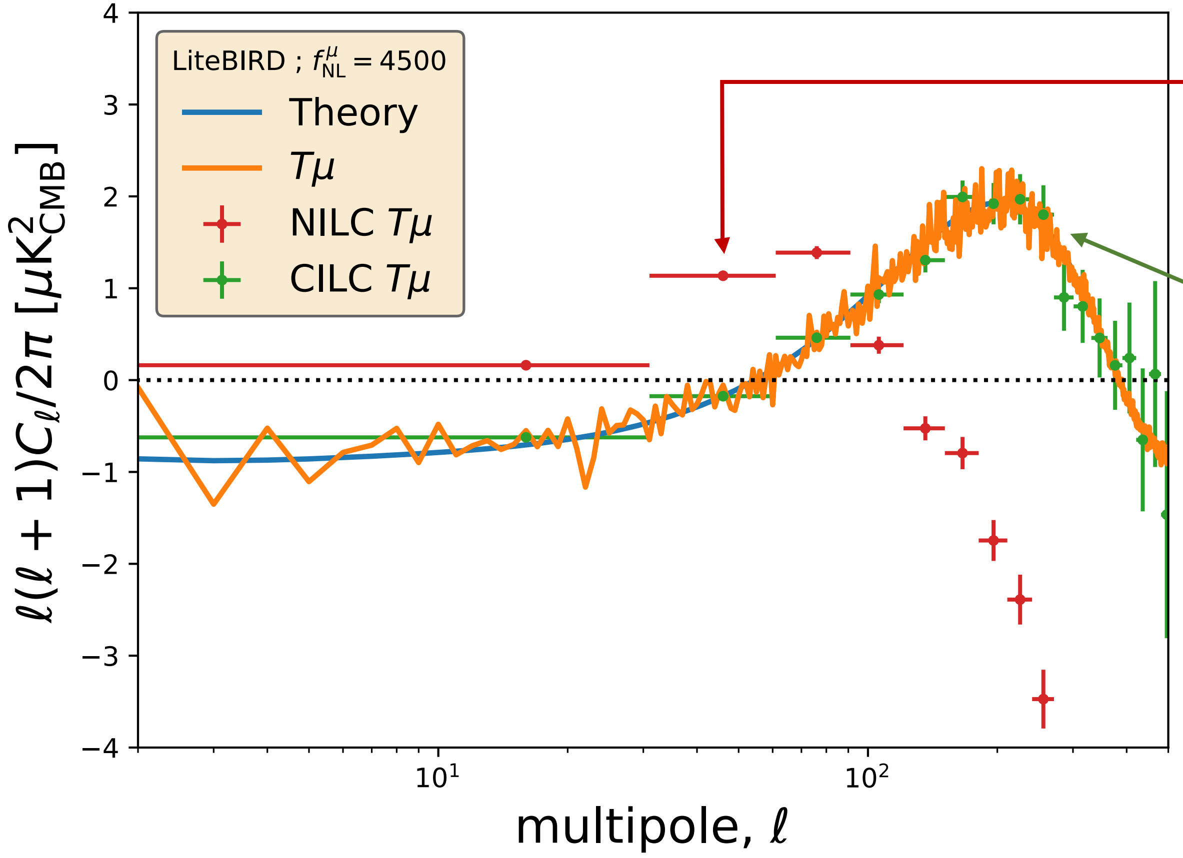

Standard ILC methods suffer from spurious TT correlations due to residual CMB anisotropies in the μ-map

The Constrained ILC fully recovers the correlated μT signal without bias

Remazeilles, Ravenni, Chluba, MNRAS 2022
Remazeilles & Chluba, MNRAS 2018

LiteBIRD, $f_{NL}^{\mu} = 4500$
without foregrounds

Remazeilles, Ravenni, Chluba MNRAS 2022

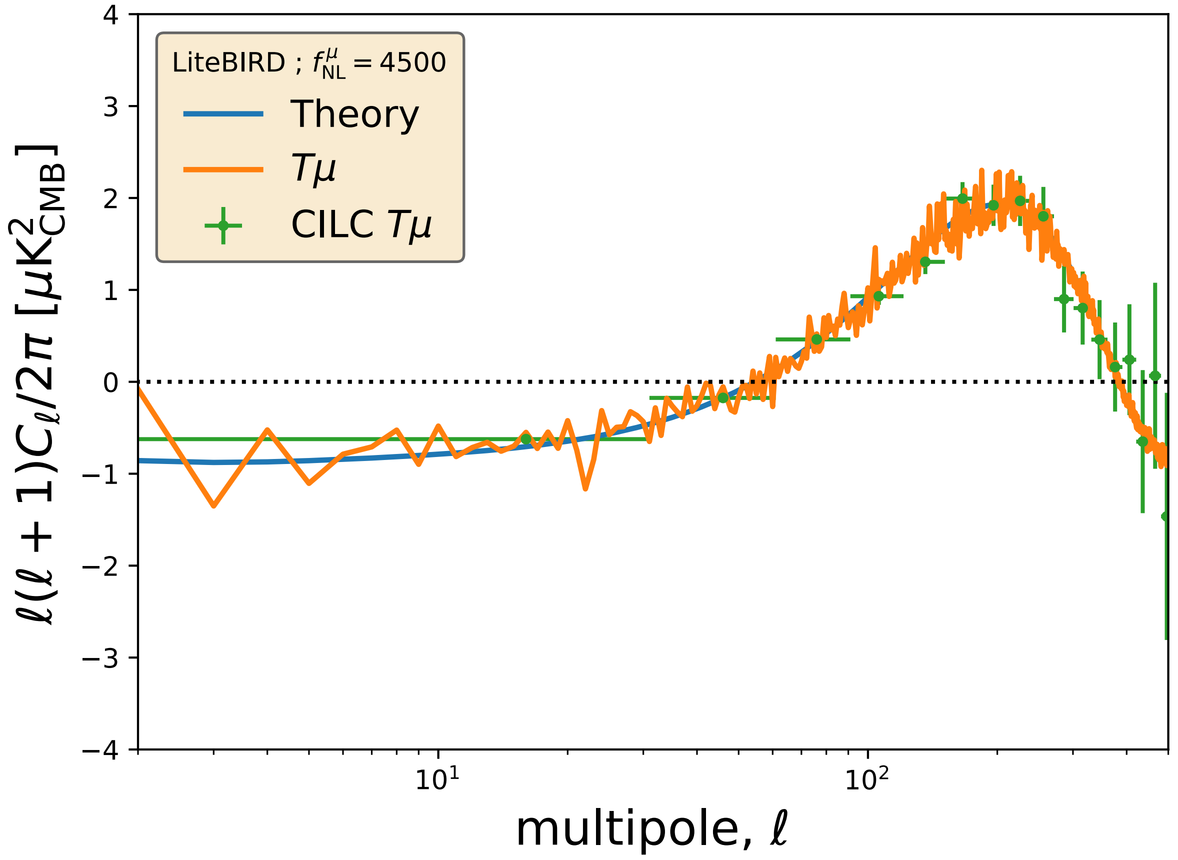

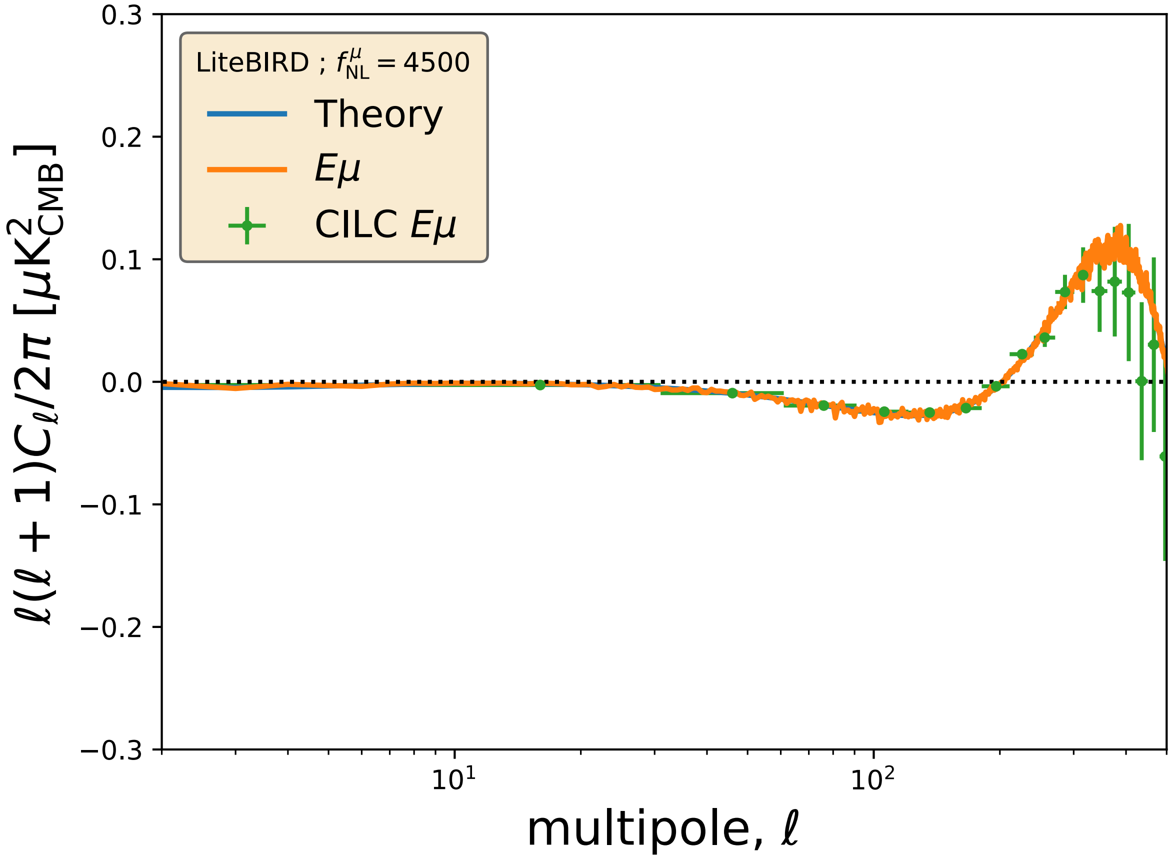

LiteBIRD, $f_{NL}^{\mu} = 4500$ with foregrounds

Remazeilles, Ravenni, Chluba MNRAS 2022

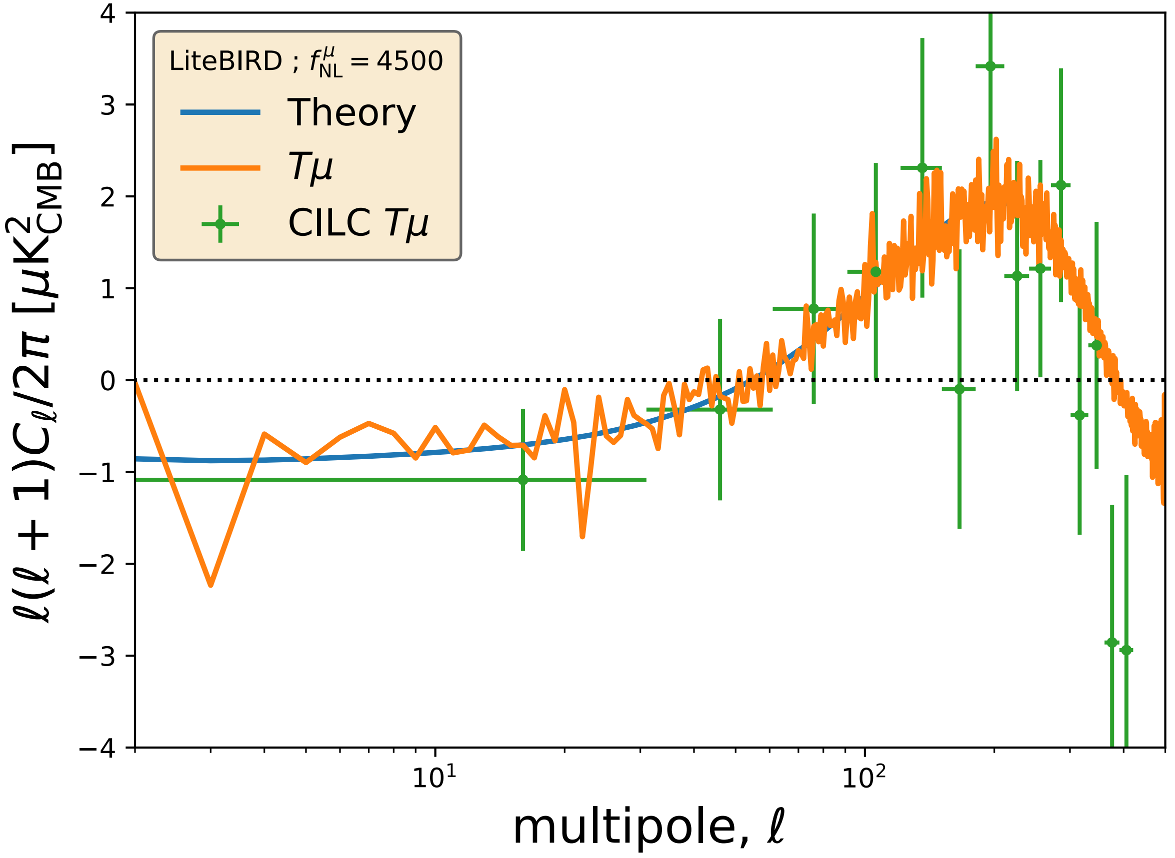

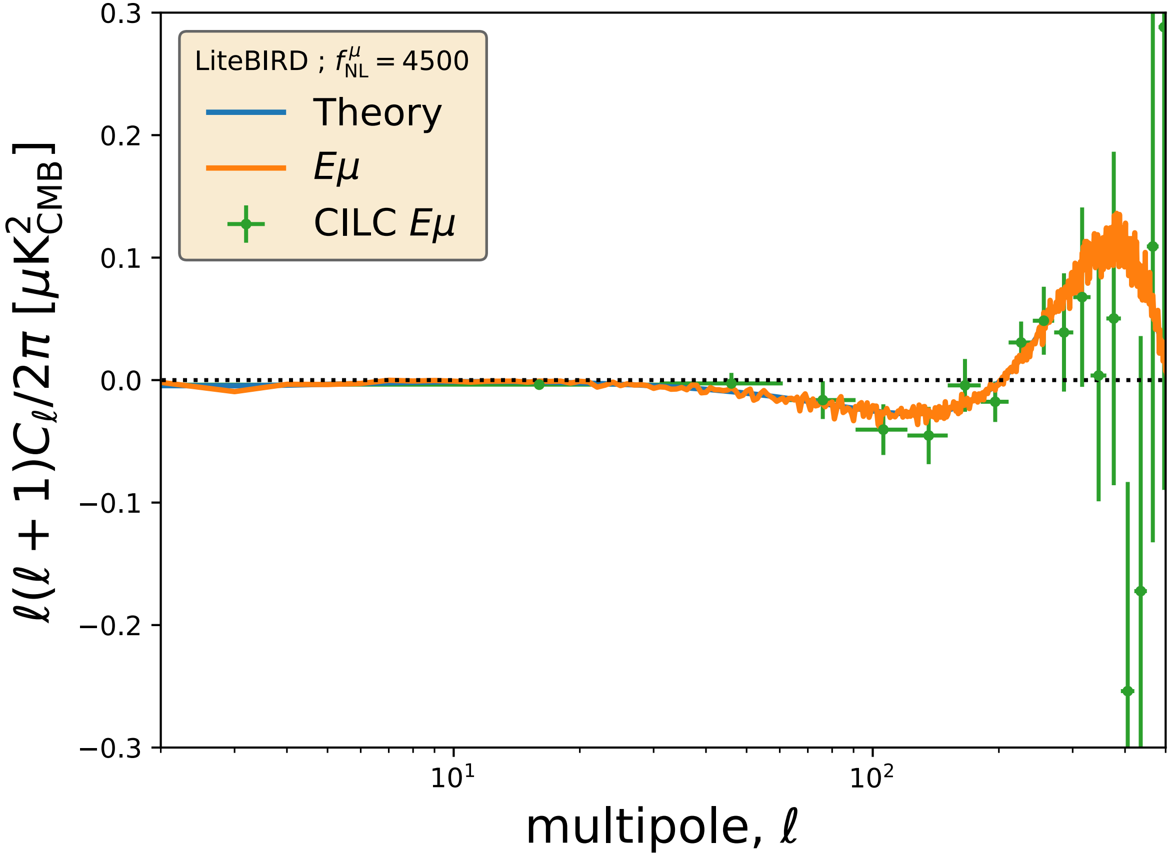

LiteBIRD, $f_{NL}^{\mu} = 10^4$ with foregrounds

Remazeilles, Ravenni, Chluba MNRAS 2022

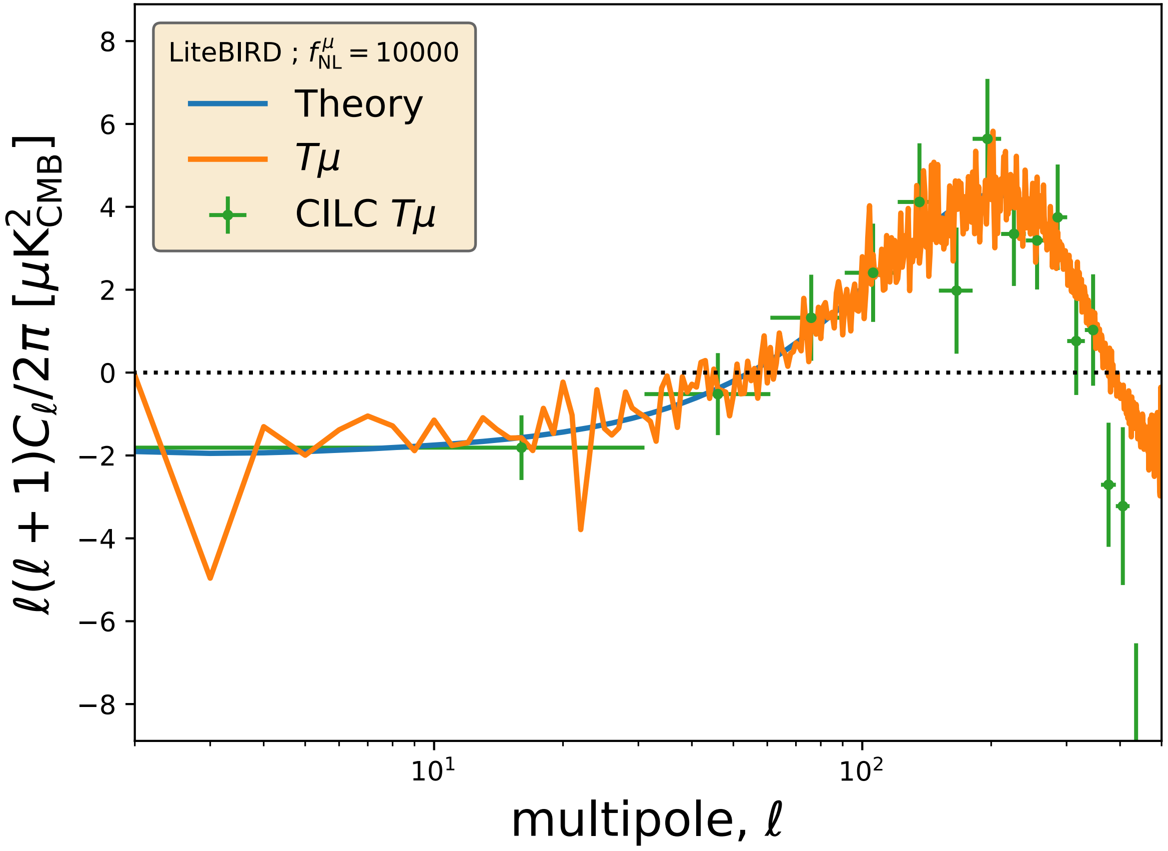

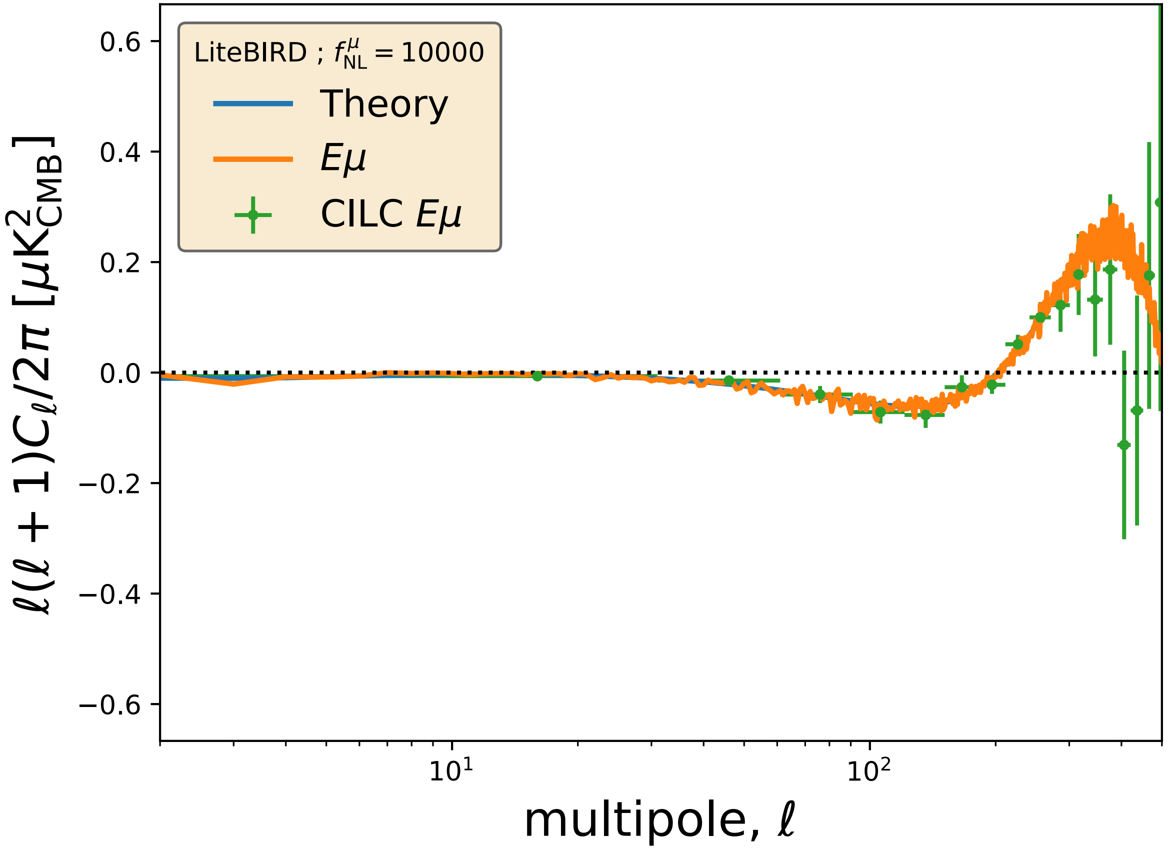

LiteBIRD, $f_{NL}^{\mu} = 10^5$
with foregrounds

Remazeilles, Ravenni, Chluba MNRAS 2022

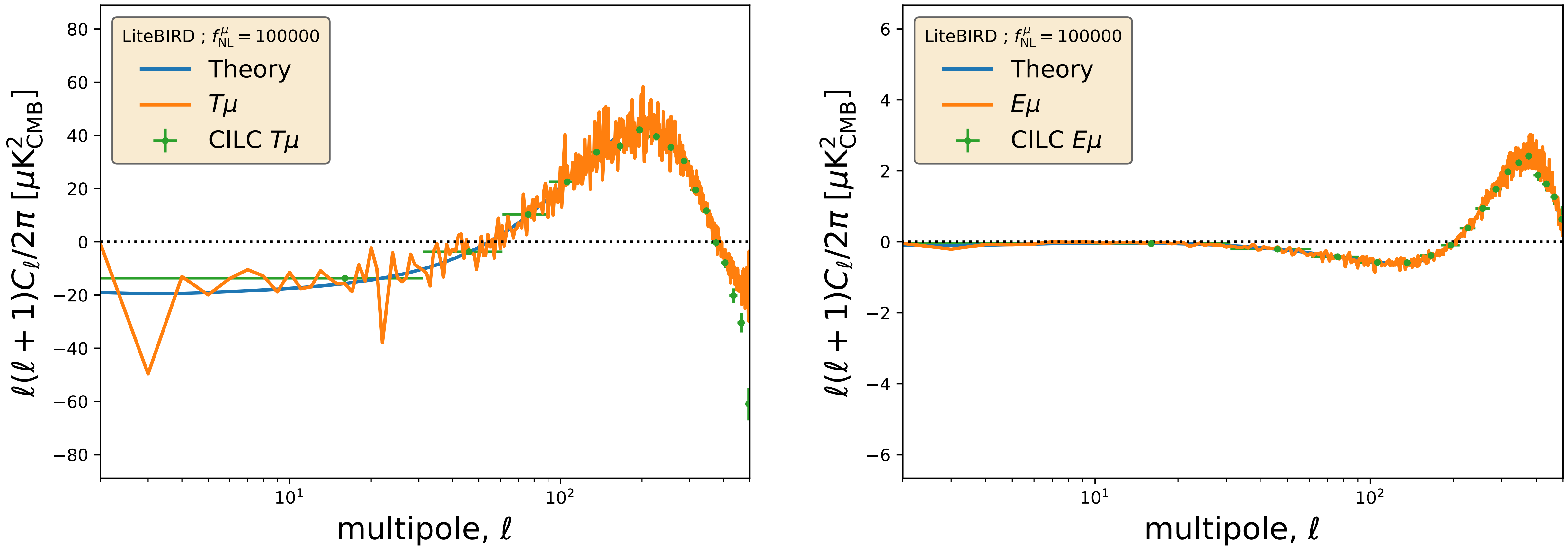

LiteBIRD null test, $f_{NL}^{\mu} = 0$ without foregrounds

Remazeilles, Ravenni, Chluba MNRAS 2022

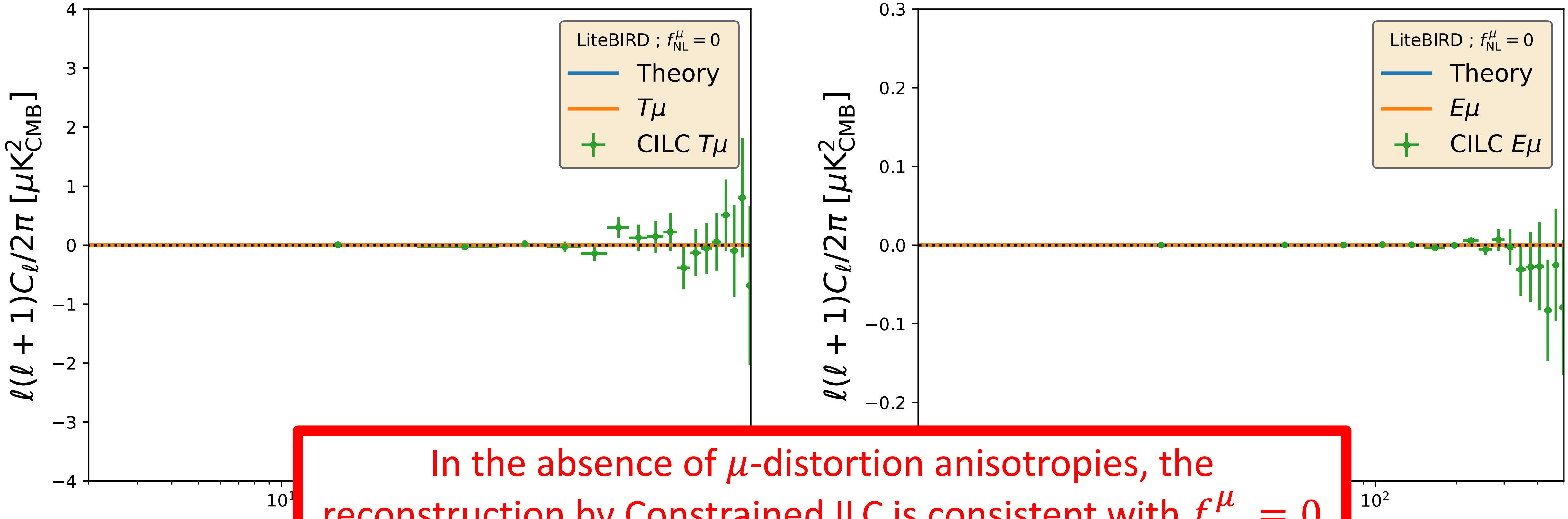

In the absence of μ-distortion anisotropies, the reconstruction by Constrained ILC is consistent with $f_{NL}^{\mu} = 0$

LiteBIRD null test, $f_{NL}^{\mu} = 0$ with foregrounds

Remazeilles, Ravenni, Chluba MNRAS 2022

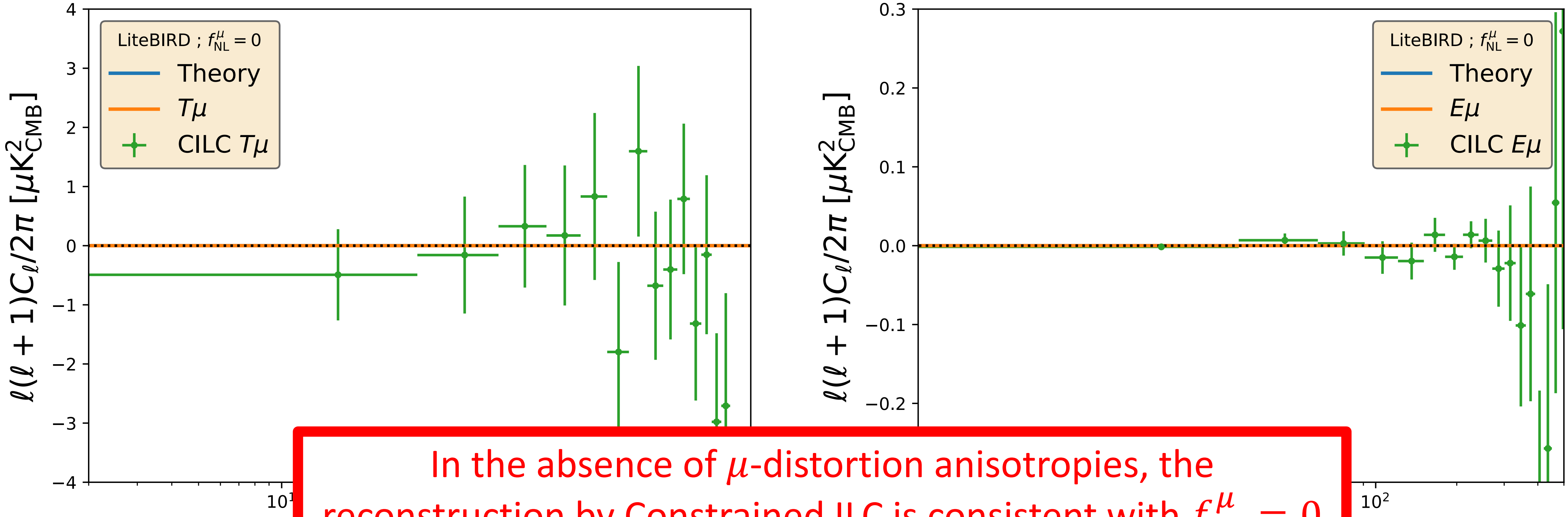

In the absence of μ-distortion anisotropies, the reconstruction by Constrained ILC is consistent with $f_{NL}^{\mu} = 0$

Forecasts on $f_{NL}^{\mu}(k \simeq 740\ \mathrm{Mpc}^{-1})$

$\mu \times T$

Remazeilles, Ravenni, Chluba, MNRAS 2022

LiteBIRD simulation

$f_{\rm NL}^{\mu}$ (fiducial)	10^5	10^4	4500	0	4500 (w/o foregrounds)	0 (w/o foregrounds)
$\mu \times T$	$(0.97 \pm 0.02) \times 10^5$ [50σ]	$(1.05 \pm 0.12) \times 10^4$ [8σ]	5264 ± 1286 [3.5σ]	951 ± 1286 -	4348 ± 152 [30σ]	8.2 ± 103 -

Forecasts on $f_{NL}^{\mu}(k \simeq 740\ \mathrm{Mpc}^{-1})$

$\boldsymbol{\mu \times T}$

LiteBIRD simulation

Remazeilles, Ravenni, Chluba, MNRAS 2022

$f_{\rm NL}^{\mu}$ (fiducial)	10^5	10^4	4500	0	4500 (w/o foregrounds)	0 (w/o foregrounds)
$\mu \times T$	$(0.97 \pm 0.02) \times 10^5$ [50σ]	$(1.05 \pm 0.12) \times 10^4$ [8σ]	5264 ± 1286 [3.5σ]	951 ± 1286 -	4348 ± 152 [30σ]	8.2 ± 103 -

Foregrounds degrade the sensitivity to $f_{\rm NL}^{\mu}$ by about a factor of 10

Forecasts on $f_{NL}^{\mu}(k \simeq 740\ \mathrm{Mpc}^{-1})$

$\mu \times E$

Remazeilles, Ravenni, Chluba, MNRAS 2022

LiteBIRD simulation

f_{NL}^{μ} (fiducial)	10^5	10^4	4500	0	4500 (w/o foregrounds)	0 (w/o foregrounds)
$\mu \times T$	$(0.97 \pm 0.02) \times 10^5$ [50σ]	$(1.05 \pm 0.12) \times 10^4$ [8σ]	5264 ± 1286 [3.5σ]	951 ± 1286 -	4348 ± 152 [30σ]	8.2 ± 103 -
$\mu \times E$	$(0.96 \pm 0.01) \times 10^5$ [100σ]	$(0.91 \pm 0.11) \times 10^4$ [9σ]	$\boxed{3779 \pm 1089\ [4\sigma]}$	-534 ± 1084 -	4366 ± 108 [42σ]	0.9 ± 76 -

μE provides more constraining power than μT on f_{NL}^{μ}

Forecasts on $f_{NL}^{\mu}(k \simeq 740\ \mathrm{Mpc}^{-1})$
$\mu \times T, E$ (joint)

Remazeilles, Ravenni, Chluba, MNRAS 2022

LiteBIRD simulation

f_{NL}^{μ} (fiducial)	10^5	10^4	4500	0	4500 (w/o foregrounds)	0 (w/o foregrounds)
$\mu \times T$	$(0.97 \pm 0.02) \times 10^5$ [50σ]	$(1.05 \pm 0.12) \times 10^4$ [8σ]	5264 ± 1286 [3.5σ]	951 ± 1286 -	4348 ± 152 [30σ]	8.2 ± 103 -
$\mu \times E$	$(0.96 \pm 0.01) \times 10^5$ [100σ]	$(0.91 \pm 0.11) \times 10^4$ [9σ]	3779 ± 1089 [4σ]	-534 ± 1084 -	4366 ± 108 [42σ]	0.9 ± 76 -
$\mu \times T, E$ (joint)	$(0.97 \pm 0.01) \times 10^5$ [100σ]	$(0.97 \pm 0.08) \times 10^4$ [11σ]	$\boxed{4425 \pm 827\ [5\sigma]}$	95 ± 824 -	4329 ± 90 [48σ]	-2.8 ± 62 -

***LiteBIRD*: 5σ detection of $f_{NL}^{\mu} = 4500$ after foreground cleaning**

***LiteBIRD*: $\sigma(f_{NL}^{\mu} = 0) \lesssim 800$ in the presence of foregrounds**

Focal plane optimization for μ-distortion anisotropies?

Optimization of focal plane for μ anisotropies?

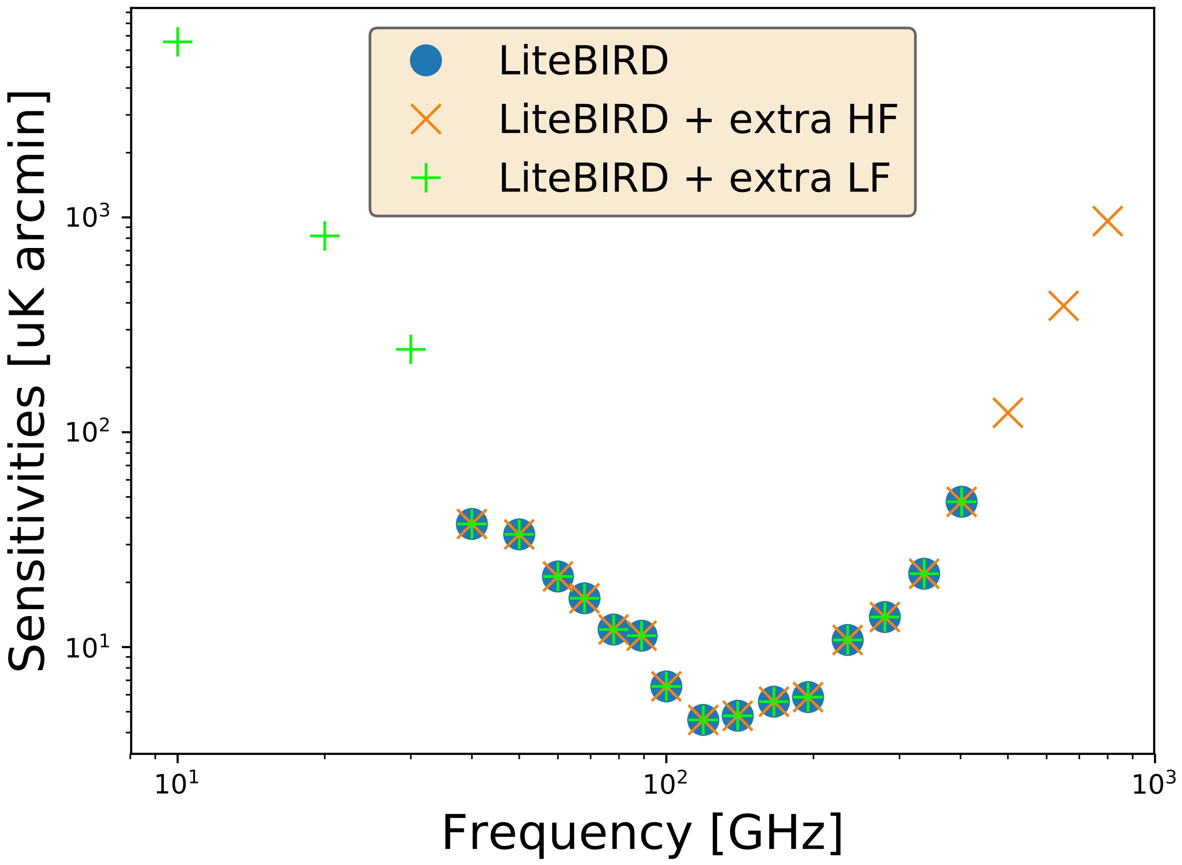

Combined sensitivity of all frequency channels:

$$\sigma = \left(\sum_{i=1}^{N} \frac{1}{\sigma_i^2} \right)^{-1/2}$$

$\sigma_{\rm LB}$ vs $\sigma_{\rm LB+HF}$ vs $\sigma_{\rm LB+LF}$?

Optimization of focal plane for μ anisotropies?

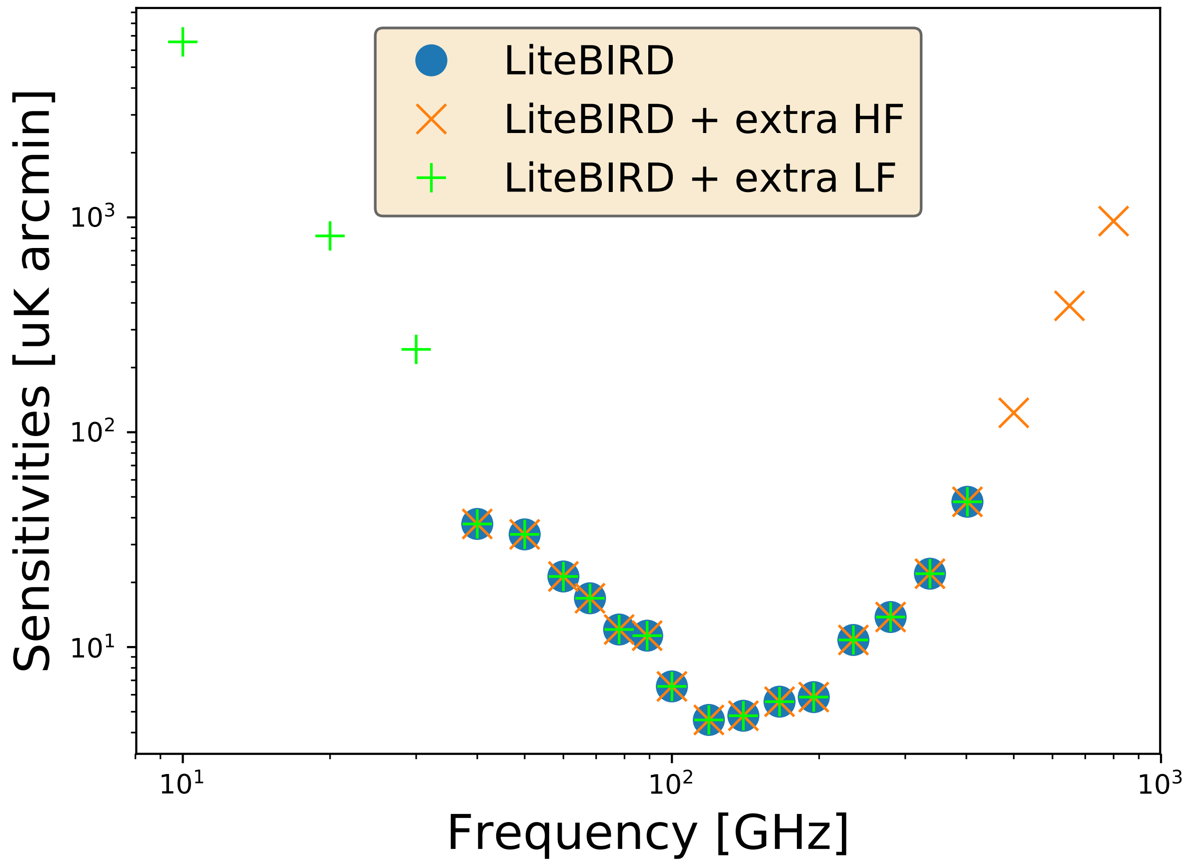

Combined sensitivity of all frequency channels:

$$\sigma = \left(\sum_{i=1}^{N} \frac{1}{\sigma_i^2} \right)^{-1/2}$$

This is the sensitivity to the **achromatic CMB signal**

Equivalently, ILC noise RMS for CMB in the absence of foregrounds

Optimization of focal plane for μ anisotropies?

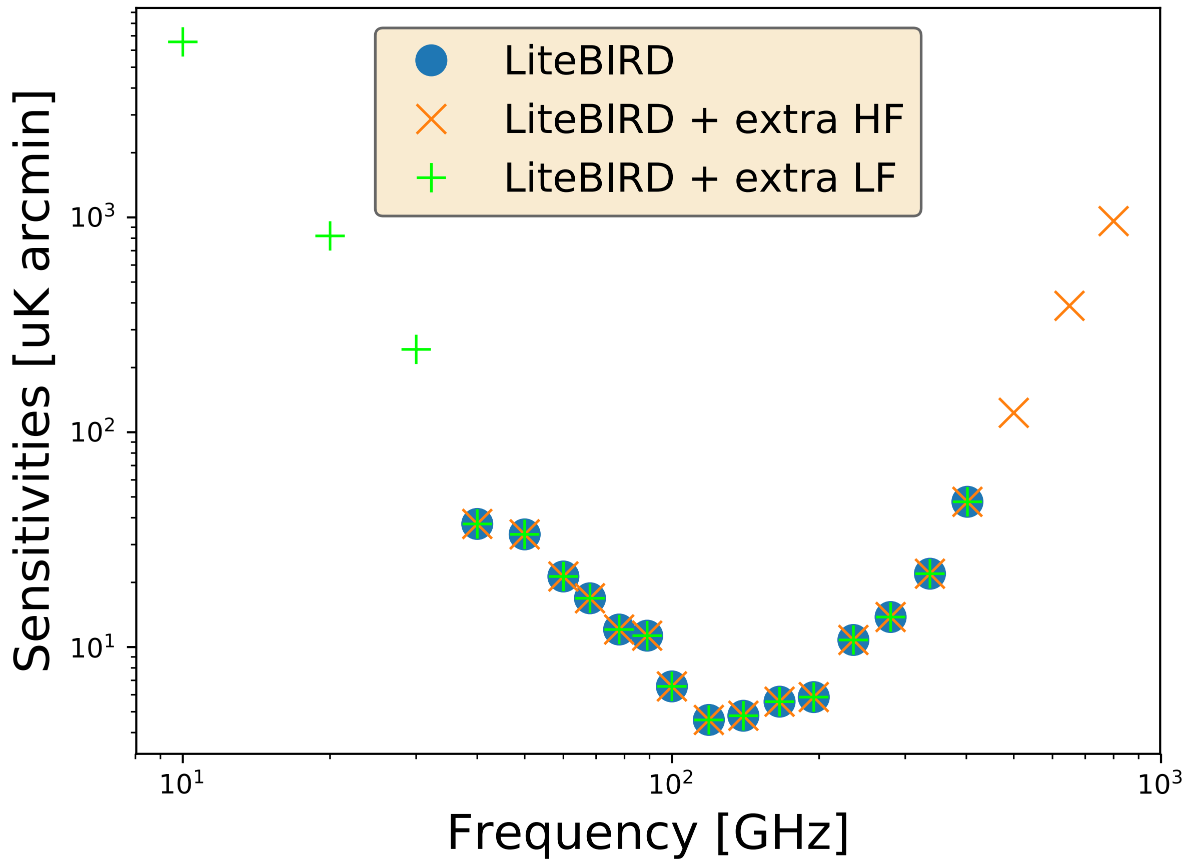

Sensitivity to **non-achromatic μ-distortion signal**:

$$\sigma = \left(\sum_{i=1}^{N} \frac{\left(a_i^{(\mu)}\right)^2}{\sigma_i^2} \right)^{-1/2}$$

extra weighting by the μ SED

Equivalently, ILC noise for μ in the absence of foregrounds

Optimization of focal plane for μ anisotropies?

$$\left(\sum_{i=1}^{N}\frac{1}{\sigma_i^2}\right)^{-1/2}$$

$$\left(\sum_{i=1}^{N}\frac{\left(a_i^{(\mu)}\right)^2}{\sigma_i^2}\right)^{-1/2}$$

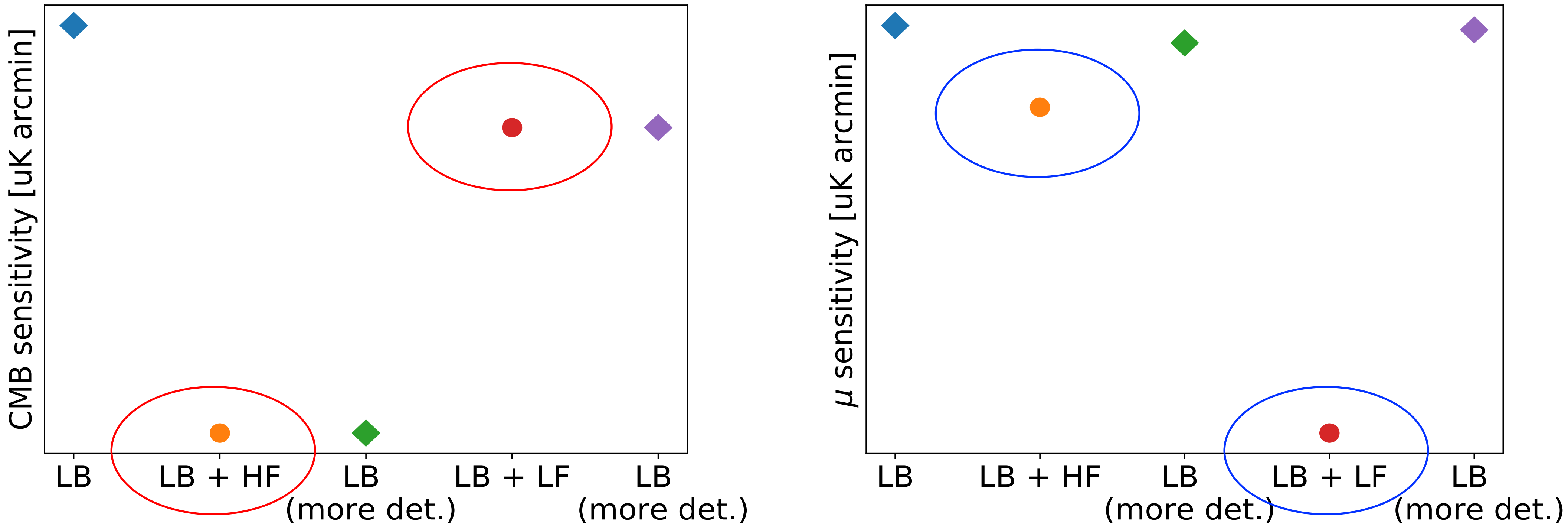

High frequencies better for CMB

Low frequencies better for μ

Optimization of focal plane for μ anisotropies?

$$\left(\sum_{i=1}^{N} \frac{1}{\sigma_i^2}\right)^{-1/2}$$

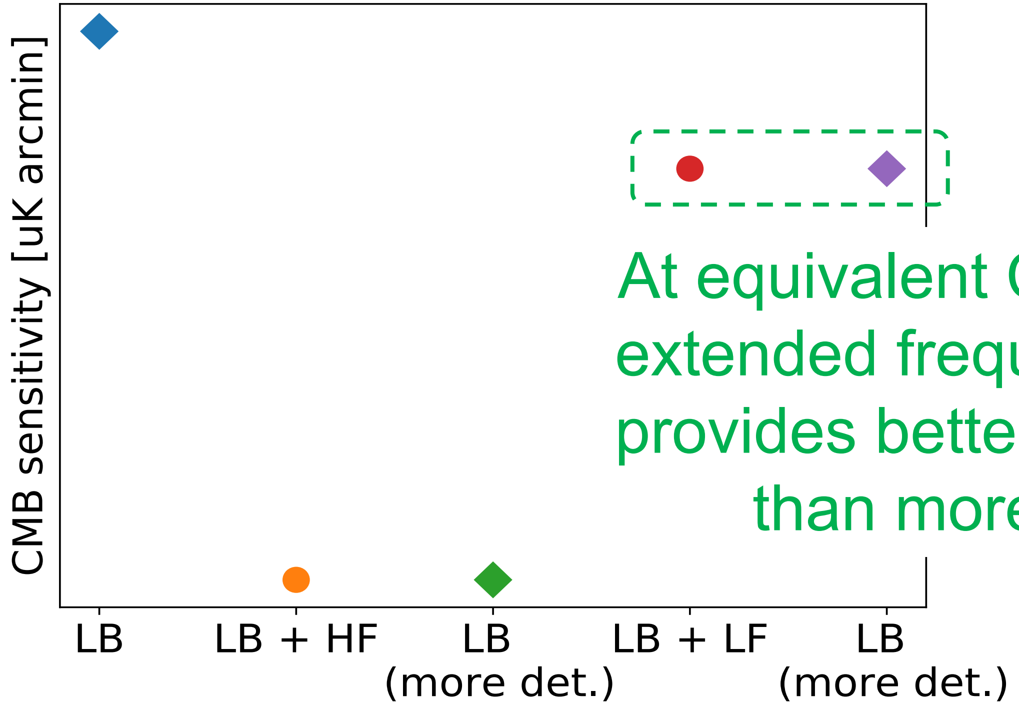

$$\left(\sum_{i=1}^{N} \frac{\left(a_i^{(\mu)}\right)^2}{\sigma_i^2}\right)^{-1/2}$$

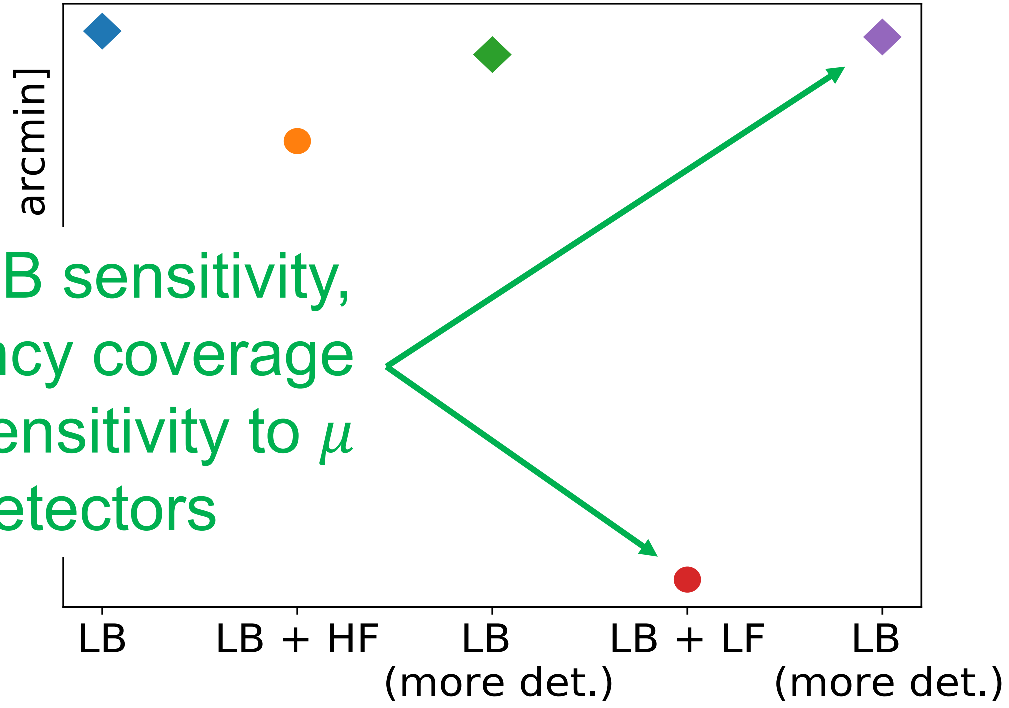

At equivalent CMB sensitivity, extended frequency coverage provides better sensitivity to μ than more detectors

High frequencies better for CMB

Low frequencies better for μ

Takeaway

- The Constrained ILC method enables to recover μT and μE correlation signals without bias
- Foregrounds degrade LiteBIRD sensitivity to $f_{\rm NL}^{\mu}(k \simeq 740\ {\rm Mpc}^{-1})$ by a factor of ten
- *LiteBIRD* detection limit $\sigma(f_{\rm NL}^{\mu} = 0) \lesssim 800$ from joint μT, μE analysis after foreground cleaning
- μE correlations provide more constraining power than μT correlations on $f_{\rm NL}^{\mu}$
  - Because the degree of correlation between μ and E is larger than that between μ and T
  - Because foregrounds are less complex in polarization than in intensity
  - Because the CMB E-mode is immune from μ-distortion anisotropies
- In contrast to CMB anisotropies, μ-distortion anisotropies would get better sensitivity by adding low frequencies to LiteBIRD than adding high frequencies
- Extended frequency coverage provides more leverage than increased detector sensitivity